ATOMIC EMISSION SPECTROSCOPY WITH AN INDUCTIVELY COUPLED RADIOFREQUENCY PLASMA

by

JAMSHID MANZOORI-LASHGAR, M.Sc., D.I.C.

A thesis submitted for the degree of
Doctor of Philosophy of the University of London

August 1977

Department of Chemistry,
Imperial College of Science and Technology,
South Kensington,
London, S.W.7.

SUMMARY

This thesis describes the development and application of a radiofrequency plasma system for trace element analysis.

Plasma emission sources in analytical spectrometry are classified and discussed. The development and characteristics of inductively coupled plasmas are described and the literature briefly reviewed. In addition, the theoretical aspects of emission spectroscopy pertaining to plasma sources are considered.

The construction and subsequent modification of a complete analytical argon plasma system operated at 36 MHz and 2.5 KW is described. The operational parameters (viz.; observation height, generator power and gas flow rates) and their interdependencies are investigated. Interference effects in the system are studied and mechanisms suggested. The detection limits for 7 elements have been determined and the results are compared with those of other workers.

The determination of Mo, Co, and B in soil extracts is discussed in detail. The method was found to be precise and rapid with detection limits equal to or superior to those obtained by other analytical techniques.

ACKNOWLEDGEMENTS

I would like to thank my supervisor, Professor T. S. West, for the opportunity to gain research experience whilst working under his guidance.

I would also like to thank Dr R. A. Chalmers and Dr I. L. Marr for allowing me to work in their laboratory and for their help during my period in Aberdeen.

I am particularly indebted to my immediate supervisor, Dr B. L. Sharp, for his encouragement, useful discussion and great concern throughout my research programme.

Finally, I would like to thank all my colleagues in the analytical research group, in particular Mr S. Cooke for his help with English during the writing of this thesis.

The research work presented in this thesis was carried out in the Chemistry Department of the Imperial College of Science and Technology and the University of Aberdeen from October 1974 to August 1977. It is entirely original except where due reference is made. No part of this work has previously been submitted for any degree.

CONTENTS

		Page
CHAPTER I	INTRODUCTION	
1.1.	DEFINITION AND DISCUSSION OF THE PLASMA STATE	9
1.2.	APPLICATIONS OF PLASMAS	9
1.3.	CLASSIFICATION OF PLASMA TYPES	10
1.3.1.	Two Electrode Plasmas	11
1.3.2.	Single Electrode Plasmas	11
1.3.3.	Electrodeless Plasmas	12
1.4.	INDUCTIVELY COUPLED RADIO FREQUENCY PLASMAS (ICP)	13
1.4.1.	Mechanism of Formation, Stabilisation and Physical Characteristics	13
1.4.2.	Properties of ICP	18
1.4.3.	Sample Introduction Methods	20
1.4.4.	Literature Review	21
CHAPTER II	THEORY OF EMISSION SPECTROMETRY AS PERTAINING TO R.F. PLASMA SOURCES	
2.1.	INTRODUCTION, CONVENTION AND NOTATION	30
2.2.	SPECTRAL LINE INTENSITY	31
2.3.	EXCITATION AND BOLTZMANN DISTRIBUTION LAW	32
2.4.	THE CONCEPT OF TEMPERATURE AND THERMODYNAMIC EQUILIBRIUM	34
2.5.	TEMPERATURE MEASUREMENT	35
2.6.	IONIZATION AND THE SAHA EQUATION	36
2.7.	DISSOCIATION EQUILIBRIA	38
2.8/		

		Page
2.8.	SELF-ABSORPTION	39
CHAPTER III	INSTRUMENTATION	
3.1.	THE PLASMA GENERATOR	45
3.2.	THE WORK COIL	46
3.3.	THE PLASMA TORCH	46
3.4.	GAS SELECTION AND FLOW RATE CONTROL SYSTEM	50
3.5.	MOUNTING OF THE TORCH	50
3.6.	THE PLASMA INITIATION	52
3.7.	NEBULIZERS	52
3.8.	AEROSOL CHAMBER	54
3.9.	MODIFICATION TO THE INJECTOR TUBE	57
3.10.	AUXILIARY DEVICE TO INCREASE S/N RATIO	57
3.11.	DETECTION SYSTEM	59
CHAPTER IV	INVESTIGATION OF THE ANALYTICAL OPERATING CHARACTERISTICS OF RF ICP	
4.1.	OPTIMISATION OF THE OPERATING PARAMETERS	62
4.1.1.	Effect of the Injector Gas Flow Rate	62
4.1.2.	Effect of the Plasma Gas Flow	63
4.1.3.	Effect of Coolant Gas Flow	66
4.1.4.	Effect of the Radiofrequency Power	69
4.1.5.	Effect of the Height of Observation	72
4.1.6/		

		Page
4.1.6.	Inter-relative Effect of the Operating Parameters	74
4.2.	INTERFERENCE EFFECTS	81
4.2.1.	Classification of Interference Effects	81
4.2.2.	Ionization Interference Study	82
4.2.3.	Dependence of Interference Effect on Interferent Concentration	87
4.2.4.	Mechanism of Al Interference on Mo	89
4.3.	DETECTION LIMITS	96
4.4.	PRECISION	98
CHAPTER V	APPLICATION OF THE ICP TO THE ANALYSIS OF SOIL SAMPLES	
5.1.	MOLYBDENUM	
5.1.1.	Introduction	100
5.1.2.	Choice of Analytical Line	101
5.1.3.	Standard Solutions	101
5.1.4.	Calibration Curves	101
5.1.5.	Emission Spectra	106
5.1.6.	Interference Effects	110
5.1.7.	Sample Preparation	111
5.1.8.	Analysis of Mo in Soil Extracts	112
5.1.9.	Effect of Organic Matter on Mo Determination	115
5.1.10.	Molybdenum Determination in the Presence of Zirconium	116
5.2.	COBALT	
5.2.1/		

		Page
5.2.1.	Introduction	119
5.2.2.	Choice of Analytical Line	119
5.2.3.	Standard Solutions	120
5.2.4.	Calibration Curves	120
5.2.5.	Interference Effects	120
5.2.6.	Sample Preparation	124
5.2.7.	Analysis of Co in Soil Extracts	124
5.3.	BORON	
5.3.1.	Introduction	125
5.3.2.	Calibration Curves	126
5.3.3.	Interference Effects	128
5.3.4.	Sample Preparation	128
5.3.5.	Analysis of B in Soil Extracts	130
CHAPTER VI	CONCLUSION	132
REFERENCES		136

CHAPTER I

INTRODUCTION

1.1 DEFINITION AND DISCUSSION OF THE PLASMA STATE

The word plasma, etymologically, means a mould or a form and is also used for the liquid part of the blood in which the corpuscules are suspended. From the modern scientific point of view it is considered as the fourth state of matter and is believed to constitute 99% of the matter in the universe. In spectrochemical terminology a plasma may be defined as a volume of gas or vapour in which a significant number of atoms or molecules are in the electrically charged or ionized state. Due to the greater mobility of electrons compared with positive ions, many plasmas have a thin outer sheath rich in electrons surrounding a main body rich in positive ions.

Plasma physics has been the concern of different scientists for over a hundred years, since Michael Faraday made observations on the glow discharge in the 1830's. A detail discussion of the origin of plasma physics can be found in reference (1). In summary the science of plasma physics may be identified as the study of electrical discharges and their interaction with magnetic fields.

1.2 APPLICATION OF PLASMAS

The applications of plasmas, generally, result from the fact that they provide higher temperatures than combustion flames. In plasma torches a temperature of 10000 K is quite easily obtainable, while flames are limited to about 3000 K. At such high temperature few molecules can survive, and noting that the boiling point of tungsten is 5600°C and molybdenum 4612°C the importance of plasmas to the analysis of such materials is clear. Analytically plasmas are used to perform the/

the functions of vaporisation, dissociation, and excitation. In certain cases only the atomisation function is employed and the plasma is used as an atom reservoir, e.g. for atomic absorption or atomic fluorescence.

It should be remembered that a large branch of physics is concerned with the plasma state and probably the most publicized plasma applications are those concerned with energy conversion by means of controlled thermonuclear (fusion) reactions and magnetohydrodynamic (MHD) power generation. Plasmas are also used in electrical communications and in metallurgy for melting metals.

1.3 CLASSIFICATION OF PLASMA TYPES

Plasmas may, roughly but usefully, be classified into three types according to the number of electrodes they employ, two electrode plasmas, single electrode plasmas and electrodeless plasmas. Boumans and de Boe r (2) have classified excitation plasma sources into:

(I) D.C. plasmas, which are either the current-carrying type (gas-stabilized arcs and disc- or wall-stabilized arcs) or the current-free type (plasma jets)

(II) High Frequency (HF) or Radiofrequency (RF) plasmas with either capacitive or inductive coupling (frequency range 1-100 MHz, power $>$ 0.5 KW)

(III) Microwave plasmas with either capacitive or inductive coupling (frequency 2450 MHz, power a few hundred W to a few KW for the capacitively-coupled type and 25-200 W for the cavity-induced type).

The author will be concerned with the first classification, as

it/

it seems to be general and encompasses all types of plasmas, Boumans' classification is more related to analytical technique.

1.3.1 Two Electrode Plasmas

Such plasmas are formed in the column joining the current-carrying electrodes. The d.c., a.c. arc and a.c. spark, classified as non-flame-like plasmas by Sharp (3), and plasma jets (transferred plasmas) are examples of this type. Non-flame-like plasmas are the most widely used excitation sources in spectrochemistry and for a detailed treatment of the subject matter the reader may refer to appropriate texts (4, 5, 6, 7), which also provide a readable account of the historical aspect and a substantial literature.

Plasma jets are in fact gas stabilized arcs and are formed when a flow of partially ionized gas emerges from a small orifice at high velocity. The principle of the plasma jet was described by Gerdien and Lotz (8) in 1922. They inserted an anode into a copper ring cooled by a vortex water stream. The arc burned in the water vapour and the gases emerged from the ring in a high velocity steam plasma jet. This form of the plasma jet received considerable attention in the 1950's by Peters (9), Weiss (10) and Giannini (11); its use for analytical purposes was described in 1959 independently by Margoshes and Scribner (12) and Korolev and Vainshtein (13). It is not within the scope of this thesis to consider such plasmas in detail and for further information reference should be made to (4, 14-16).

1.3.2 Single Electrode Plasmas

These can be divided into, high-frequency single electrode and single-electrode microwave plasmas. High-frequency single electrode plasmas/

plasmas are obtained when a high-frequency oscillation is transferred to a point shaped electrode. A high field strength is produced at the electrode tip and a discharge is formed once the surrounding gas has been ionized by external means. A discharge tube with a central electrode can be used to form microwave plasmas. The electrode is coupled via a waveguide to the microwave oscillator and the plasma is formed at the tip. A review on the history and development of single electrode plasmas has been given by Greenfield (17), other reviews of interest are to be found in references (4, 18).

1.3.3 Electrodeless Plasmas

The description covers electrodeless discharge lamps, electrodeless microwave and inductively coupled plasmas.

Electrodeless discharge lamps (EDLs) consist of a sealed-off bulb containing an inert gas at low pressure and a small sample of the metal or metal salt. Such lamps are operated at radiofrequency or microwave frequency by suitable coils, antennas or waveguides. Winefordner and Browner (19) have critically reviewed the development of EDLs and have demonstrated techniques for the production and operation of lamps.

The free flowing microwave plasma is a low power device, generally (0-200 W), operated in a resonant cavity designed to oscillate at 2450 MHz. An exception was the work of Tsemko et al (20, 21) who used a generator which was capable of supplying more than 2 KW to an argon plasma with tangential flow at atmospheric pressure. Since the thermal temperature of the microwave plasma is relatively low, thermal vaporization of particulate samples is inefficient. However, it is an efficient excitation source that possesses a sufficient number of high/

high energy electrons to excite at even quite energetic levels. Therefore, if possible the sample should be presented to the source in a pre-atomized condition and ready for excitation. Limitations of sampling, and interference effects generally place limitations on the use of the microwave plasma for emission spectrometry. It is, therefore, most suited to dedicated applications, for example as a detector in chromatographic systems, or as a gas analyser or trace-metal analyser for small samples, where its low cost is of importance. Sharp (3) has recently made an excellent review of the analytical development and application of the microwave plasma.

1.4 INDUCTIVELY COUPLED RADIO FREQUENCY PLASMAS (ICP)

1.4.1 Mechanism of Formation, Stabilization and Physical Characteristics of ICP

Plasmas are by definition gases in which a significant fraction of the atoms or molecules are ionized and therefore they readily interact with a magnetic field. One such interaction is inductive coupling to time varying magnetic fields. In order to fully understand the plasma mechanism, consider a quartz tube placed inside a coil which is connected to a high frequency generator (Fig. 1.1). Now, if the radiofrequency field is applied with argon flowing through the quartz tube, nothing happens because argon gas is not a conductor. It is, therefore, necessary to seed the plasma with electrons. The easiest method is to introduce a graphite rod into the plasma. The carbon is quickly heated by radiofrequency induction and produces thermal electrons. The free electrons and ions are accelerated by the high frequency oscillating

magnetic/

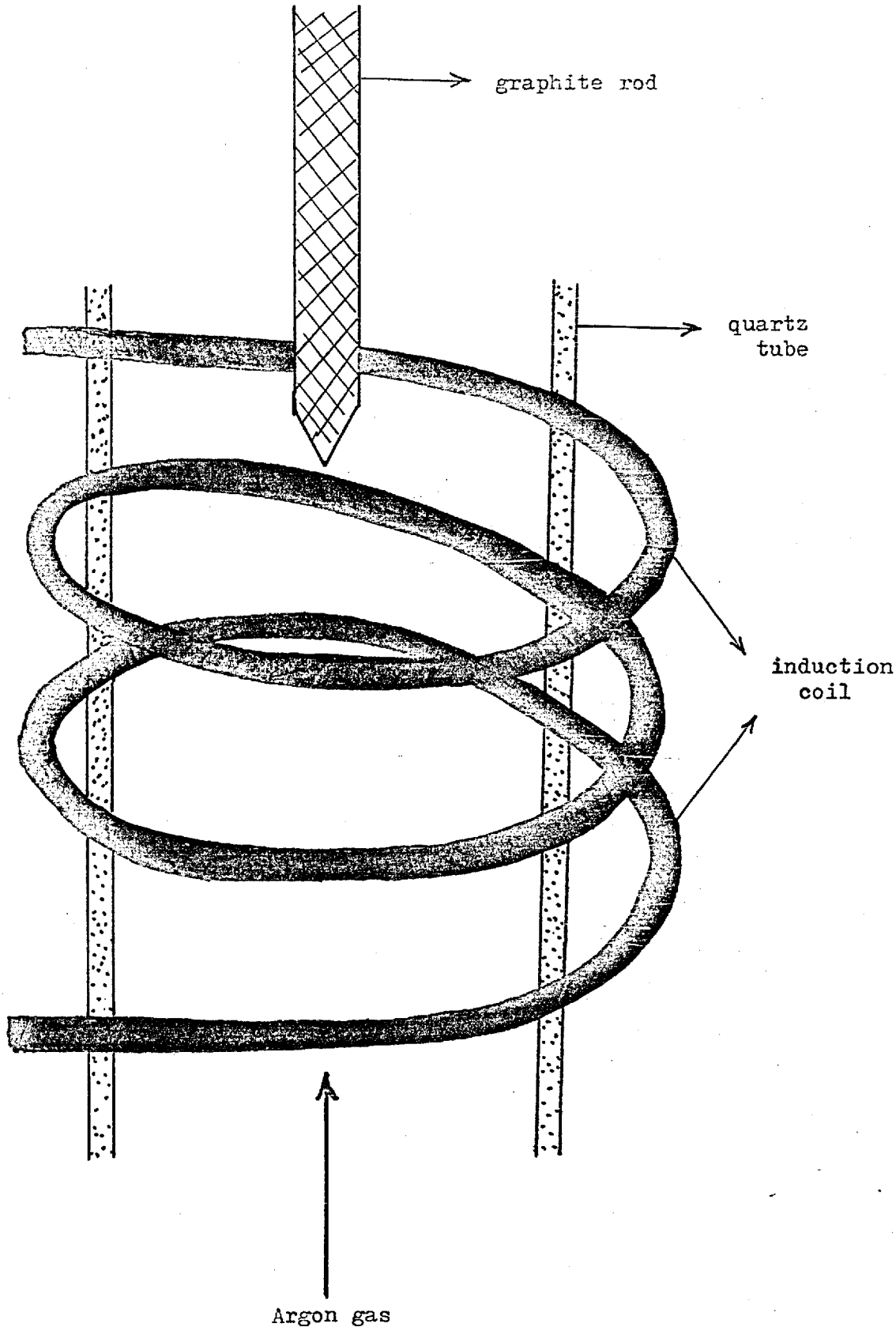


Fig. 1.1. Ignition of the Inductively Coupled Plasma

magnetic field induced in the axial direction. The accelerated electrons or ions meet resistance to their flow and joule or ohmic heating results. This process leads to the almost instantaneous formation of the plasma.

The plasma is thermally very hot and attains a gas temperature of 9000-10000 K (22) in the region of maximum eddy current flow. Thus, the plasma has to be thermally isolated from the tube walls to prevent overheating of the quartz tube. This isolation is accomplished by Reed's vortex stabilization technique (23, 24). As shown in (Fig. 1.2), a high velocity flow of argon is introduced tangentially into the annular gap between two quartz tubes and then streams upward cooling the tube walls and centering the plasma radially in the tube. (Fig. 1.2) also shows the complete assembly of concentric quartz tubes and argon flow patterns necessary for sustaining the plasma after it is formed. The third tube (injection tube) is used to transport the sample to the plasma either as an aerosol, a powder or a thermally generated vapour.

The plasma has the overall appearance of a very intense, brilliant white, nontransparent core and a flame-like tail (25). If the plasma is generated at low frequencies ~5 MHz (26-29), a teardrop shaped plasma as shown in (Fig. 1.3a) is formed. In this form of plasma the sample particles do not experience the high temperature of the plasma center, they follow a path around the plasma.

As shown in (Fig. 1.3b) an increase in the oscillating frequency of the power source to ~30 MHz (30-35) causes the eddy current to flow more closely to the outer or skin portions of the plasma. This results

from/

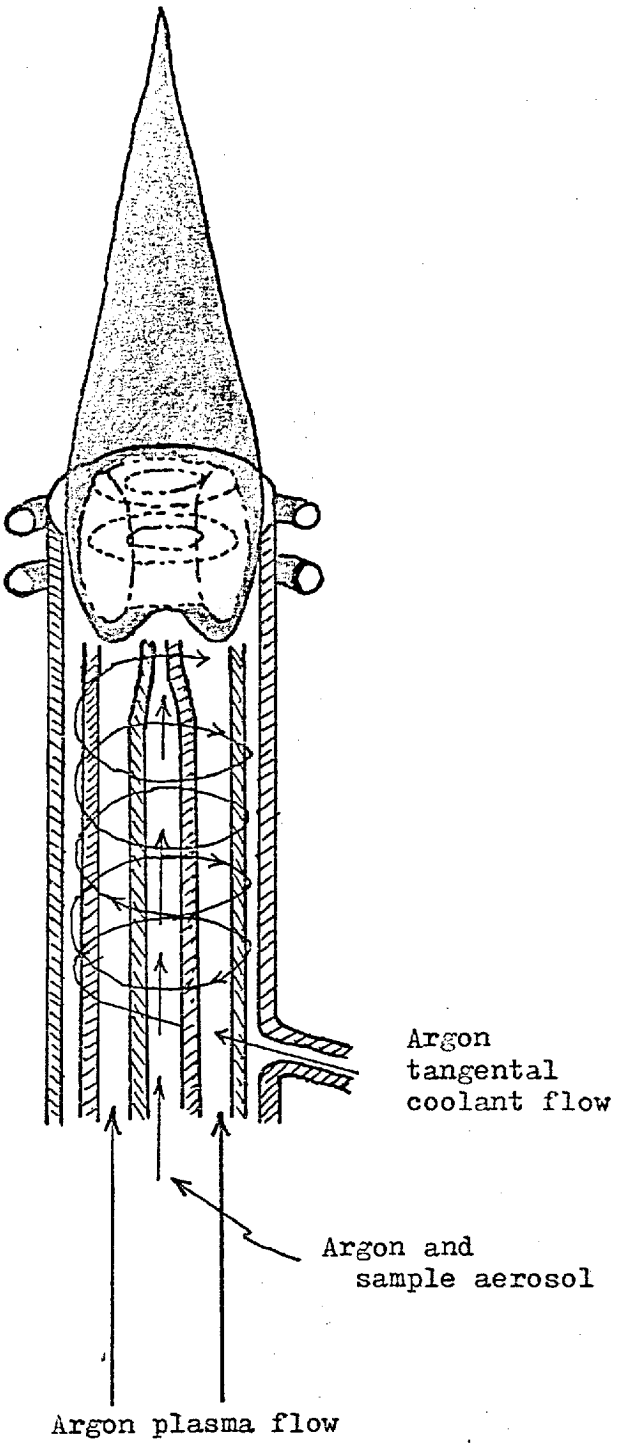


Fig. 1.2. Complete plasma configuration(25)

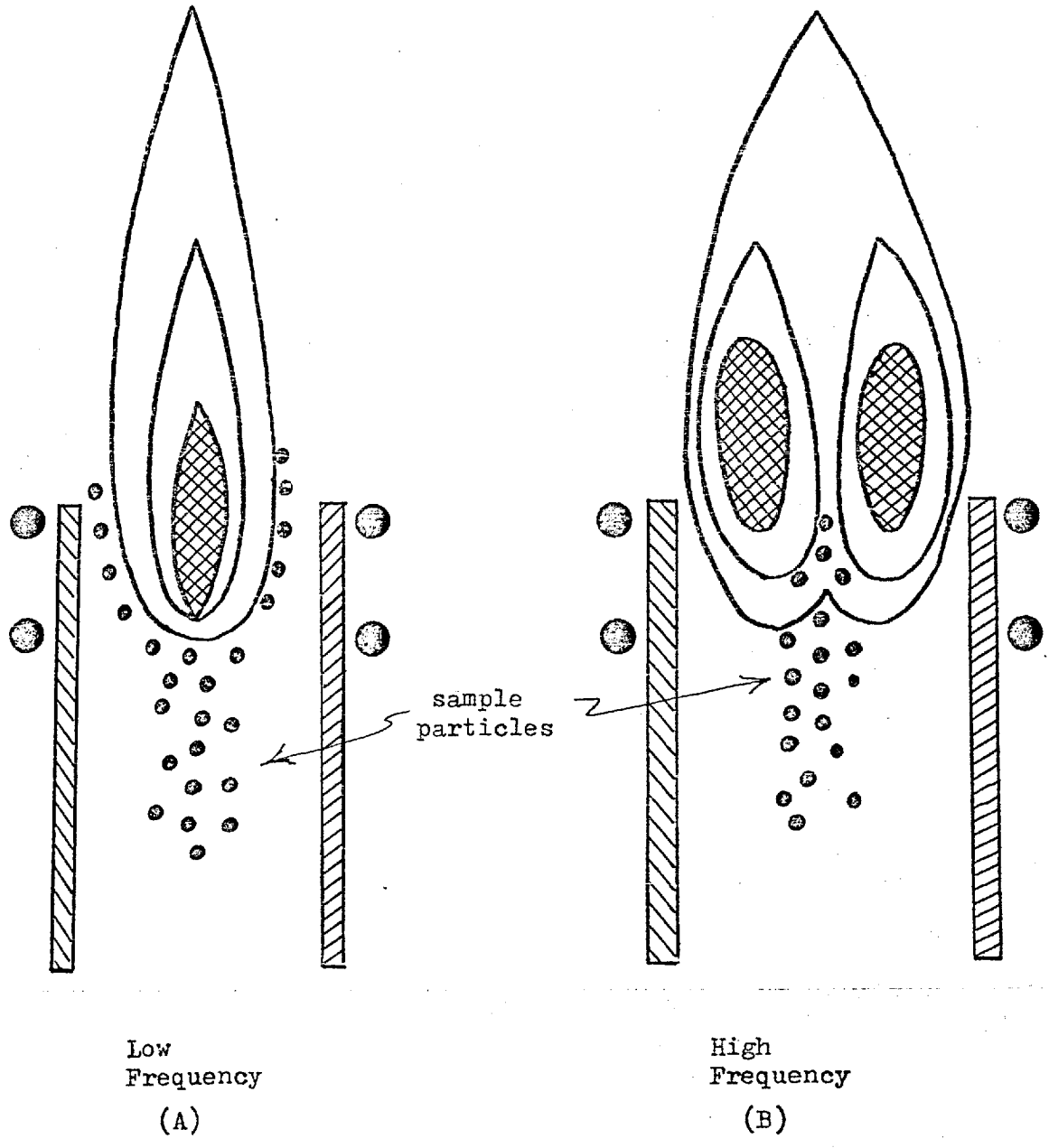


Fig. 1.3. Aerosol path for tear drop and doughnut plasma shape

from the well known skin depth effect (32, 36, 37). The skin depth is defined as the depth at which the eddy current declines to $1/e$ (~37%) of its maximum value near the surface and it is inversely proportional to the square root of the applied frequency. Thus an annular shape or doughnut shaped plasma is formed. The hole in the doughnut is cooler than the doughnut itself and it offers less resistance to the injection of sample material. Axial viewing of the plasma reveals the central channel as a dark region at the centre of the plasma anulus. The sample does not experience the highest temperature of the plasma core, but rather the temperature of the axial channel which still is higher than the sampling temperature that can be achieved with most other sources.

The degree to which the doughnut hole is developed is jointly controlled by the frequency of the current generator and the flow velocity of the carrier gas that injects the sample into the plasma.

1.4.2 Properties of ICP

The desirable analytical properties of ICP are as follows:-

(I) Because of its annular shape the nebulized liquids or finely ground powders can be easily introduced into the excitation region without seriously disturbing the coupling between the plasma and power source.

(II) A high gas temperature, which enables the source to atomise and excite a large number of elements. Also, the continuous temperature gradient from about 10000 K down to room temperature allows greater latitude in selection of the optimum analysis temperature. Furthermore, free atoms may be generated in the hotter zones and then observed in lower temperature regions where the background emission is lower.

(III)/

(III) The relatively long residence time of the sample in the plasma, [the residence time for an analyte particle in the plasma tail-flame is 3.3 ms compared with 77 μs in the flame] (117), makes the high temperature of the gas effective in producing complete sample atomisation even though the thermal conductivity of the gas is low. The additional advantage of the longer residence time is that for samples whose rate of vaporization is low, complete vaporization may be possible during their residence in the plasma.

(IV) Stable spatial and temporal behaviour comparable with flame sources.

(V) An inert atmosphere which reduces chemical interferences, associated with stable compound formation, such as are commonly encountered in flames.

Furthermore, species like , CH, C_2, CO, CN, CO_2, NH, NO etc. which are produced in flames are absent. Thus, the intense background radiation occurring over a considerable proportion of the visible and near U.V. spectrum related to these species and also the quenching effect produced by CO, NO and CN are eliminated.

(VI) the radiating free atoms are conveniently distributed in a narrow channel, therefore, the slit width of the monochromator or the viewing field of spectrophotometer can be readily filled by the resulting emission (25).

(VII) The absence of electrodes eliminates source contamination.

(VIII) The ICP provides ideal conditions for simultaneous multielement (SME) analysis. Even though much effort has been directed towards devising viable flame atomic absorption or atomic fluorescence systems (38, 39) for multielement analysis, the requirement for an auxiliary

primary/

primary source and the limitations imposed by optical configuration pose serious experimental difficulties.

(IX) It operates on non-combustible inert gases which are safe to store.

1.4.3 Sample Introduction Methods

Gases, liquids and solids may all readily be introduced into the plasma channel.

The introduction of gases into the ICP has been fully investigated by Tuilt and Robinson (40-41). They introduced gases into the plasma via the coolant, plasma and injector flows and reported that better detection limits were obtained when gases were introduced through the injector tube. Alder and Mermet (42) studied the introduction of sulphur dioxide, hydrogen sulphide, carbon tetrachloride, chlorine, phosphorus trichloride and sulphur hexafluoride into an inductively coupled radiofrequency plasma. The introduction of gases for subsequent analysis has not attracted much attention and very little work has appeared in the literature.

The introduction of solids into the plasma poses several difficult problems such as obtaining a steady flow without segregation of the powder and ensuring that all the material entering the plasma is volatilised. Even though a considerable amount of work has been carried out in this field a complete solution to all the problems has not been achieved and undoubtedly more work is necessary. Methods of solid sample introduction are the subject of references (3, 43).

The introduction of liquid samples is probably the easiest and most widely used technique. Most work on solutions has been carried out using nebulisers of either the pneumatic or ultrasonic type. In

the/

the plasma, however, the solvent has a quenching effect and this limits the amount of sample that can be introduced. The molecular gases released by the solvent not only cause an impedance mismatch but also absorb energy from the plasma for their excitation and dissociation. Therefore, the energy available for sustaining the ionization equilibrium that maintains the discharge is diminished. This difficulty may be overcome by increasing the radiofrequency generator power or by using an aerosol desolvation system (28, 32, 36)

The introduction of micro-samples into the plasma has also been reported. Greenfield et al (66) have carried out the analysis of fuel oils on 25 µl samples. Fassel et al (93) have described work with 100 µl samples vaporised into the plasma from a tantalum filament.

1.4.4 Literature Review

The development of radiofrequency inductively coupled plasmas has been reviewed in detail by Fassel (18) in 1971 and recently by Greenfield and co-workers (43) and Sharp (3). A brief account will be given here and only the more important papers published will be reviewed. The ICP torch was first described by Reed (23) to whom should be given most of the credit for the development of the technology of these plasmas. Reed's apparatus which was used for growing crystals is shown in (Fig. 1.4). Although Reed recognised that these plasmas offered attractive possibilities for the excitation of spectra, the initial exploitation as atomisation and excitation sources was pioneered independently by Greenfield in England (30, 45, 46) and by Fassel in the U.S.A. (26, 31, 32, 27 , 47). (Fig. 1.5) shows the typical radiofrequency plasma torch configuration which is now in common use. Since the initial work a succession/

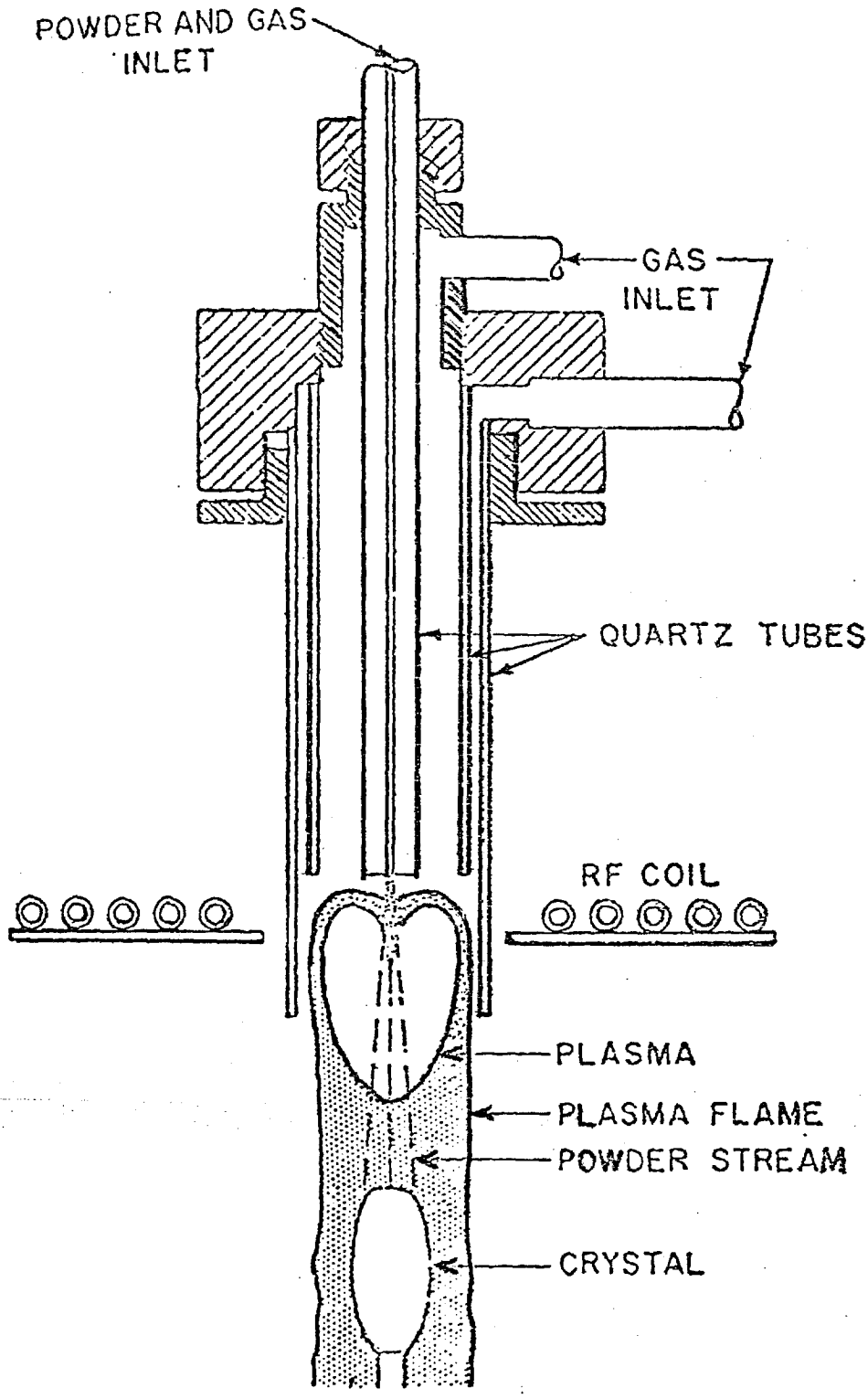


Fig. 1.4. Schematic drawing of Reed's torch used for crystal growth studies

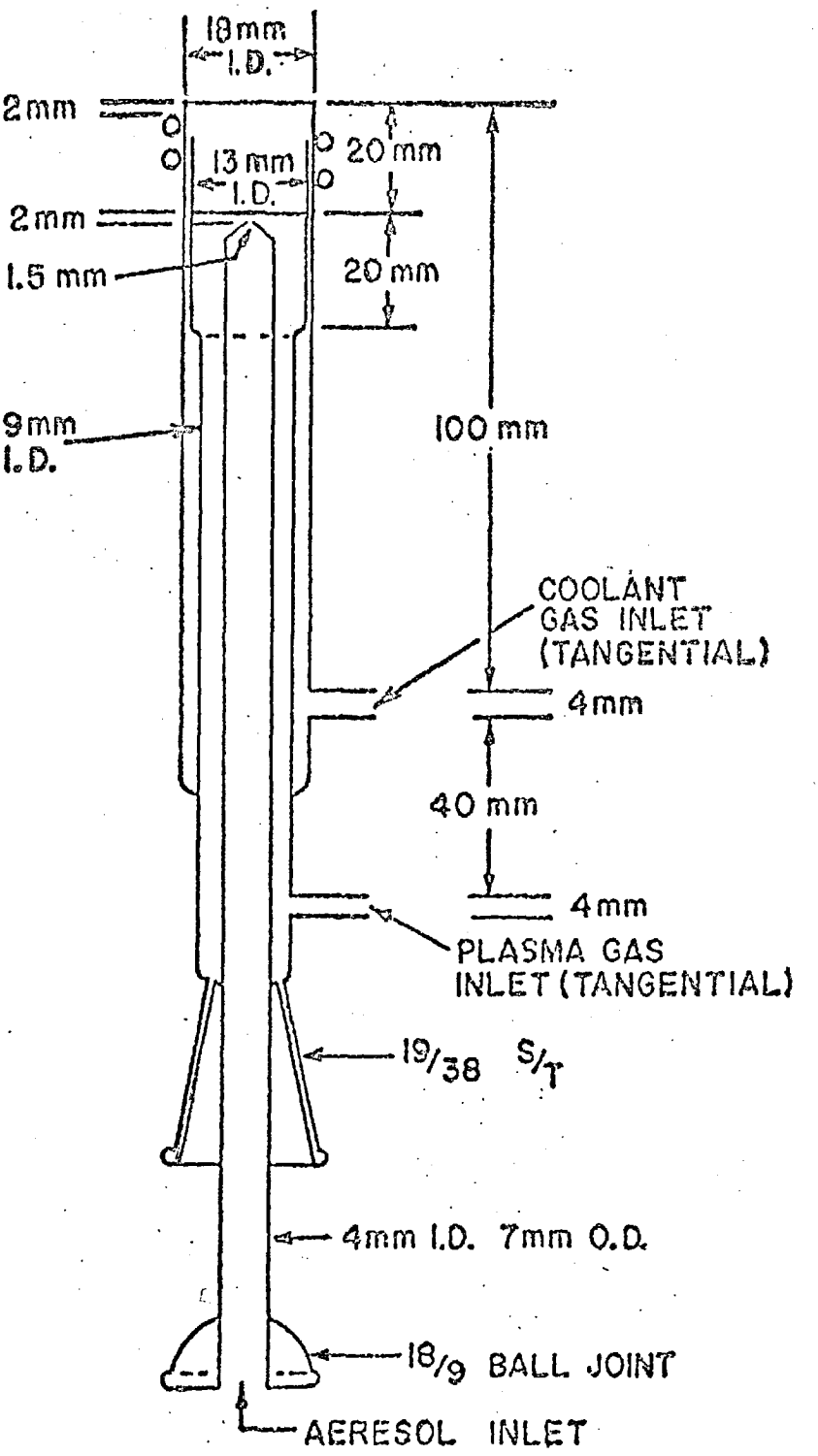


Fig. 1. 5. Typical plasma torch as used by Fassel and associates

succession of authors in various countries have investigated the analytical potential of ICP (28, 33,35, 48—55).

Greenfield et al (30) have used a direct pneumatic nebulizer to inject powders and slurries through an annular plasma and have reported the tail-flame as being intense and the plasma stable. This school of workers (56) have shown that the central hole can be produced as easily in a plasma at 7 MHz as in one at 36 MHz and have shown photographs demonstrating that the two resultant annular plasmas are very similar. These authors are of the opinion that the tunnel effect is more a function of injector gas-flow than skin-depth. This view is supported by Thorpe (57). Greenfield (58) in his invited lecture 'Why Plasma Torch?' has considered some outstanding characteristics of plasmas such as sensitivity in terms of temperature and stability. It has been reported in this paper that nitrogen gives better sensitivity for nearly all elements and better detection limits for high-energy lines than argon as coolant gas.

Fassel's group has in the last two years published several interesting papers on the application of ICPs as excitation sources. They have used three different ICP optical emission spectrometry systems for the determination of residual impurities and alloying constituents in solutions of high and low alloy steels of widely varying composition (59). Further papers have dealt with the simultaneous multielement (SME) determination of 15 different wear metals in lubricating oils (60) and the application of ICPs as atomisation cells for atomic fluorescence spectroscopy (61). Fassel and Larson (62) have made a comparison of the interelement effects in a microwave single electrode plasma (SEP) and/

and the ICP. They found severe interference effects from easily ionizable elements in the SEP whereas only small effects were observed in the ICP. Similar results were obtained when the effect of concomitants on MO emission and the effect of Al and PO_4^{3-} on Ca emission were studied.

Boumans and de Boer (36, 63, 64) in three related papers have studied the potential of the plasma torch for SME. They have compared flame sources with plasmas and have concluded that the experimental parameters of the ICP can be chosen so that there exists excellent condition for SME. They have also concluded that even though interference effects do occur in the ICP, the operational parameters can be chosen so that the interference effects are eliminated or are small. In another paper (65) these authors have made a comparative assessment of four important spectroscopic analytical methods, the results of which are summarized in (Fig. 1.6). It was concluded that the ICP is an outstanding source not only for accurate routine determination of a few elements, say four to ten, as is commonly required in a large variety of materials, but also for the general analysis of solutions. Boumans and de Boer (2) have also made a comparative investigation of some analytical performance characteristics of the ICP and a capacitively-coupled microwave plasma. Their work demonstrated the overall superiority of the ICP to the capacitively-coupled microwave plasma. This superiority manifested itself in better overall detection power, far smaller matrix effects, better reproducibility and the possibility of defining for the ICP compromise parameter values suitable for SME analysis on a wide range of samples.

Human/

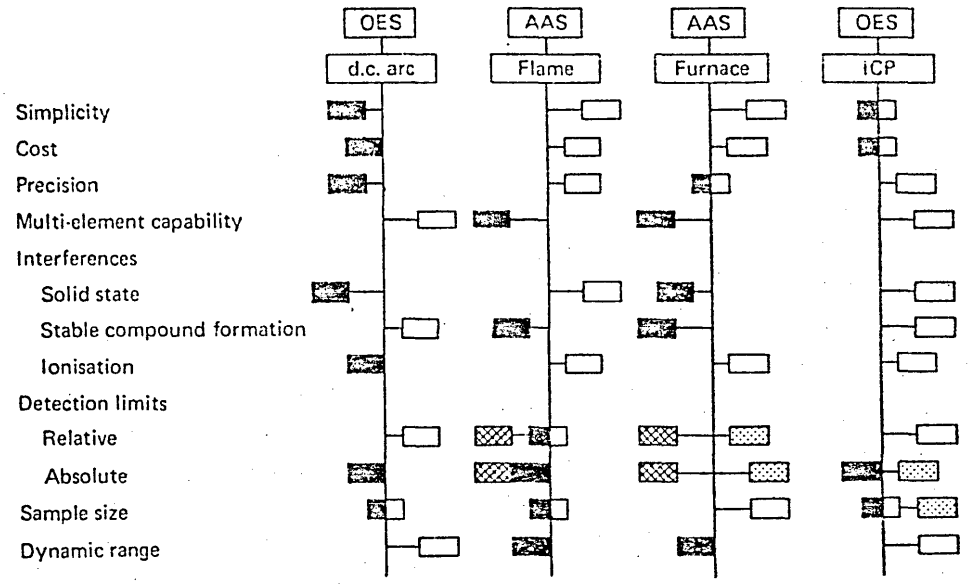


Fig. 1.6. Comparative assessment of d.c. arc optical emission spectrometry (d.c. arc OES), flame atomic absorption spectrometry (flame AAS), furnace atomic absorption spectrometry (furnace AAS) and inductively coupled high frequency plasma optical emission spectrometry (ICP OES). (ICP OES) (65).

The characteristics upon which an appraisal is based are listed in the left hand column of Fig. 1.6. Appraisals of the separate items are expressed by the position and shading of blocks for each method and characteristic. A white block indicates a positive and a black one a negative judgement. The further a block is displaced to the right from the vertical axis the more positive the characteristic is judged to be. For further detail see reference 65.

Human and co-workers (113) have used a conventional high-voltage spark for sampling and nebulizing material from solid conducting samples. The sample was connected to the negative terminal of the source, and gas fed through the spark chamber transported the metal particles into an ICP for analysis. This method removes the requirement for pretreatment of the sample.

Recently, reports concerning the application of ICP spectrometers in analytical laboratories for routine analysis have been published. Jones (114) has used a direct reading spectrometer-inductively coupled plasma emission system for the analysis of 16 elements in soil extracts and plant tissue. The instrument has been found to be capable of determining the elemental content at a very rapid rate and at sensitivity levels equal to or better than that obtained using the atomic absorption technique. Alder and co-workers (115) have applied an inductively coupled argon plasma source to the determination of the exchangeable ammonium-nitrogen content of soil samples. The ammonium ion was oxidised with sodium hypobromite in alkaline medium, the evalved nitrogen was passed into the argon plasma and the NH emission intensity produced in the plasma was monitored.

The growth in the literature pertaining to ICP sources has been so considerable in the last few years that it is beyond the scope of this review to give a comprehensive literature survey. The reader's attention is directed, however, to the plasma section of Annual Reports on Analytical Atomic Spectroscopy (116). This reviews work published during 1976 on fundamental studies, instrumentation, interference effects and applications. Also of note is the ICP Newsletter, edited by Barnes (Dept of Chemistry, University of Massachusetts, U.S.A.), which contains much valuable material/

material and includes correspondence, abstracts, reports of meetings and original papers.

CHAPTER II

THEORY OF EMISSION SPECTROMETRY AS PERTAINING TO R.F. PLASMA SOURCES

2.1 INTRODUCTION, CONVENTION AND NOTATION

The general theoretical basis of the emission technique has been well covered although only one review, that of Sharp (3), has specifically discussed the theory in relation to plasma sources. In this chapter the most important aspects of the theory which are relevant to plasma sources will be discussed. The most useful text books concerned with the fundamentals of emission spectroscopy are as follows: Theory of Spectrochemical Excitation (6), Resonance Radiation and Excited Atoms (110), Comprehensive Analytical Chemistry (5) and Analytical Emission Spectroscopy (4).

The electrons in an atom are distributed in discrete energy levels. The energy of an electron in each level can be described in terms of its quantum numbers. These are:

I The principal quantum number, n, which designates the main energy level of the electron and may have integral values of 1, 2, 3, ... n.

II The orbital quantum number, l , which designates the energy sublevel within the main energy level and may take values from zero to n-1.

III The magnetic quantum number, m, which designates the particular orbital within the energy sublevel. This is significant if the excited atom is exposed to an electrical or magnetic field and can have any integral value from +l through -l including zero.

IV The spin quantum number, s, which describes the two ways in which an electron may be aligned with a magnetic field and has only two values $+\frac{1}{2}$, or $-\frac{1}{2}$.

The total angular momentum of an electron is the resultant of the angular momentum vector and the electron spin angular momentum vector which/

which is described by a new quantum number j. For atoms with one valence electron $j = l + s = l \pm \frac{1}{2}$. There are $(2j + 1)$ possible orientations of j in respect to an applied magnetic field, each orientation being associated with a slightly different energy change. The term $2j + 1$ is known as statistical weight (symbol g) for a particular state.

2.2 SPECTRAL LINE INTENSITY

According to quantum mechanics spectral lines, which are characterised by their frequency ν, originate from transitions between energy levels of atoms or ions. An atom emits radiation when an electron falls from a higher state (q) of energy E_q to a lower state (p) of energy E_p. The radiative transition from excited state to lower state occurs spontaneously. The frequency is related to the energy difference between the two states by the Bohr frequency rule

$$h\nu_{qp} = E_q - E_p \qquad (2.1)$$

where h is Planck's constant. When the lower state is the ground state the emitted spectral line is known as resonance line. The process was described by Einstein (1917) in terms of transition probability A_{qp}, which is the probability per second that an atom in state q will spontaneously radiate its energy and return to a lower state. According to Einstein the spontaneous emission of atoms in a given state of excitation is governed by a law similar to that of radioactive disintegration. If n_q is the number of atoms in the excited level q at a given time the following equation governs $q \rightarrow p$ transition

$$-\frac{dn_q}{dt} = A_{qp}\, n_q \qquad (2.2)$$

This/

This equation is equivalent to saying that the number of atoms leaving the state q per second by spontaneous emission is proportional to the number of n_q present in that state.

If n_q is assumed to be the number of excited atoms per unit volume of a uniform source then the number of photons having a frequency of ν_{qp} emitted per second in all directions from the unit volume will be $A_{qp}\, n_q$. Therefore, the power radiated in all directions is $A_{qp}\, n_q\, h\, \nu_{qp}$. Detection systems are not generally capable of measuring the total power emitted, but they accept radiation emitted into a given solid angle. Dividing the total power by 4π results in the spectral emittance per unit volume per unit solid angle which is known as the brightness or radiance of the source (B)

$$B = \frac{1}{4\pi} A_{qp}\, n_q\, h\, \nu_{qp} \qquad (2.3)$$

Throughout this work the absolute intensity will be identified with the concept of radiance, therefore,

$$I \equiv B \qquad (2.4)$$

2.3 EXCITATION AND BOLTZMAN^{N} DISTRIBUTION LAW

In a state of complete thermodynamic equilibrium, the population of energy levels for each kind of particle follows a Boltzman^{n} distribution, i.e.

$$\frac{n_q}{n_o} = \frac{g_q}{g_o} \exp\left(-E_q/kT\right) \qquad (2.5)$$

where n_o is the concentration of the particles in the ground state, k is the Boltzman^{n} constant, T is the absolute temperature, and g_q and g_o are the statistical weights of the excited and ground state.

The equation 2.5 is extremely useful and is widely used in calculations involving/

involving relative intensities. However, the concentration of the ground state atoms does not remain constant when the temperature increases. It is often convenient, therefore, if the population of any one level can be expressed in terms of the total number N, of particles present. If the Boltzmann distribution expression is written for each state we obtain:

$$\begin{aligned} n_o &= g_o \exp(-E_o/kT) \\ n_1 &= g_1 \exp(-E_1/kT) \\ n_2 &= g_2 \exp(-E_2/kT) \\ &\vdots \\ n_J &= g_J \exp(-E_m/kT) \end{aligned} \qquad (2.6)$$

Then, summing the equations 2.6 we have:

$$\sum_{o}^{J} n_m = N = \sum_{o}^{J} g_m \exp(-E_m/kT) \qquad (2.7)$$

where J is the highest state to be considered. Hence, equation 2.5 can be written:

$$\frac{n_q}{N} = \frac{g_q \exp(-E_q/kT)}{\sum_{m=o}^{m=J} g_m \exp(-E_m/kT)} \qquad (2.8)$$

The quantity in the denominator on the right-hand side of 2.8 is known as the partition function which expresses the population of states as a function of temperature.

$$Z = \sum_{o}^{J} g_m \exp(-E_m/kT) \qquad (2.9)$$

From equation 2.8 n_q can be calculated,

$$n_q = N \frac{g_q}{Z} \exp(-E_q/kT) \qquad (2.10)$$

substituting n_q into equation 2.3 yields

I/

$$I = B = \frac{1}{4\pi} \; h \nu_{qp} \; A_{qp} \; N \frac{g_q \exp(-E_q/kT)}{Z} \qquad (2.11)$$

Equation 2.11 is correct for the ideal model but is only an approximation for all real plasma sources.

2.4 THE CONCEPT OF TEMPERATURE AND THERMODYNAMIC EQUILIBRIUM

The temperature of a plasma is the most vital parameter which controls its characteristics. The conditions of a plasma are determined by different temperatures each of which describes a distinct aspect of the physical state of the system. The term can only have significant meaning when related to a defined equilibrium. A monatomic gas may be characterised by four temperatures:

(a) The electron temperature, which governs the distribution of the kinetic energy of the electrons.

(b) The gas temperature, which governs the distribution of the kinetic energy of the neutral atoms.

(c) The excitation temperature, which governs the populations of the atoms in different states of excitation.

(d) The ionisation temperature, which governs ionisation equilibria.

In summary, in an atomic gas, translation, excitation and ionisation temperatures are recognized. In molecular gases, however, temperatures are also assigned to the dissociation equilibria and the population of vibrational and rotational levels. If all definitions of temperature yield the same numerical values the system is said to be in thermodynamic or thermal equilibrium. This state is characterized by the following conditions:

(a) the velocity distribution of all particles (atoms, molecules, electrons/

electrons and ions) in all energy states is Maxwellian,

(b) the ionisation equilibrium is defined by the Saha equation,

(c) the relative population of states for each kind of particle conforms to Boltzmann's Law,

(d) the chemical dissocation equilibrium is defined by the Law of Mass Action,

(e) the radiation density is given by Planks' Law,

(f) the principle of detailed balancing applies strictly, so that every process of energy transfer is perfectly balanced by the reverse process, thus excitation collisions by atoms, electrons or molecules are exactly balanced by quenching collisions with the same species, and the absorption of radiation quanta is exactly balanced by spontaneous and stimulated emission.

Thermodynamic equilibrium is an idealized state which can not be observed because practical sources suffer energy losses (by conduction, convection and radiation), and these are not balanced by the surroundings. If, however, the temperature change along a mean free path, within a localised volume element, is small compared with the mean temperature of that element the equilibrium is only slightly effected. Thus, it is common to refer to "local thermal equilibrium" LTE existing in defined regions of the source.

2.5 TEMPERATURE MEASUREMENT

The most frequently used method for the determination of the temperature of a plasma is by the measurement of the intensity ratios of two or more spectroscopic lines emitted by atoms of the same element.

If/

If the transition probabilities are known the temperature can be calculated from the Boltzmann equation. Unfortunately the transition probabilities are not accurately known for all species, therefore most temperature measurements are subject to error. It should be noted here that recently Kornblum and De Galan (111) have proposed a novel method for measuring excitation temperatures that does not require a knowledge of transition probabilities.

Physical studies of plasmas usually involve determination of the radial temperature distribution. Lateral scanning of the plasma does not produce this directly. A proper temperature profile can be reconstructed from the inversion of a measured lateral intensity distribution into a radial distribution. This is commonly called an Abel inversion. (See P.135 of Theory of Spectrochemical Excitation (6).)

2.6 IONISATION AND THE SAHA EQUATION

A necessary condition for the existence of a plasma is the partial ionisation of the gas mixture in the discharge. In a thermal plasma, all charged particles originate from thermal ionisation of the gas, therefore the concentrations of electrons and ions are uniquely related to the gas temperature and to the gas composition. Saha's treatment of thermal ionisation is based essentially on the application of the Law of Mass Action. For each component of a composite gas an equilibrium of the following form can be considered.

$$\text{neutral atom} \rightleftharpoons \text{ion} + \text{electron} \qquad (2.12)$$

By applying the Nernst heat theorem, the equilibrium constant can be calculated as a function of the temperature, which is known as Saha equation/

equation

$$K_n = S\ (T) = \frac{n_i\ n_e}{n_a} \qquad (2.13)$$

where n_i, n_e and n_a are the concentration of ions, electrons and atoms respectively and $S(T)$ the Saha ionization constant.

In the study of ionization equilibria it is convenient to introduce the concept of degree of ionization and relate it to the Saha ionization constant. The degree of ionization α in a gas is:

$$\alpha = \frac{n_i}{n_a + n_i} \qquad (2.14)$$

Using the degree of ionization, n_a and n_i can be expressed in terms of the total concentration n where

$$n = n_a + n_i \qquad (2.15)$$

$$n_i = \alpha n \qquad (2.16)$$

and

$$n_a = (1 - \alpha)n \qquad (2.17)$$

Substituting into equation 2.13

$$S(T) = \frac{\alpha n\ n_e}{n(1 - \alpha)} \qquad (2.18)$$

Therefore

$$\alpha = \frac{S(T)}{n_e + S(T)} \qquad (2.19)$$

The equation shows that α depends both on temperature and electron concentration. The full Saha equation governing the ionization equilibrium is

$$S(T) = \frac{n_i\ n_e}{n_a} = \frac{(2\pi\ m_e\ kT)^{3/2}}{h^3}\ \frac{2\ Z_i}{Z_a} \exp\ (-\ E_i/kT) \qquad (2.20)$$

where m_e is the electronic mass, k is the Boltzman constant, h Plank's constant/

constant, Z the partition function and E_i the ionization energy.

The electron concentration n_e in equation 2.20 depends on temperature, therefore in an arc plasma exhibiting thermal equilibrium, the electron concentration is approximately equal to that of the positive ions. As a metal of low ionization potential is evaporated, the ion concentration in the plasma, and the conductivity increase. This, in turn, causes a decrease in the electric field strength and, according to the equation $W = E\,I$, dissipation of power in the plasma will be reduced. The decrease in energy released per unit time will obviously result in a decrease in temperature, and hence ionization and conductivity will again be reduced. Therefore, by means of these processes the ion and electron concentrations are self-regulating in the plasma. Because of the self-regulating character of the system, the changes in the composition of the plasma have a considerable effect on the plasma temperature and thus on spectral line intensity. In contrast, in high temperature plasmas, the major components of the plasma are ionized to such a degree that the electron pressure becomes of the order of the total gas pressure, therefore the precise value of the temperature in the discharge depends much less on the presence of added metal vapour. Summarizing, it can be said that one of the fundamental parameters of the plasma processes is the electron concentration. Electron concentration is generally determined by application of the Saha equation; details may be found in Grove's book (4).

2.7 DISSOCIATION EQUILIBRIA

In the preceding sections, it has been assumed that all chemical species/

species are present in the form of free atoms or ions. In general this condition does not exist. Chemical reactions occurring in the plasma may considerably influence the concentration of free metal atoms. For a chemical equilibrium in the general form of

$$xy \rightleftharpoons x + y \qquad (2.21)$$

the following relationship holds:

$$K_n = \frac{n_x\, n_y}{n_{xy}} = \left(\frac{2\pi}{h^2}\,\frac{M_x\, M_y}{M_{xy}}\right)^{3/2} \frac{Z_x\, Z_y}{Z_{xy}} \exp\,(E_d/kT) \qquad (2.22)$$

where K_n is the dissociation constant, M the molecular weight and E_d the dissociation energy.

In spectrochemical excitation sources the incomplete dissociation of molecular species or the association of atoms of one kind with those of another to form a molecule or radical, results in a reduction of the concentration of the free atoms. When this happens they can not emit their characteristic radiations, therefore dissociation equilibria play an important role in the excitation process. It should be noted that at the temperatures prevailing in ICPs, the energy acquired by the molecules is generally sufficient to dissociate them. For the carbon arc in air at atmospheric pressure, oxide formation must be taken into account for diatomic oxides. One of the reasons for this is that several metal oxides possess relatively high dissociation energies and that as the oxygen molecule has a relatively low dissociation energy, there is considerable concentration of oxygen atoms in the plasma.

2.8 SELF-ABSORPTION

Radiation generated by atoms in the interior of a source is subject to/

to absorption by atoms of the same kind, during its passage to the outside. This phenomenon is called self-absorption, it decreases the relative intensity of the source, so destroying the proportionality between the intensity of radiation and atomic concentration, and also causes an apparent broadening of the spectral line. An understanding of the theory of self-absorption requires acquaintance with some classical concepts (absorption coefficient, total absorption factor, the Einstein transition probability, etc.).

If a homogeneous cloud of atoms of depth L, absorbing radiation from a continuum source I_o, is considered, the absorption coefficient k_ν at a discrete frequency ν is defined by the equation

$$I_\nu = I_o \, e^{-k_\nu L} \qquad (2.23)$$

the absorbed power is therefore

$$\Delta I_\nu = I_o - I_\nu = I_o \, [1-\exp(-k_\nu L)] \qquad (2.24)$$

The ratio of the absorbed power to the incident power is generally known as the absorptivity and is given the symbol A_ν, thus

$$A_\nu = 1 - \exp(-k_\nu L) \qquad (2.25)$$

If I_o equals the intensity of a black body I_B having the same temperature as the vapour, according to Kirchhoff's Law, the emitted power I is equal to absorbed power

$$I_{\nu_E} = I_B \, [1-\exp(-k_\nu L)] = I_B \, A_\nu \qquad (2.26)$$

Obtaining I_B from Plank's Law and recognizing that A_ν varies across the spectral profiles, the spectral intensity of the line at the frequency ν becomes:

$$I_{\nu_E} = A_\nu \, \frac{2h\nu^3}{c^2} \, \exp\,(-E_q/kT) \qquad (2.27)$$

where/

where c is velocity of light. The radiated photons are not monochromatic, but are spread over a range of frequencies distributed about the central frequency ν_o. Therefore, the spectral profile of a line is usually expressed in the form of a normalized integral.

Integrating equation 2.27:

$$I = \int_o^\infty [1-\exp(-k_\nu L)]\, d\nu \; \frac{2h\nu^3}{c^2} \; \exp(-E_q/kT) \qquad (2.28)$$

The quantity $A_T = \int_o^\infty [1-\exp(-k_\nu L)]\, d\nu$ is known as the total absorption factor.

Evaluation of A_T

(a) Small $k_\nu L$

When k_ν is small [i.e. N (the total number of atoms) is not large] and the source depth, L, is not too great, the equation giving A_T may be simplified to

$$A_T = \int_o^\infty k_\nu L\, d\nu = L \int_o^\infty k_\nu\, d\nu \qquad (2.29)$$

$(1-e^{-x}) \longrightarrow x$ as $x \longrightarrow o$

From the Einstein theory of radiation and Milne's treatment [P.95 of Resonance and Excited Atoms (110)] it can be shown that

$$K = \int_o^\infty k_\nu\, d\nu = \frac{\lambda_o^2\, g_q\, N\, A_{qp}}{8\pi\, g_p} \qquad (2.30)$$

This equation is important since it shows that K may be represented by a simple, linear relationship with N and that this relationship is quite independent of whatever physical processes are responsible for the formation of the absorption line. Substituting the value of integrated absorption coefficient in equation 2.28 yields

$$I = \frac{\lambda_o^2\, g_q\, N\, A_{qp}}{8\pi\, g_p} \; \frac{2h\nu^3 L}{c^2} \; \exp(-E_q/kT) \qquad (2.31)$$

since/

since $\lambda = c/\nu$

$$I = \frac{h\nu_o N g_q L A_{qp}}{4\pi g_p} \exp(-E_q/kT) \qquad (2.32)$$

Under these conditions self-absorption is minimal and the analytical growth curve of log I versus log N is a straight line with a slope of unity. The integrated area A_T grows linearly with N, but the spectral half-width remains approximately constant

(b) Large $k_\nu L$

When optical density becomes sufficiently large, i.e. at high atomic concentrations or when extended sources are encountered, the approximation made previously no longer holds, and for a line having a mixed Doppler-Lorentz profile, i.e. a Voigt profile (3) it can be shown that

$$A_T = \left\{ \frac{\lambda_o^2 g_q NL a A_{qp} \Delta\nu_D}{4\pi g_p (Ln\ 2)^{\frac{1}{2}}} \right\}^{\frac{1}{2}} \qquad (2.33)$$

where $\Delta\nu_D$ is the Doppler half width

and $a = (Ln2)^{\frac{1}{2}} \Delta\nu_L/\Delta\nu_D$

where $\Delta\nu_L$ is the Lorentz half-width

Hence equation 2.28 becomes:

$$I = \frac{h\nu_o^2}{c} \left\{ \frac{g_q NL a A_{qp} \Delta\nu D}{g_p \pi (Ln2)^{\frac{1}{2}}} \right\}^{\frac{1}{2}} \exp(-E_q/kT) \qquad (2.34)$$

Equation 2.34 shows that, at high optical density, because of self-absorption the relationship between intensity and atomic concentration is no longer linear and there is a square-root relationship between them. Under these conditions, the radiation at the line centre is equivalent to that from a black body at the same temperature, being independent of atomic concentration/

concentration. Further emission can only occur in the line wings, where the absorption is weaker, hence an apparent broadening of the lines occurs. In special cases, an intensity minimum appears which is termed self-reversal of the line. The product of the total number of atoms and the optical length and also the temperature gradient determine the degree of self-reversal. Self-reversal is discussed in greater detail in reference 3.

CHAPTER III

INSTRUMENTATION

3.1 THE PLASMA GENERATOR

Most of the generators that have been used to produce radio-frequency plasmas utilize free running oscillators (30, 35, 36, 48, 56, 67, 68). In these oscillators the power leads and the plasma are part of the resonant circuit. The frequency of the oscillator is fixed by the values of the components in the circuit and, therefore, changes in the plasma impedance, due to sample loading for example, affect the frequency of operation. However, with the doughnut plasma, the sample is heated indirectly and therefore the electrical characteristics of the plasma are not radically changed by the presence of the sample. Hence, effects of sample loading are minimal, this is particularly true with high power generators.

Modern developments of the free running valve oscillator overcome the problem of frequency variation by loosely coupling the plasma to the oscillator circuit. Efficient power transfer to the load is ensured by matching source and load impedances.

Recently a new type of radiofrequency generator which consists of a crystal controlled oscillator and an air-cooled power amplifier has become available (37). These generators provide fixed frequency output and are bench-top size. Efficient impedance matching of the generator, cable combination to the plasma is accomplished with variable capacitors which on some units are tuned automatically.

One of the most important factors in choosing radiofrequency generator is its power. Most workers have used generators of between 2-5 KW. Boumans and de Boer (36) and Fassel et al (37) have shown a trend towards low powered (1-2 KW) generators. Reduction in power entails/

entails a reduction in the size and price of the equipment and also results in lower operating costs. Greenfield et al (56) have worked with a large (15 KW) generator and they cite numerous advantages such as greater sensitivity, improvements in precision, and elimination of the band spectra and chemical interferences. They have also demonstrated that the high power enables diatomic gases to be used with more freedom in the torch, furthermore the torch is not easily extinguished when high material loads, such as powders, are put through.

During the course of this study a Radyne SC15 generator (Radyne Ltd., Wokingham, Berkshire) was used. The oscillator valve produced a radio-frequency of 36 MHz and the power output was adjustable to a maximum nominal value of 2.5 KW via a variable capacitor. Due to the fact that generator was some 12 years old and had been modified by previous workers, the maximum output power was 1.5 KW at a frequency of 32 MHz.

3.2 THE WORK COIL

In the standard commercial Radyne plasma generator the work coils consist of $2.\frac{1}{2}$ turns of 6.3 mm outside diameter cylindrical copper tubing. The coil diameter is 32 mm inside and 44.5 mm outside. The overall height of the coil is 22 mm and the separation between turns of the coil is 1.5 mm. The work coil is connected to two flexible copper tubes, made from copper braids (armoured hoses), which supply cooling water and power to the coil via BSP fittings. This also allows the coil to be moved within the torch compartment.

3.3 THE PLASMA TORCH

The/

The design of torch was similar to that used by other workers (73, 74) Figure 3.1. It consisted of a two part brass body with appropriate O-ring seals to prevent gas leakage, two lengths of straight quartz tube and an injector tube. The brass body accommodated two gas inlets for the plasma and coolant gas flows. The coolant gas was tangentially fed into the upper torch body while plasma gas flowed into the lower torch body in the same manner (see Figure 3.2). Tangential gas flows produce vortex stabilization of the plasma and result in longer life of the quartz tubes. The base of the torch was designed to accommodate an axial B14 cone to accept the injector tube.

The quartz tubes were of 25 mm id, 28 mm od and 22 mm id, 24 mm od for the coolant and plasma tubes respectively. The outer tube was 100 mm long and extended 35 mm above the top of the inner tube. The work coil was positioned concentrically with the torch so that the base of the coil was 3 mm above the top of the inner tube and the top of the coil was 10 mm below the top of the outer tube. The sample injector tube, 11 mm id, 9 mm od, constricted to 4 mm at the tip, was placed in the center of the plasma tube terminating at the top of the inner tube.

Recently further work has been reported on the development of plasma torches. Lichte and Koirtyohann (118) have described a demountable torch in which the quartz tubes were set in epoxy resin which yielded stability similar to that obtained with silica one-piece torches and had the additional advantage of being easily constructed and repaired. Ohls and Krefta(119) have designed an adjustable torch which allowed optimum positioning of the three silica tubes with respect to each other. Allemand and Barnes(120) have discussed the electrical parameters affecting the/

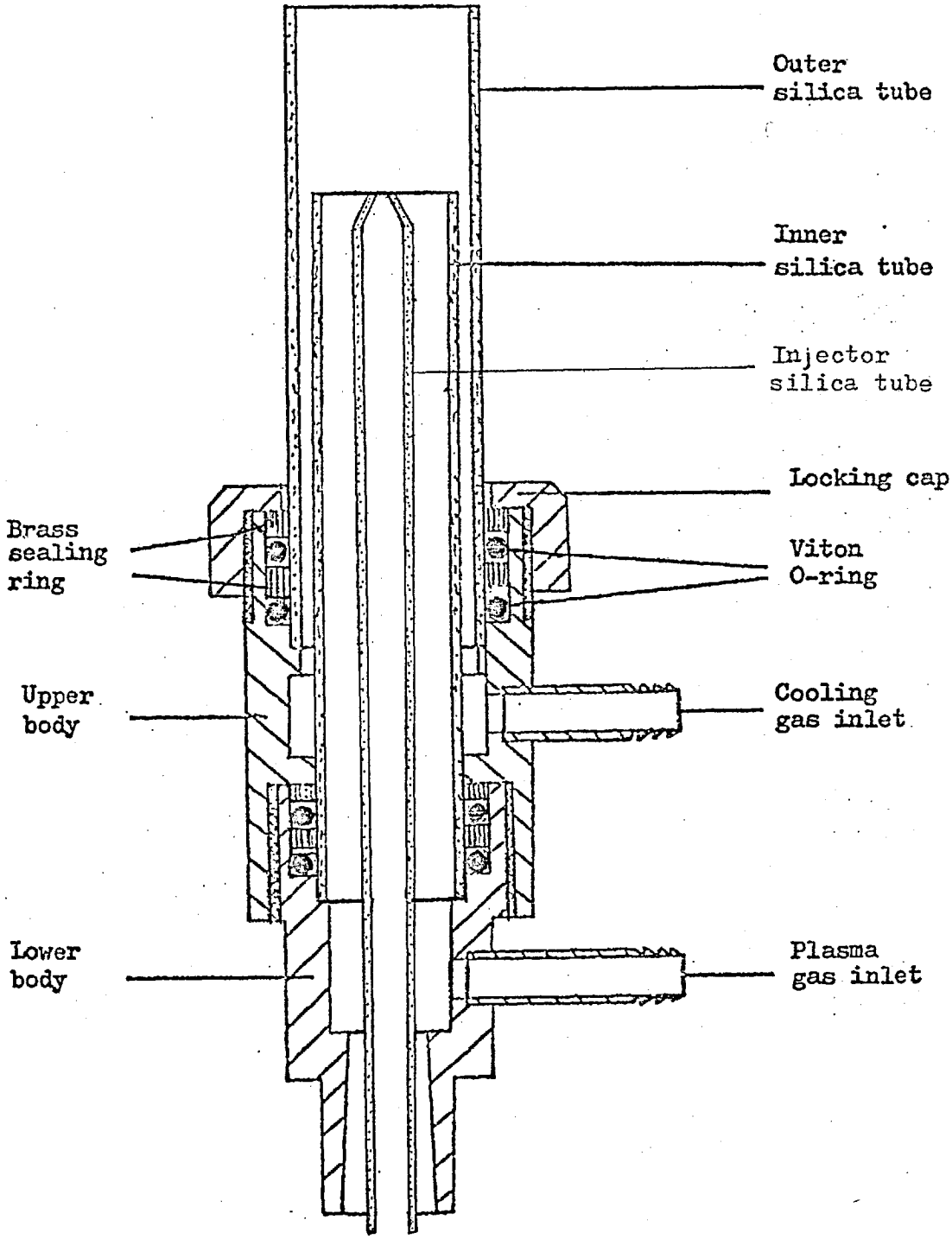
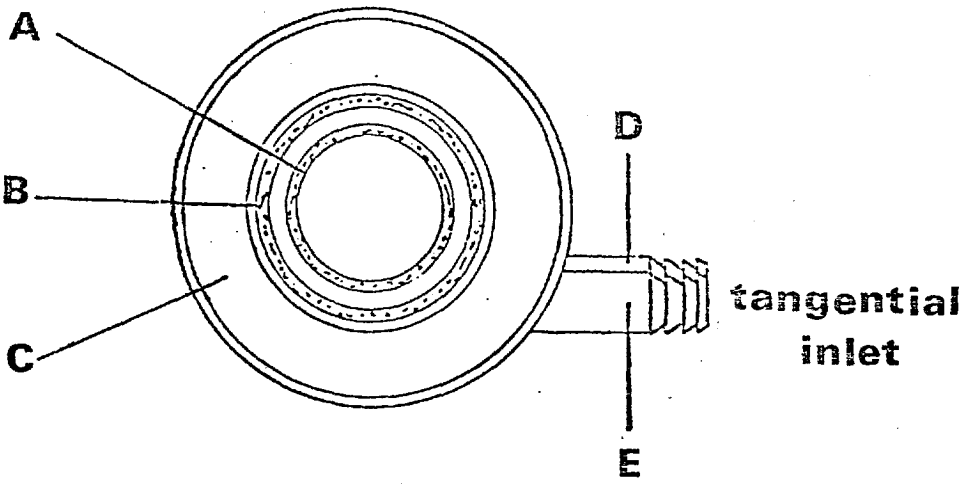
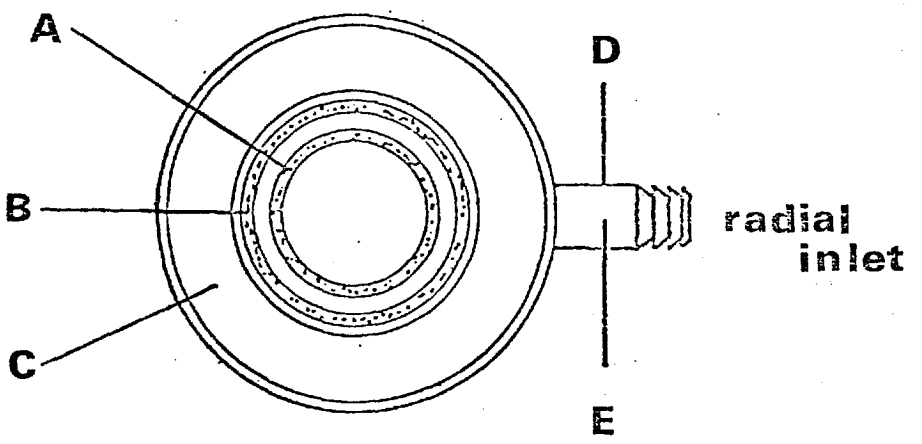


Fig 3.1 Demountable Plasma Torch





A	Inner silica tube	D	Plasma gas inlet
B	Outer silica tube	E	Cooling gas inlet
C	Torch body		

Fig. 3. 2. Tangential and radial introduction of gases into the plasma torch

the discharge initiation process in ICP torches, and have also reported the initiation and operational characteristics of various plasma torch configurations employed during the development of their ICP system (121).

3.4 GAS SELECTION AND FLOW RATE CONTROL SYSTEM

Argon was used for both the plasma and coolant flows. Polyatomic gases could not be used since not enough power was available and among the inert monoatomic gases argon is the cheapest.

The flow rates of the various gases were controlled by three rotameters. The coolant and plasma gas flows were operated at a pressure of 15 psi with a flow rate of 0.0-20 $^{l}/_{min}$ and the injector gas flow at a pressure of 30 psi with a flow rate of 0.0-2.6 $^{l}/_{min}$. The schematic diagram of the gas flow system is shown in Figure 3.3.

3.5 MOUNTING OF THE TORCH

The torch, coil and leads must be adequately shielded so that emitted radiofrequency radiation does not interfere with the detection equipment. In order to fulfil this requirement an aluminium shielding box (17 x 20 x 25 cm) was used and the tube assembly was mounted inside the box on the torch holder. The torch was held in a cradle screwed to the torch holder which allowed adjustment of the relative positions of the torch and work coil in order to obtain concentric alignment. The torch holder with the box and the coil was fitted to a carriage which allowed movement of the plasma torch and work coil as a whole along the vertical axis at right angles to the optical axis.

The/

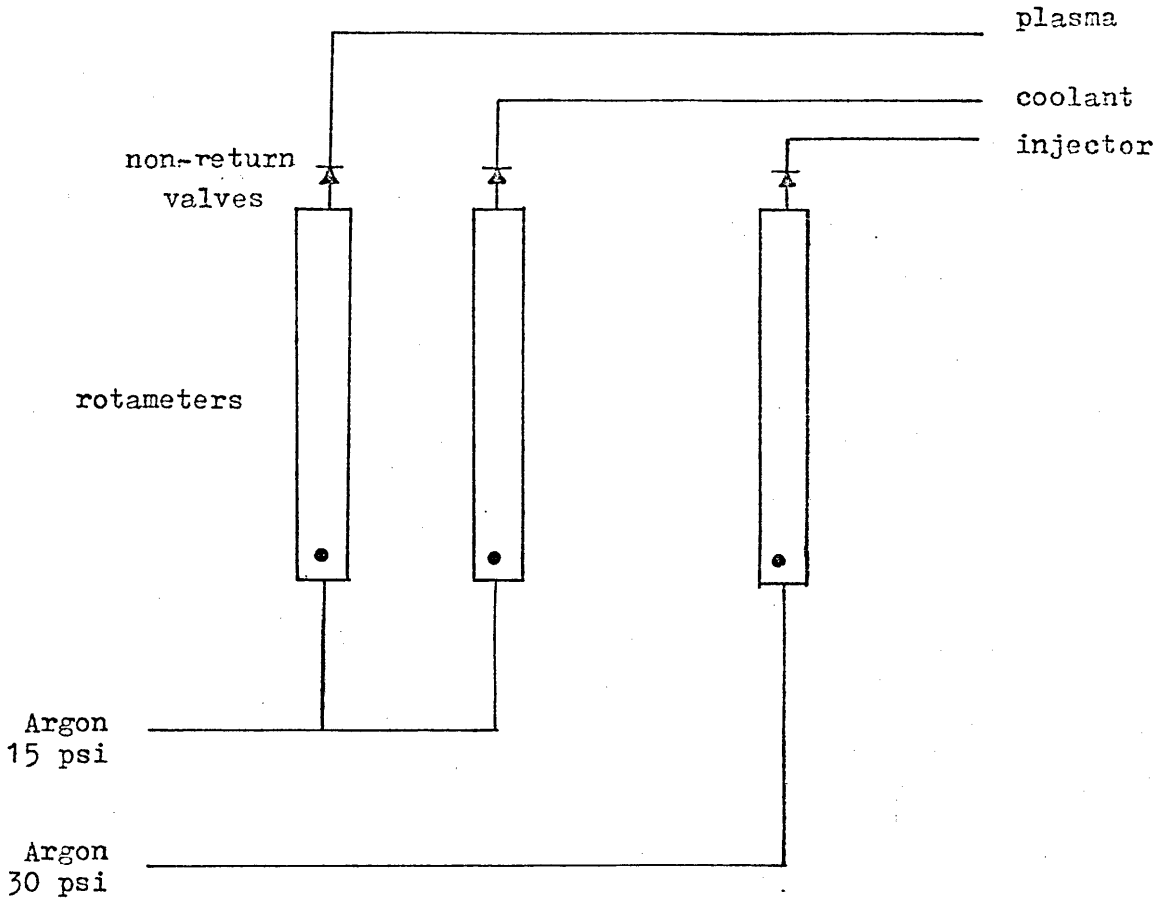


Fig. 3.3. Gas Flow System

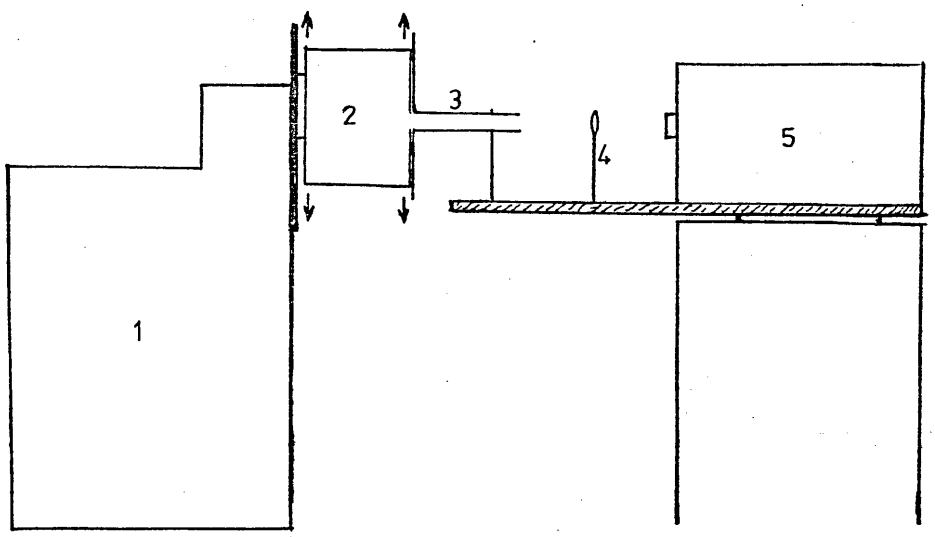


Fig. 3.4. Schematic diagram of 1- generator 2- shielding box 3- observation aperture 4- lens 5- monochromator

The shielding box was provided with a door, and apertures for plasma observation and gas exhaust. To preserve electrical screening, apertures were fitted with a metal tube having a length at least four times their diameter. The observation part was mounted on a slide so that the plasma could be moved up and down whilst the observation tube remained firmly clamped to the optic axis (see Figure 3.4).

3.6 THE PLASMA INITIATION

The torch is first flushed with argon for a few minutes and the generator allowed to warm up. The plasma is then ignited by touching the quartz tube with a carbon rod, thermionic electrons from the hot rod initiate the plasma discharge. It is important to stop the aerosol flow during this operation, while maintaining a coolant and plasma flow rate of approximately 14 $^{l}/_{min}$. Next, the argon carrying the sample is slowly introduced through the central tube and the plasma flow rate is simultaneously reduced to about 6 $^{l}/_{min}$. The introduction of the sample results in a visible axial passage through the plasma channel. Initiation of the plasma requires a minimum power of 1 KW. Any difficulties in generating the plasma are usually attributable to incorrect alignment of the torch tubes, this is overcome by the realignment of the torch.

3.7 NEBULIZERS

Two types of nebulizer have been used in emission spectrometry, ultrasonic and pneumatic. In the former, a ceramic crystal transducer is employed to focus ultrasonic energy onto a thin film coupled to the transducer/

transducer by a liquid medium or a velocity transformer. The sample liquid is fed on to the film and ultrasonic energy produces capillary waves (69) on the surface which then rupture to form droplets. Ultrasonic nebulizers produce finer droplets (less than 2 μm) than do pneumatic type and more material is conveyed to the plasma per unit time (70). Furthermore, the gas flow rate can be varied independently of the solution uptake rate, an important factor in use with plasmas where flow rates tend to be more critical than in flames. However, difficulty of sample interchange and tendency towards memory effects which leads to difficulties with time taken for washing out of sample solution after measurement is a practical disadvantage. Attempts have been made to overcome this problem by the use of pumps to change the sample (48, 71, 55). Hoare and Mostyn (33) have used a multicell sample vessel to overcome memory effects.

Very recently Olson (75) and co-workers developed a new ultrasonic nebulizer which was used combined with a conventional aerosol desolvation system. They used a peristaltic pump Teflon-tube sampling introduction arrangement which provided continuous, constant-rate delivery of sample solution directly onto the nebulizing surface. The rate of sample delivery to the plasma torch was tenfold greater than that of pneumatic nebulizers, which resulted in improvement of detection limits. The transducer was protected against chemical attack by being completely enclosed in an acoustically coupled borosilicate glass cylinder. Furthermore, convenient sample change and rapid clean out were possible with this system.

In pneumatic nebulizer devices the liquid sample is introduced into/

into a high velocity jet of gas. The most frequently used pneumatic nebulizer is the concentric one as shown in Figure 3.5. The sample orifice is surrounded by the concentric outlet for the nebulizing gas. The high velocity gas stream produces a pressure drop at the tip of the capillary carrying the liquid to be nebulized. The liquid is thus drawn out of the capillary and shattered into many droplets by the gas stream. The pressure drop along the capillary, and the solution uptake rate, depends critically on the position of the sample capillary with respect to the gas outlet. A variety of adjustable nebulizers have been built, in which, by variation of the position of the capillary in the gas stream, it is possible to control the solution flow rate independent of the operating pressure.

An adjustable pneumatic nebulizer made of stainless steel and designed by Goulter (92) was used for this work. The solution uptake rate of the nebulizer was 1.5 $m^{l}/_{min}$ at an argon flow of 2 $^{l}/_{min}$.

3.8 AEROSOL CHAMBER

A dual tube aerosol chamber (37) was used to reduce random fluctuations in signal intensity commonly caused by the process of pneumatic aerosol generation. A schematic diagram is shown in Figure 3.6. The central tube was used to separate the forward and reverse aerosol flows, the reverse flow is produced as a result of the low pressure in the region of high aerosol velocity. The turbulence within the chamber was reduced and less condensation occurred on the nebulizer, this resulted in an improvement in the signal/noise in the plasma. No external desolvation apparatus was used, the aerosol being fed directly into/

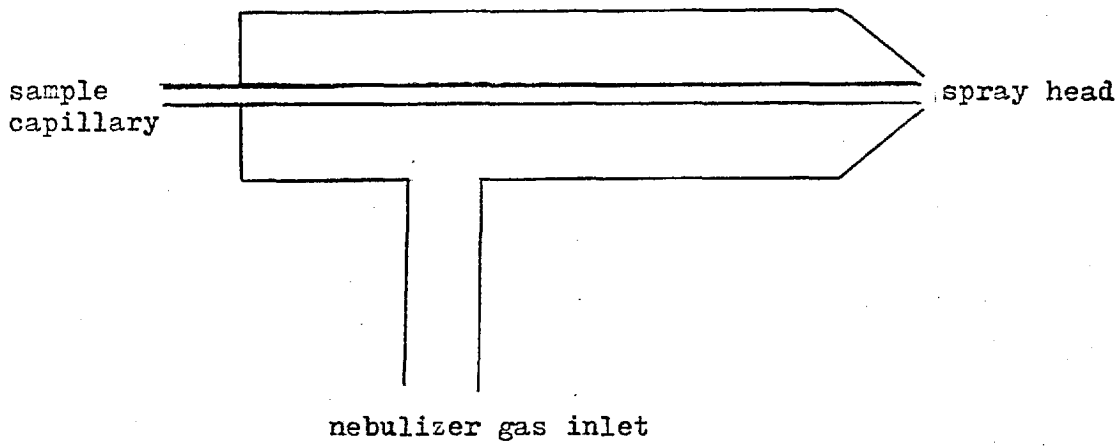


Fig. 3.5. Diagram of concentric nebulizer

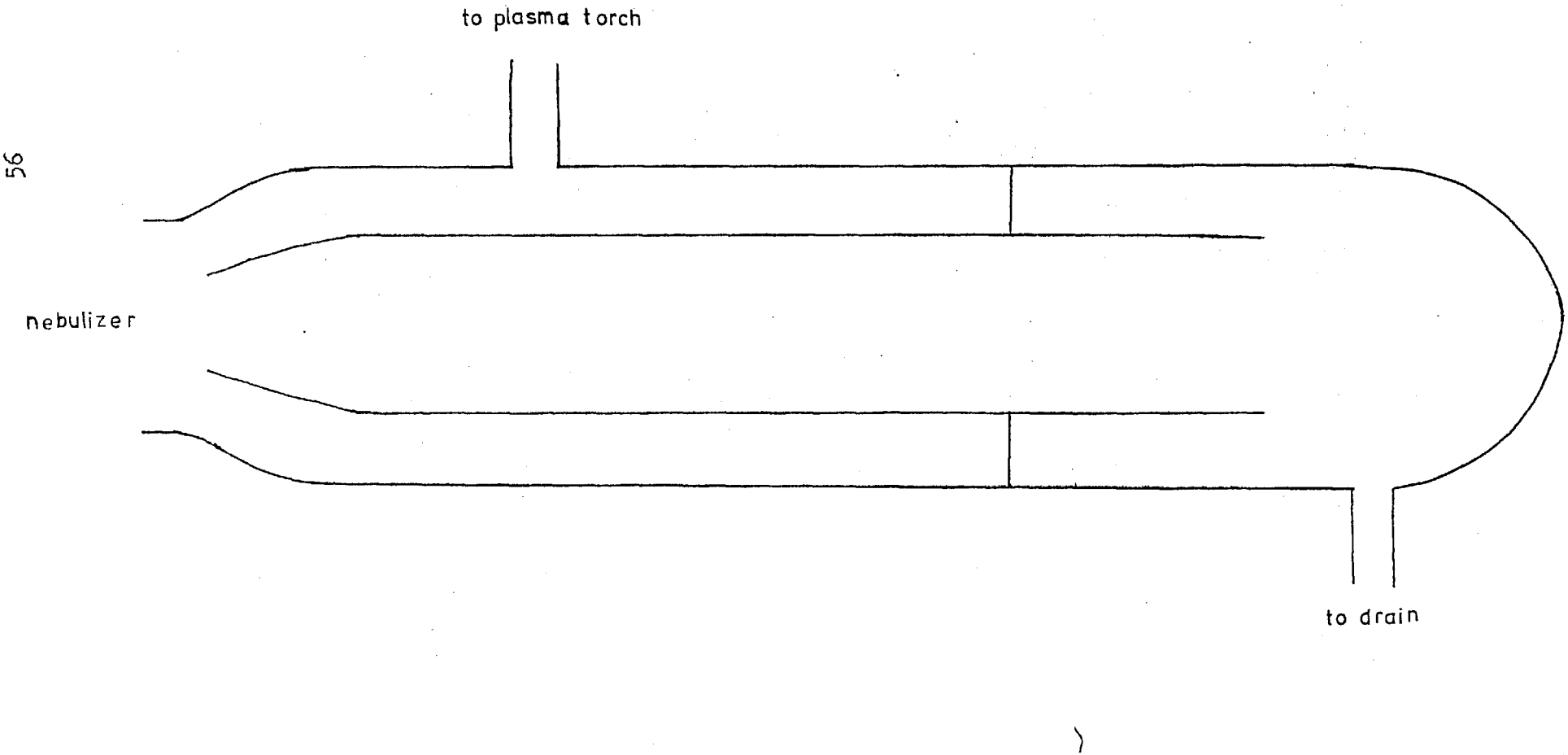


Fig 3.6 Diagram of Aerosol Chamber

into the plasma.

Dead volume between the end of the expansion chamber and the base of the torch was kept to an absolute minimum to allow efficient transfer of sample into the plasma. The rate at which the aerosol entered the plasma was approximately 0.1 ml of solution per minute for an argon flow rate of 2 $^{l}/_{min}$. This was derived by measuring the difference between the volume of run off solution and the uptake volume over a period of 30 min. The efficiency of the nebulizer was found to be ~7%.

3.9 MODIFICATION TO THE INJECTOR TUBE

Figure 3.7a shows the most frequently used type of injector tube. It was suspected that this design caused a fraction of the sample to follow a path around the outer surface of the plasma as shown in the diagram. It was also possible that the diverging gas jet was causing instability in the plasma tor oid.

A modified injector tube was designed, therefore (see Figure 3.7b) with an extended tip to direct the particles more accurately through the centre of the tor oid. The upper constricted part of the tube had a length of 10 mm and internal diameter of 4 mm. Using this injector tube not only did $^{S}/_{N}$ ratio increase, but the discharge became visually more stable and easier to initiate.

3.10 AUXILIARY DEVICE TO INCREASE $^{S}/_{N}$ RATIO

In atomic spectrometry the intensity of the emitted radiation is proportional to the number of analyte atoms reaching the source. In order to increase the number of sample particles in the plasma, it is, however/

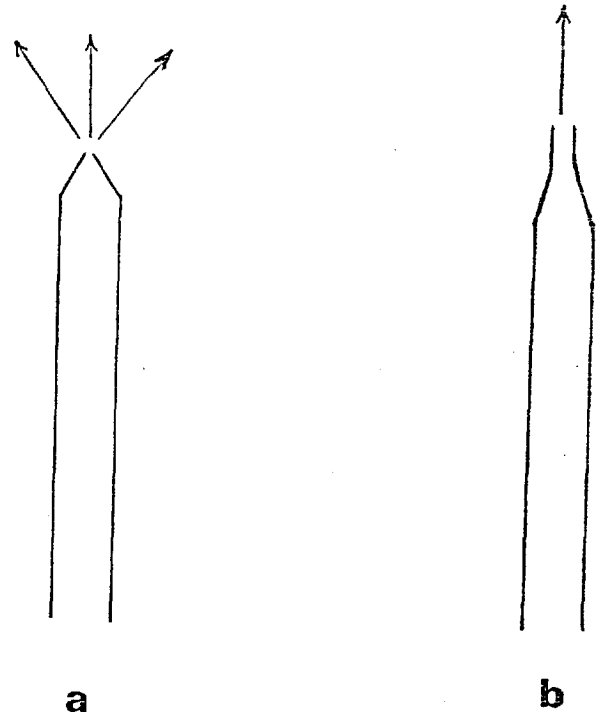


Fig. 3.7. Different injector tube shapes

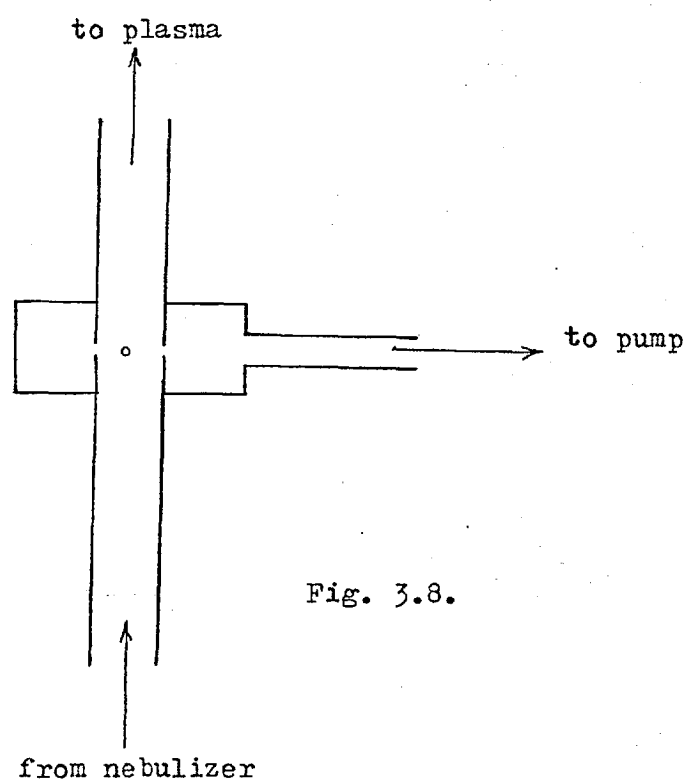


Fig. 3.8.

however, necessary to increase the injector gas flow rate which can cause instability in some plasmas and can even extinguish them. It also causes the sample particles to pass through the plasma too quickly to be totally atomized.

A device was designed, therefore, to get more sample particles into the plasma without an increase in the gas flow reaching the plasma, i.e. to increase the sample to gas ratio in the injection flow. This device was made of stainless steel and is shown in Figure 3.8. It was fitted between the aerosol chamber and the injector tube. The central tube had three holes (120° spacing) and was surrounded by the outer tube which was connected to a vacuum pump. The gas/sample mixture passed through the central tube where a greater proportion of the gas than sample was pumped out, leaving a higher sample to gas ratio in the main flow to pass on to the injector tube. Using this device, the signal increased by a factor of two.

However, critical adjustment of gas flow and pump was required and since the sensitivity of the apparatus was enough for the present work, the device was not used again during the course of the project.

A jet/orifice and a cyclone chamber were constructed in order to achieve similar effects but no significant improvement of the analytical signal was observed.

3.11 DETECTION SYSTEM

Both photographic spectrography (72) and photoelectric recording (32, 36) of the emission spectra from plasmas have been used. The photographic/

photographic method has the following advantages. There is no restriction on the choice of analytical lines, spectral interferences and the background over the whole of the wavelength range investigated are more readily observed and there is a permanent record of the experimental spectra. In electric recording the cables used to supply the photomultiplier (PMT) with high tension current and the cable carrying the PMT output current must be adequately protected from interference from the strong radiofrequency field produced by the generator. Spectrographic technique does not suffer from this disadvantage.

The existing photoelectric system was used for this work. The monochromator was a grating instrument type AA4 manufactured by Techtron PTV Ltd, Melbourne, Australia. The monochromator was positioned on a platform so that the optical axis of the entrance slit intersected the plasma axis. Using a simple silica convex lens of 71 mm focal length and 1.5" diameter, the plasma was imaged onto the entrance slit of the monochromator. The magnification of the lens was $^{1}/_{3.8}$, i.e. the plasma was imaged down in size a factor of 3.8.

The power to the PMT was supplied from a Brandenburg PMT power supply model 472R. This yielded a maximum EHT of 2 KV, which could be reduced in 10 V steps down to 0.0 V.

The output of the PMT after being amplified by a D.C. amplifier was finally displayed on a Servoscribe model RE 511-20 (Smith Industries Ltd, Wembley, Middlesex).

CHAPTER IV

INVESTIGATION OF THE ANALYTICAL OPERATING CHARACTERISTICS OF RADIOFREQUENCY INDUCTIVELY COUPLED PLASMA

4.1 OPTIMISATION OF THE OPERATING PARAMETERS

Optimisation of the different parameters was performed with the aim of improving plasma stability and achieving adequately low detection limits with relative freedom from interference effects. Various parameters critically affect the stability and the sensitivity of the plasma and they require optimisation before any analysis can be performed. The plasma, coolant, and aerosol gas flow rates, as well as observational heights in the plasma and the power input were the main operational parameters investigated. It was evident from the literature that the various operational parameters of the plasma source are inter-related. However, initial studies were carried out treating only one parameter as the variable whilst keeping the others fixed. Inter-relative effects were studied later. The effect of each parameter on emission intensity, rms (root mean square) noise and consequently signal/noise ratio were investigated. Since the analysis of Mo, Co and B in soil extracts was the main concern of this work, these elements were chosen for the optimisation experiments.

4.1.1 Effect of the Injector Gas Flow Rate

The injector gas flow rate was varied up to 2.6 l min^{-1}, i.e. the maximum attainable gas flow, while the height of observation was fixed at 20 mm above the working coil, the power at 1.2 KW, coolant gas at 14 l min^{-1} and the plasma flow at 6 l min^{-1}.

Effect of the Injector Gas Flow on Analytical Signal

When the injector gas flow rate is increased the sample uptake rate increases and the analytical signal approaches a maximum. The high injection stream gas velocity assists and ensures the formation of a toroidal/

toroidal plasma. Excessive gas flow reduces the residence time of the injected material and sample excitation is consequently reduced significantly. Therefore, the intensity of the analytical signal increases to a maximum and then decreases again. The background of the plasma decreases uniformly with increase in the injector gas flow. At flows above ca 1.6 l min^{-1}, the variation in the background is minimal.

Fig. 4.1 shows the effect of injector gas flow on analytical signal for 10 ppm Mo I at 379.8 nm. The variation of analytical signals obtained for B I and Co I are similar, with all the curves exhibiting maxima at an injector flow of ca 1.6 l min^{-1}.

Effect of the Injector Gas Flow on the Plasma Noise Level

At very low gas flow rates, fluctuations in the sample uptake rate are relatively large. Therefore, even with an aerosol expansion chamber in the system the plasma was still noisy. As the flow rate was increased the noise decreased passing through a minimum and then rising again at higher flow rates. This was attributed to the presence of large concentrations of molecular species, formed by breakdown of the water, which tended to quench the plasma. This effect is shown in Fig. 4.2 for Mo I at 379.8 nm. Similar graphs have been obtained for Co and B.

By considering Figs 4.1 and 4.2, it is clear that an argon flow rate of 1.6 l min^{-1} which corresponded to a solution uptake rate of 0.45 ml/min gave the maximum S/N ratio under the conditions given above.

4.1.2. Effect of the Plasma Gas Flow

The injector flow rate was set to 1.6 l min^{-1} and the coolant flow rate to 14 l min^{-1}. The height of observation was fixed at 20 mm above the top of the work coil and the power at 1.2 KW. The plasma gas flow was then varied up to a maximum of 12 l min^{-1}.

Effect/

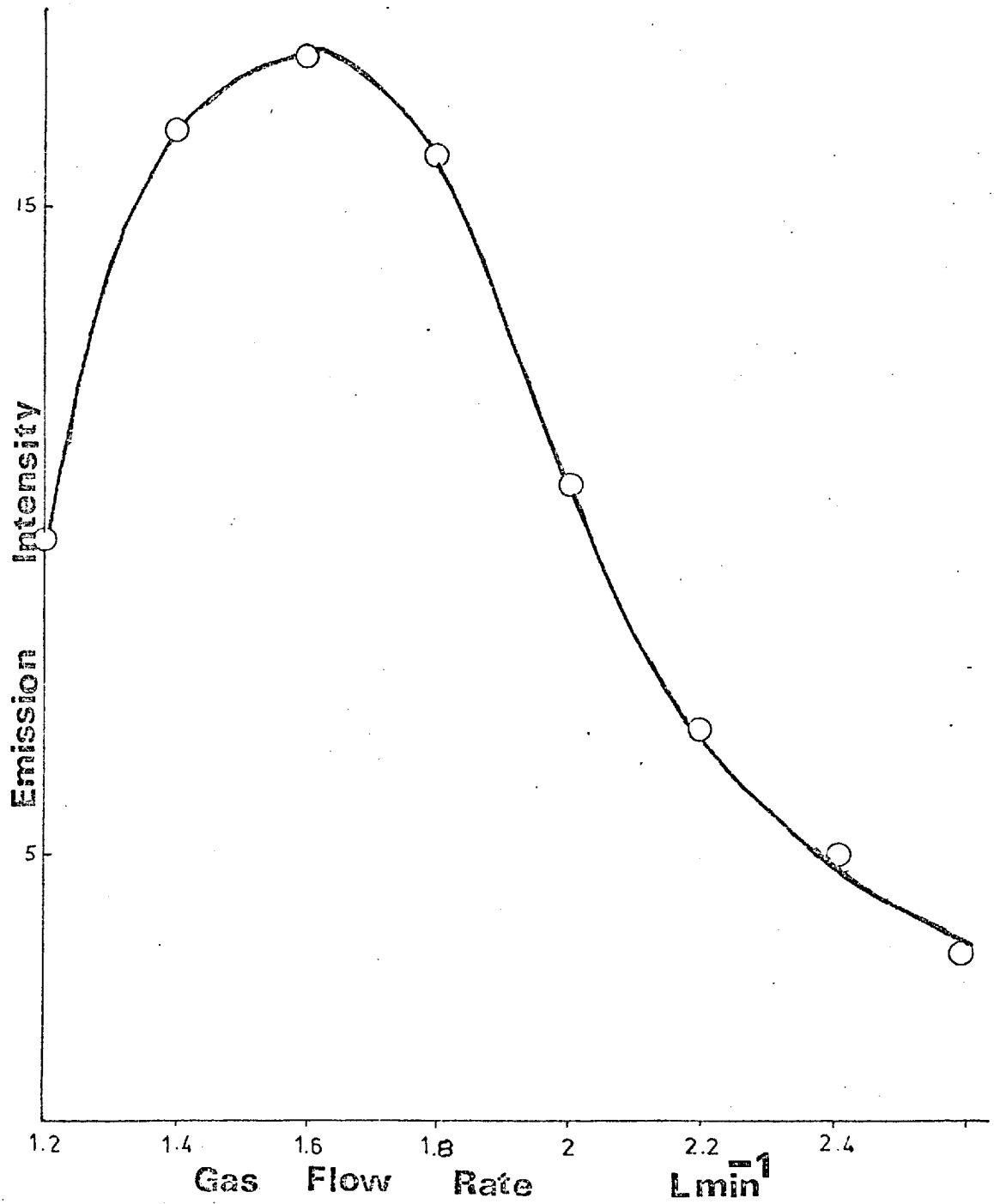


Fig 4. 1. Variation of the emission intensity at 379.8 nm. with injector gas flow rate observed from an aqueous ammonium molybdate solution containing 10 ppm. Mo.

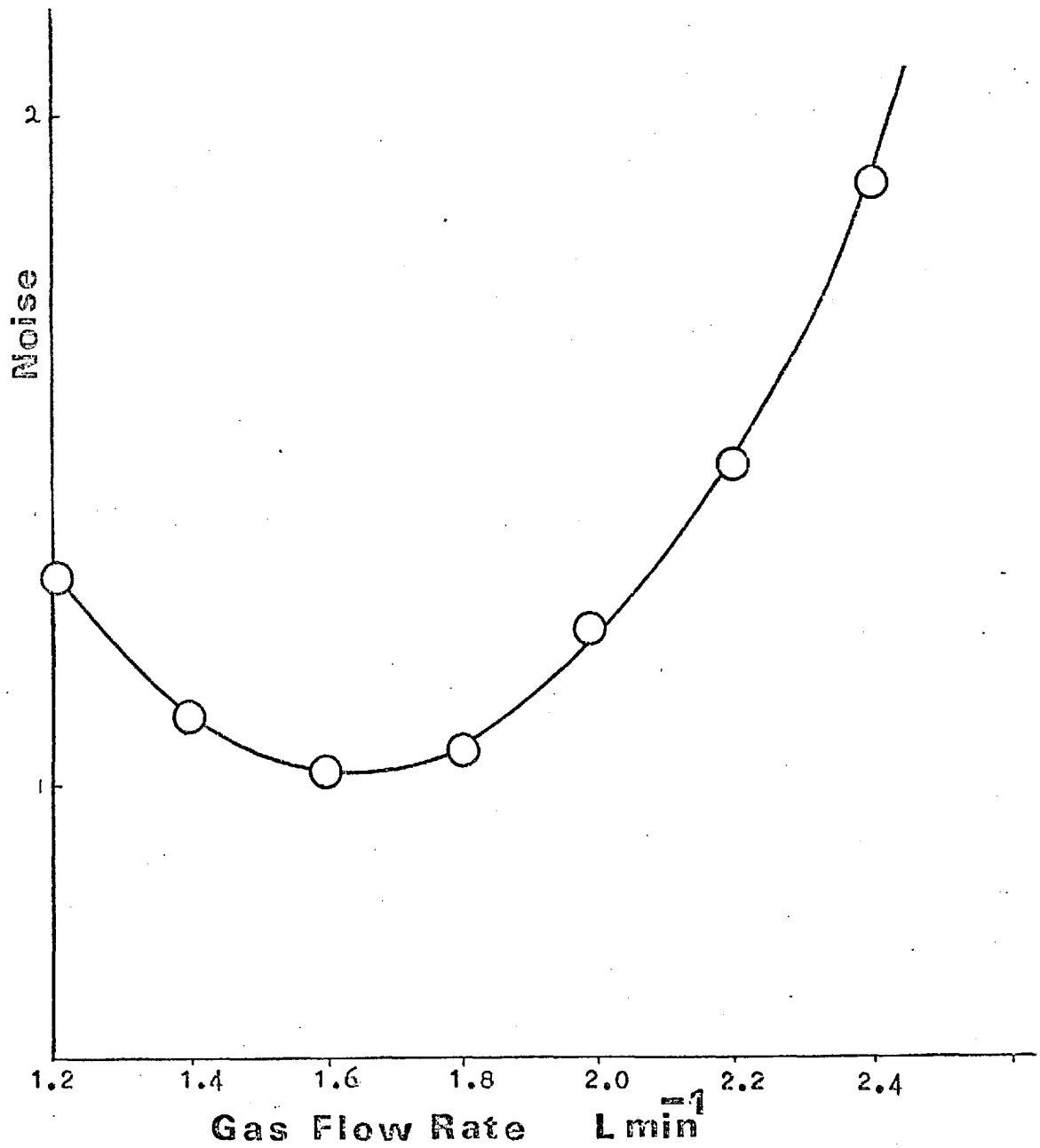


Fig. 4. 2. Variation of the noise at 379.8 nm. with injector gas flow rate observed from an aqueous ammonium molybdate solution containing 10 ppm. Mo.

Effect of the Plasma Gas Flow Rate on Analytical Signal

The variation of the analytical signal with plasma gas flow is shown in Fig. 4.3. Ward (74) has shown that the temperature decreases fairly uniformly with increasing plasma gas flow, also of course the particle density of the argon increases. The temperature decrease and the dilution of the atomic concentration causes the intensity of the signal to decrease as the plasma gas flow increases.

Effect of Plasma Gas Flow on Plasma Stability

The variation of the rms noise with plasma gas flow for Mo at 379.8 nm is shown in Fig. 4.4. Similar curves have been obtained for Co and B. The noise is lowest at 6 l min^{-1} and rises to maximum at 12 l min^{-1}. Above this gas flow, the plasma flickered and tended to extinguish.

Figs. 4.3 and 4.4 indicate that in order to obtain the highest S/N ratio, the plasma gas flow should be kept as low as possible. Unfortunately with the available plasma torch design, a flow of less than 5.5 l min^{-1} was not obtainable. Below this flow rate, heating of the tip of the injector tube occurred which caused instability in the plasma. However, systems with no plasma gas flowing have been used, see for example (2, 74).

4.1.3 Effect of Coolant Gas Flow

The injector flow rate, height of observation and the generator power were the same as reported in 4.1.2. The plasma gas flow was fixed at 6 l min^{-1}.

The variation of the coolant flow rate did not affect the spectral performance to a great extent, but it was necessary to maintain flow rates of at least 12 l min^{-1} to prevent damage to the torch. Below this/

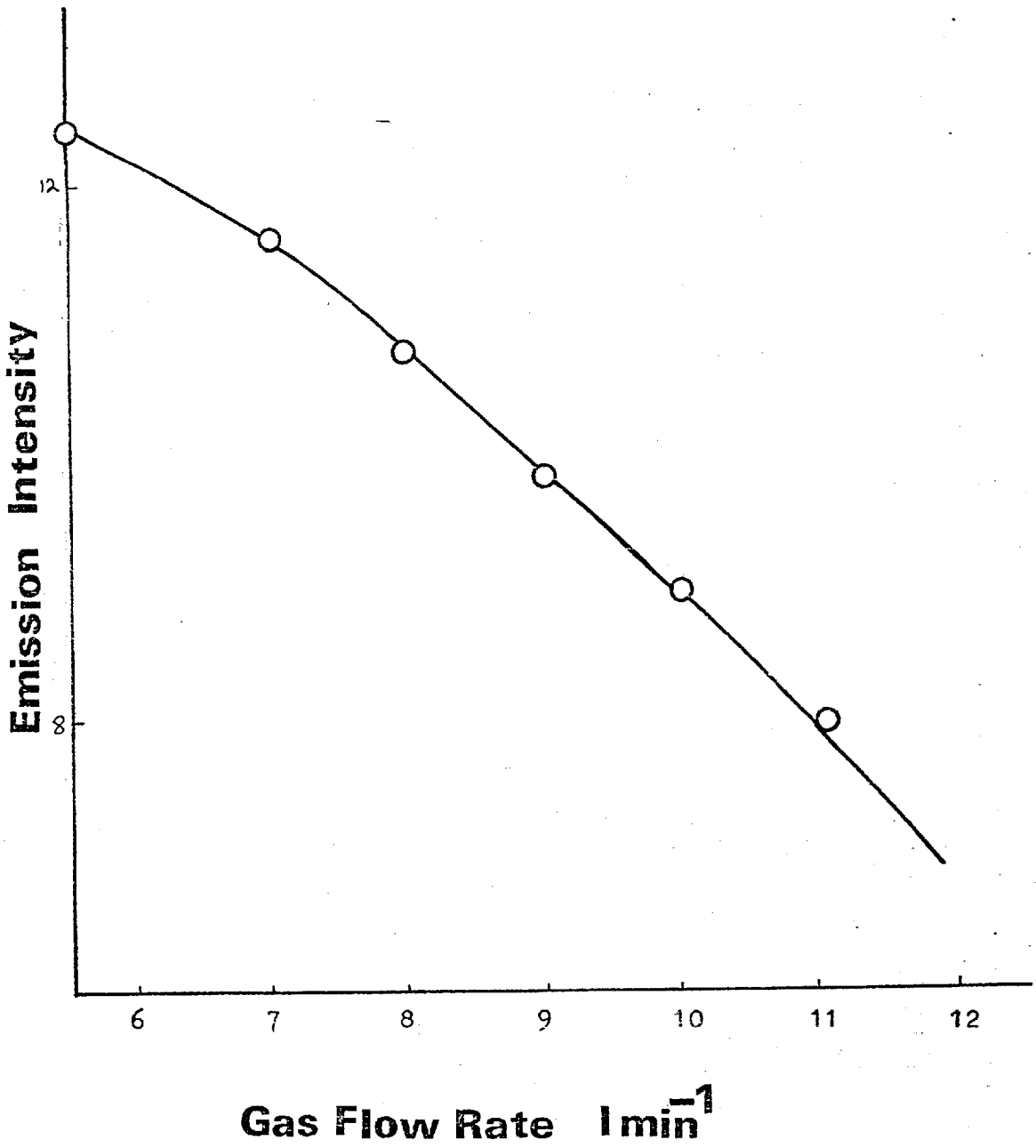


Fig. 4.3. Variation of emission intensity at 379.8 nm. with plasma gas flow rate observed from a solution containing 10 ppm Mo.

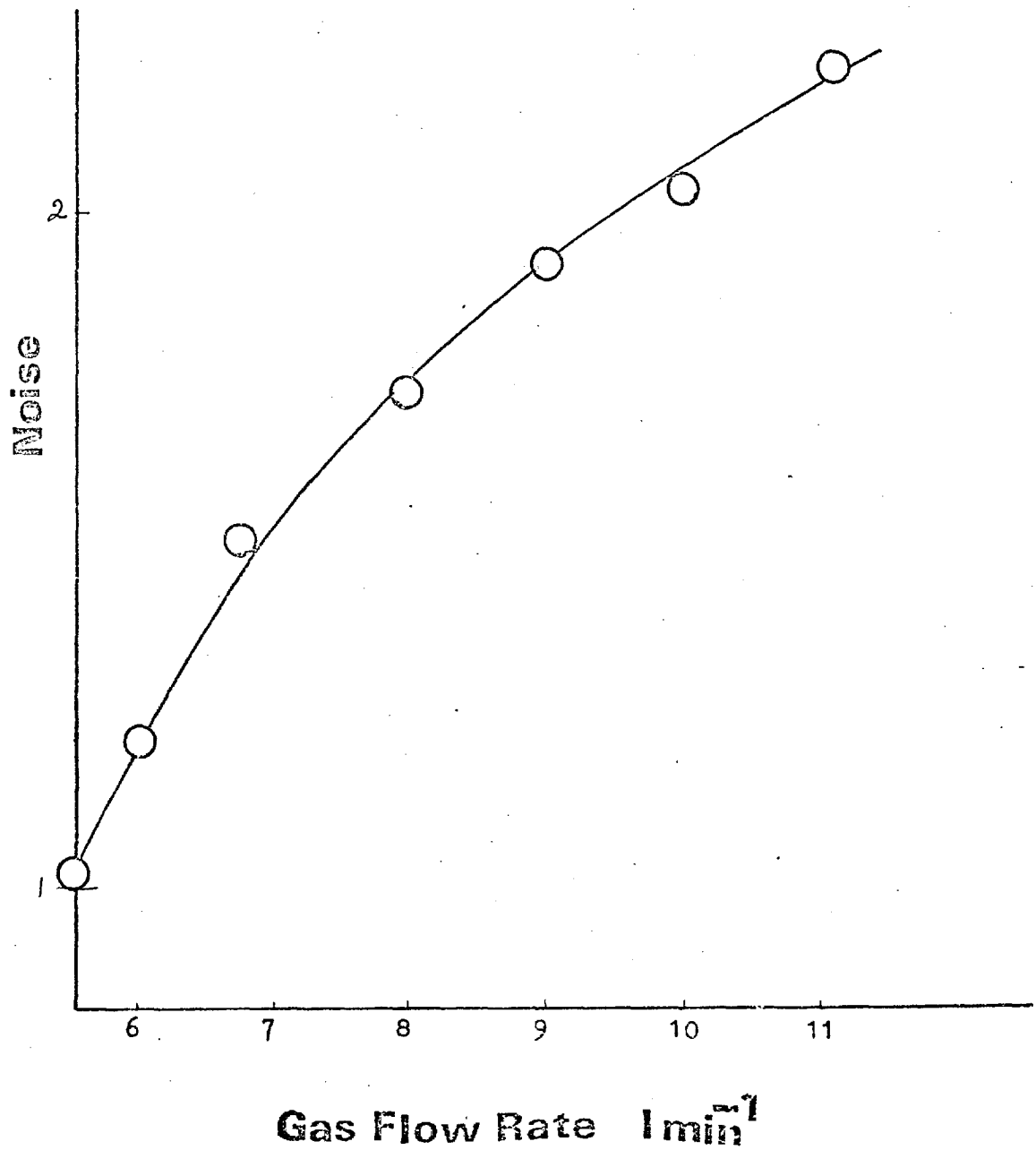


Fig. 4. 4. Variation of noise at 379.8 nm. with plasma gas flow rate observed from a solution containing 10 ppm. Mo.

this flow rate overheating of the silica tube occurred. As the coolant gas flow was increased to more than 17 l min^{-1}, the plasma tended to extinguish. Therefore, the effect of coolant gas flow rate was studied in the range 12-17 l min^{-1}. Although the coolant gas is mainly used for cooling and separating the plasma from the tube walls, it does contribute to the plasma discharge to some extent. The analytical signal was relatively unaffected by the coolant gas flow over much of the range, but the noise was found to increase slightly with a low coolant gas flow which could be because of direct attack of the plasma upon the silica tube walls. At very high coolant gas flows, the noise increased as the stability of the plasma decreased. Fig. 4.5 shows the variation of the S/N ratio with coolant gas flow rate for Mo I at 379.8 nm. (The curves for Co and B were similar.) The optimum coolant gas flow rate was therefore found to be approximately 14 l min^{-1}.

4.1.4 Effect of the Radiofrequency Power

The three gas flow rates were fixed at the optimum values determined and the observation height was set at 20 mm above the top of the working coil. The nominal power was altered from 0.75-1.5 KW via the tuning capacitor. (ca 50-70% of this power finds its way into the plasma.)

Fig. 4.6 shows the variation in the analytical signal with power observed for Mo at 379.8 nm. The temperature of the plasma increases directly with the power dissipated in the coil, therefore, the analytical signal increases with power up to high values. For elements with relatively high excitation potentials such as Mo, Co, and B, a high power is required in order to obtain an appreciable signal. Increase of the power also increases the background, although background can be reduced/

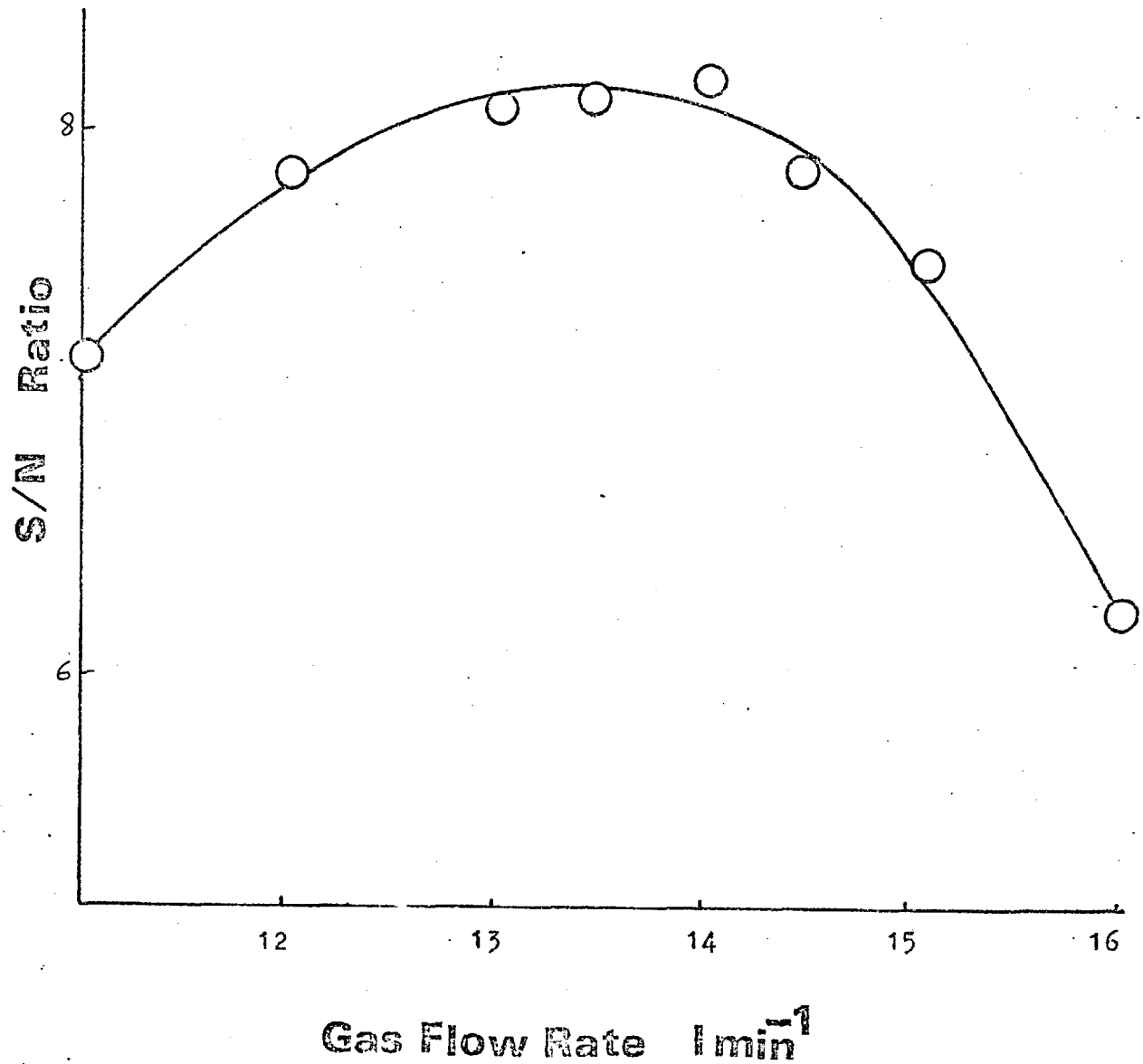


Fig. 4.5. Variation of signal to noise ratio at 379.8nm with coolant gas flow rate observed from a solution containing 10 ppm Mo.

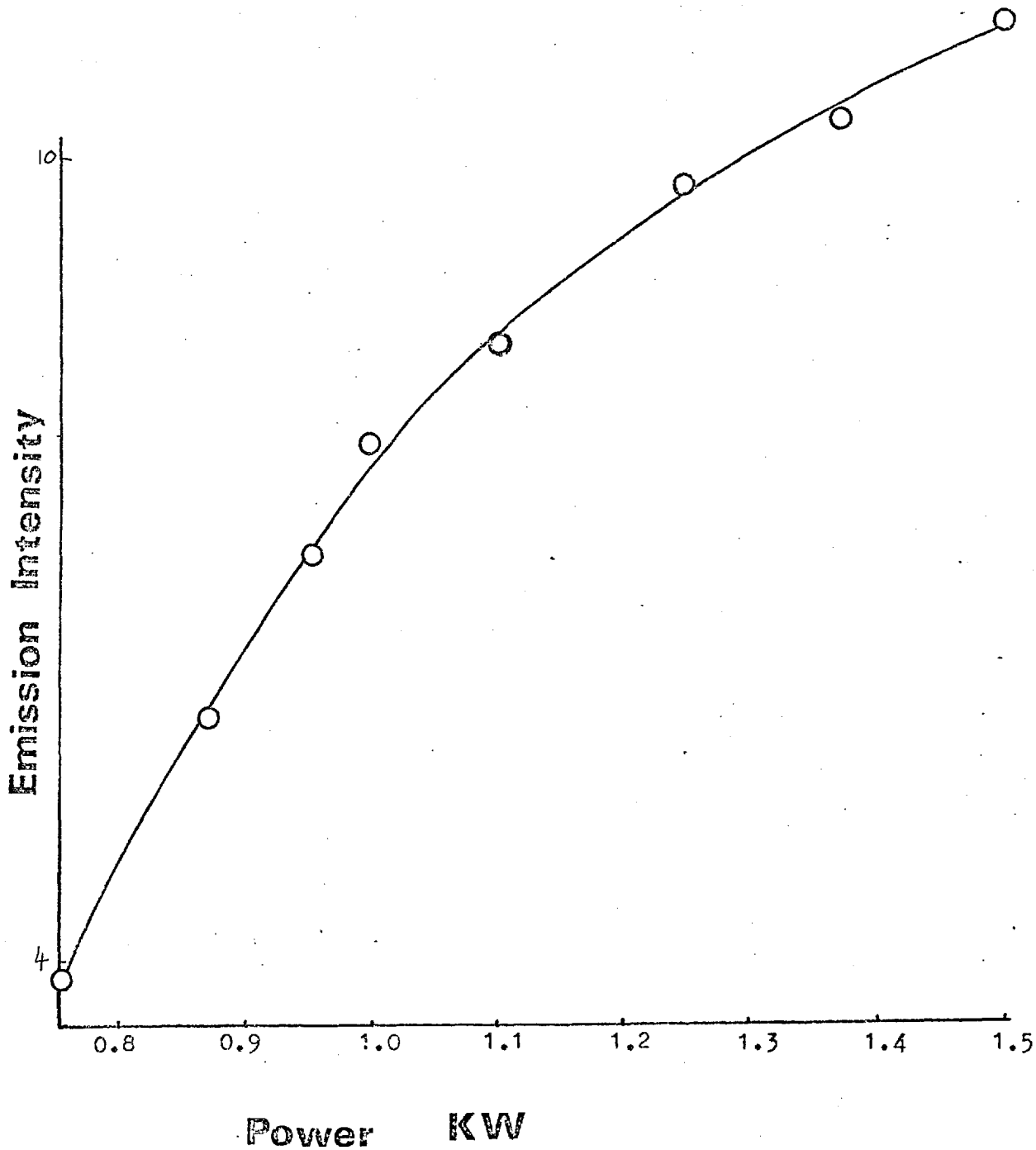


Fig. 4.6. Variation of emission intensity at 379.8 nm with generator power observed from a solution containing 10 ppm Mo.

reduced by an increase in the flow rate of the injector or plasma flow.

Variation of the power in the range 0.75-1.25 KW did not significantly change the rms noise. Above this range the noise increased sharply with power. This was probably due to instability caused by plasma expansion and resulting contact of the plasma with the silica tubing. This effect is illustrated in Fig. 4.7 for Mo at 379.8 nm (similar curves were obtained for Co and B). A power of 1.2 KW was selected as optimal since although it did not correspond to maximum intensity, it did give the lowest detection limit.

4.1.5 Effect of the Height of Observation

The height of observation above the top of the work coil was varied, keeping the other parameters at the determined optimum values.

The effective temperature of the ICP varies from about 6000 K to room temperature along a vertical and horizontal profile of the tailflame. Taking into account the excitation energy, the degree of ionization and the atomization, each spectral line has an optimal temperature at which its radiance reaches a maximum for a given atomic concentration; therefore the optimal viewing height in the plasma varies from element to element. Since the temperature of the plasma decreases with increasing observational height, elements with low excitation energies exhibit their maximum emission higher up the plasma, while elements with high excitation energies have maxima lower in the plasma. It has been found that atom lines with excitation energies above 4 ev. are best observed in the range of 5-20 mm above the work coil and those elements with lines below 4 ev. usually have peak emission in the 20-30 mm region. However, for the ion lines, the spatial emission profiles seem to be independent of the excitation characteristics of the species. In addition/

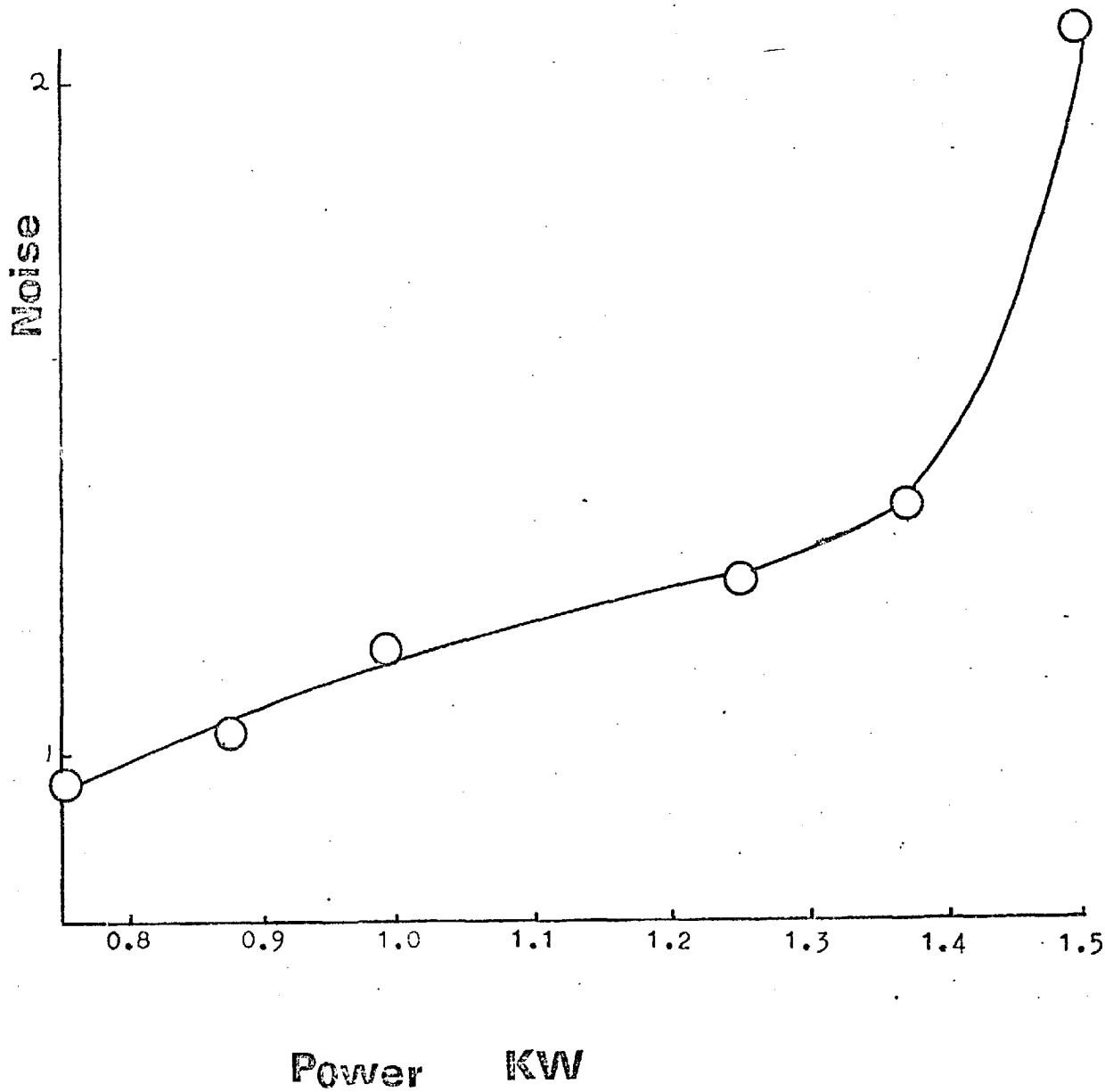


Fig. 4. 7. Variation of noise at 379.8 nm with generator power observed from a solution containing 10 ppm Mo.

addition, the ion lines have their peak emissions higher in the plasma than the corresponding neutral atom lines.

Fig. 4.8 shows the variation of the emission intensity with height of observation for Zn I at 213.8, B I at 249.8, Mo I at 379.8, Ca I at 422.6, Ba I at 552.6 and Co I at 345.3 nm (10 ppm solutions). Zn and B having excitation potentials of more than 4 ev. are best observed at 5-10 and 15 mm respectively. Mo, Ba and Ca with excitation energies of less than 4 ev. have their peak emissions in the range of 20-25 mm above the work coil. The graphs have been normalized to the same amplitude.

The rms noise increased as the height of observation increased and the background radiation decreased higher up the plasma. In the upper regions of the tailflame the plasma becomes turbulent which results in high flicker noise on the emission signal. The variation of signal noise with the height of observation is shown in Fig. 4.9 for Mo at 379.8 nm.

4.1.6 Inter-relative Effect of the Operating Parameters

The optimisation of the different parameters studied so far is only correct under the specified conditions. A change in one parameter can alter the optimised condition for another. These inter-relative effects make plasma behaviour difficult to predict. Though some work (63, 76-80) on the spatial characteristics of R.F. plasmas has been done the source is yet far from being well characterized or understood. However, a knowledge of the emission characteristics of the plasma as a function of spatial position is necessary. This is particularly important in choosing compromise condition for SME and studying interference effects. The effects of power and injector flow rate on

heights/

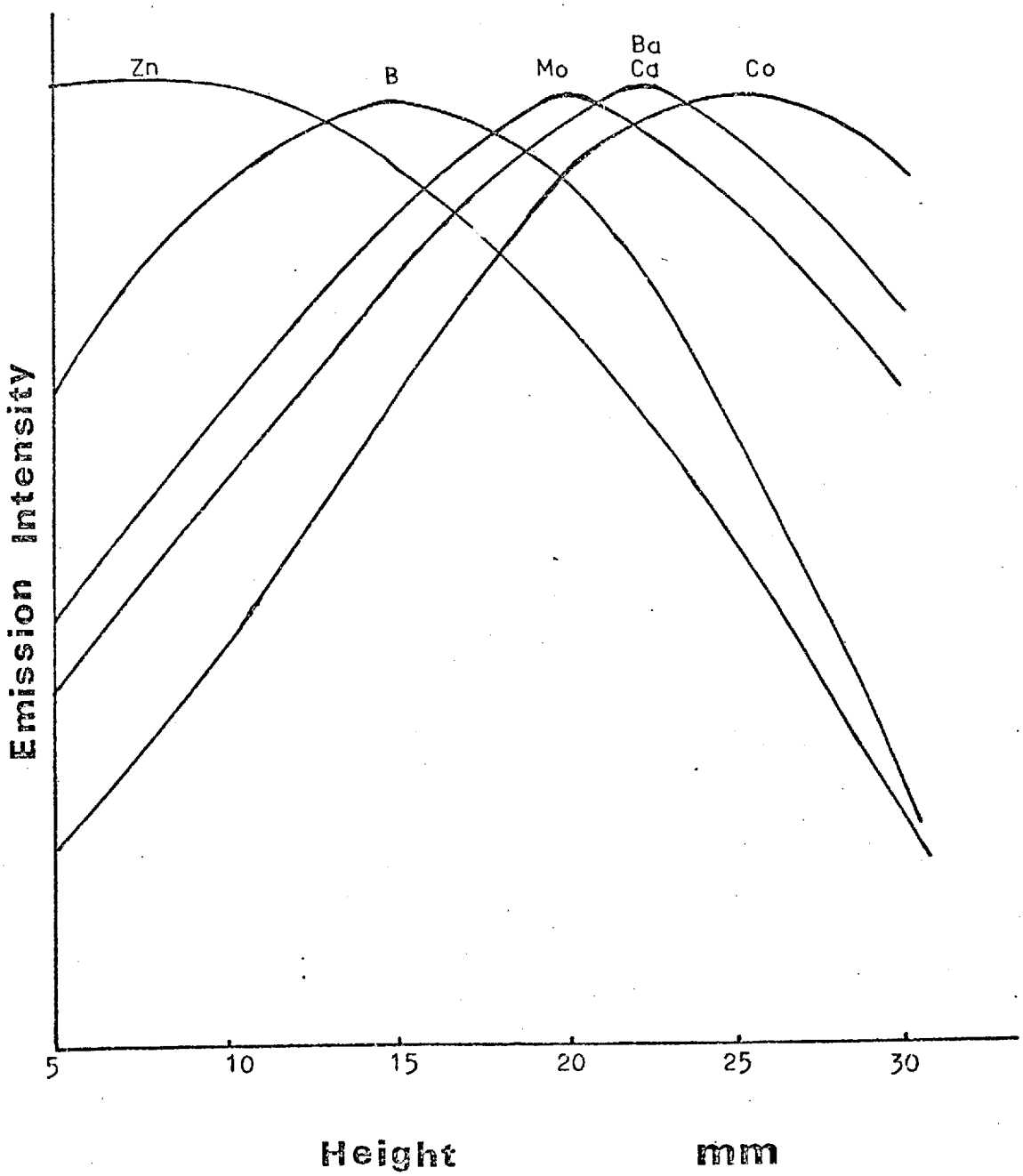


Fig. 4. 8. Variation of emission intensity with height of observation observed from solutions containing 10 ppm Zn, B, Mo, Ba, Ca, and Co at 213.8, 249.8, 379.8, 553.5, 422.6, and 345.4 nm. respectively.

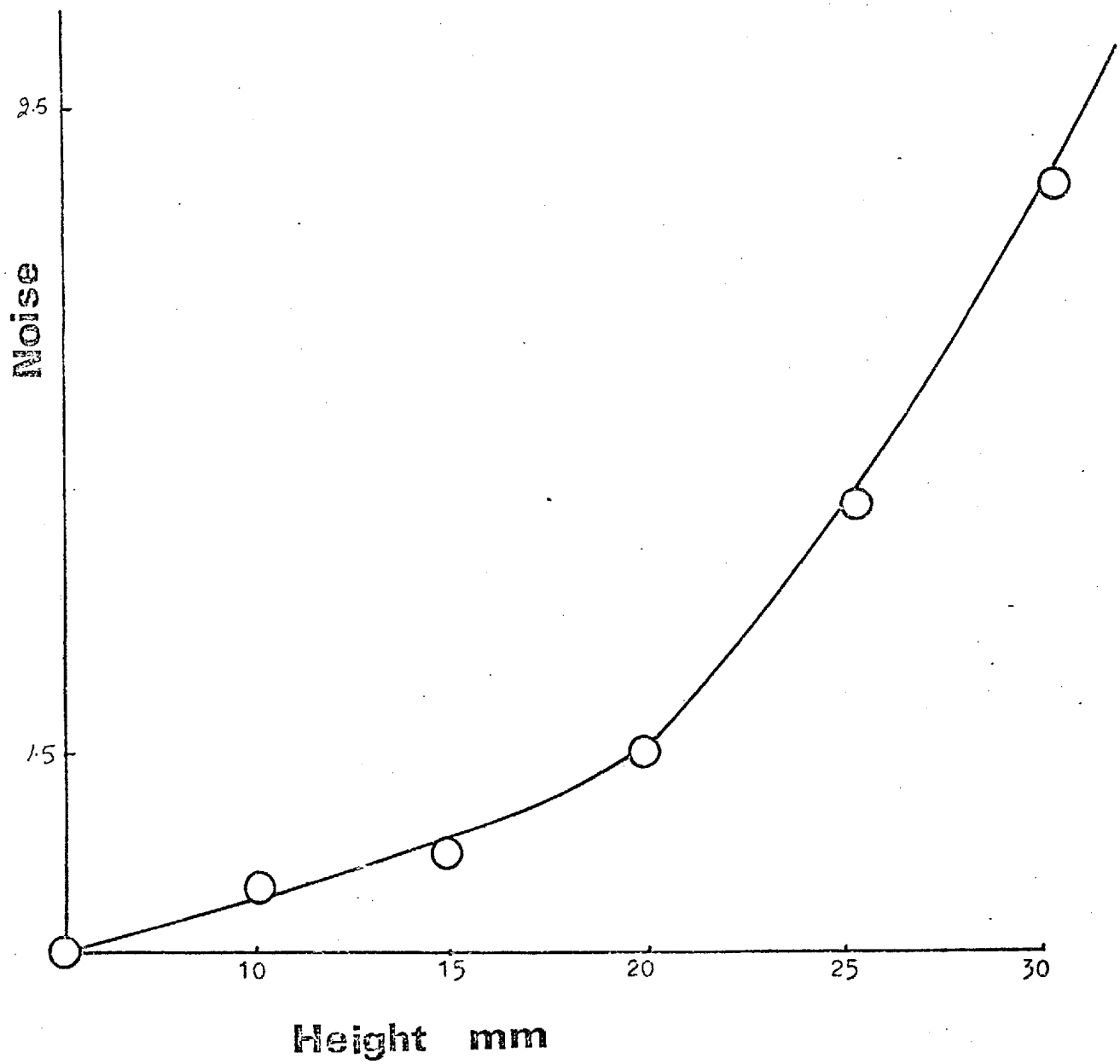


Fig. 4. 9. Variation of noise at 379.8 nm. with height of observation observed from a solution containing 10 ppm Mo

heights of observation have been studied and reported here.

Fig. 4.10 shows the spatial profile of B I emission at 249.8 nm as a function of the generator power. The gas flow rates were fixed at previously optimised values. As shown on the graph with increasing power the optimum height moved higher up in the plasma. It was also found that at decreased power the optimum height in the plasma peaked sharply, whereas with increasing power this tendency became less pronounced. The shift of the optimum height with increasing power could be attributed to expansion of the plasma caused by the rise in temperature. This expansion was clearly visible and probably results in the excitation region of each element being extended upwards. Similar pattern profiles were obtained for Mo I at 379.8 and Co I at 345.3 nm.

Fig. 4.11 shows the effect of injector gas flow rate on optimum height of observation for B I at 249.8 nm. Similar profiles were obtained for Mo, Ba, and Ca. With increase of the injector flow rate the optimum height of observation generally moved higher up the plasma for most of the elements tested. However, exceptions could be found, for instance, the optimum height of observation for Co moved slightly lower in the plasma as the gas flow was changed from 1.6 l min^{-1} to 2.1 l min^{-1} (see Fig. 4.12).

Another interesting point to note about Fig. 4.11 is that at high flow rates the height of observation becomes less important, i.e. the intensity of emission does not change much with height of observation. Comparing Figs 4.10 and 4.11, it was concluded that the reduction in the emission intensity caused by an increase in injector gas flow rate can be exactly compensated by an appropriate increase in the plasma power.

4.2/

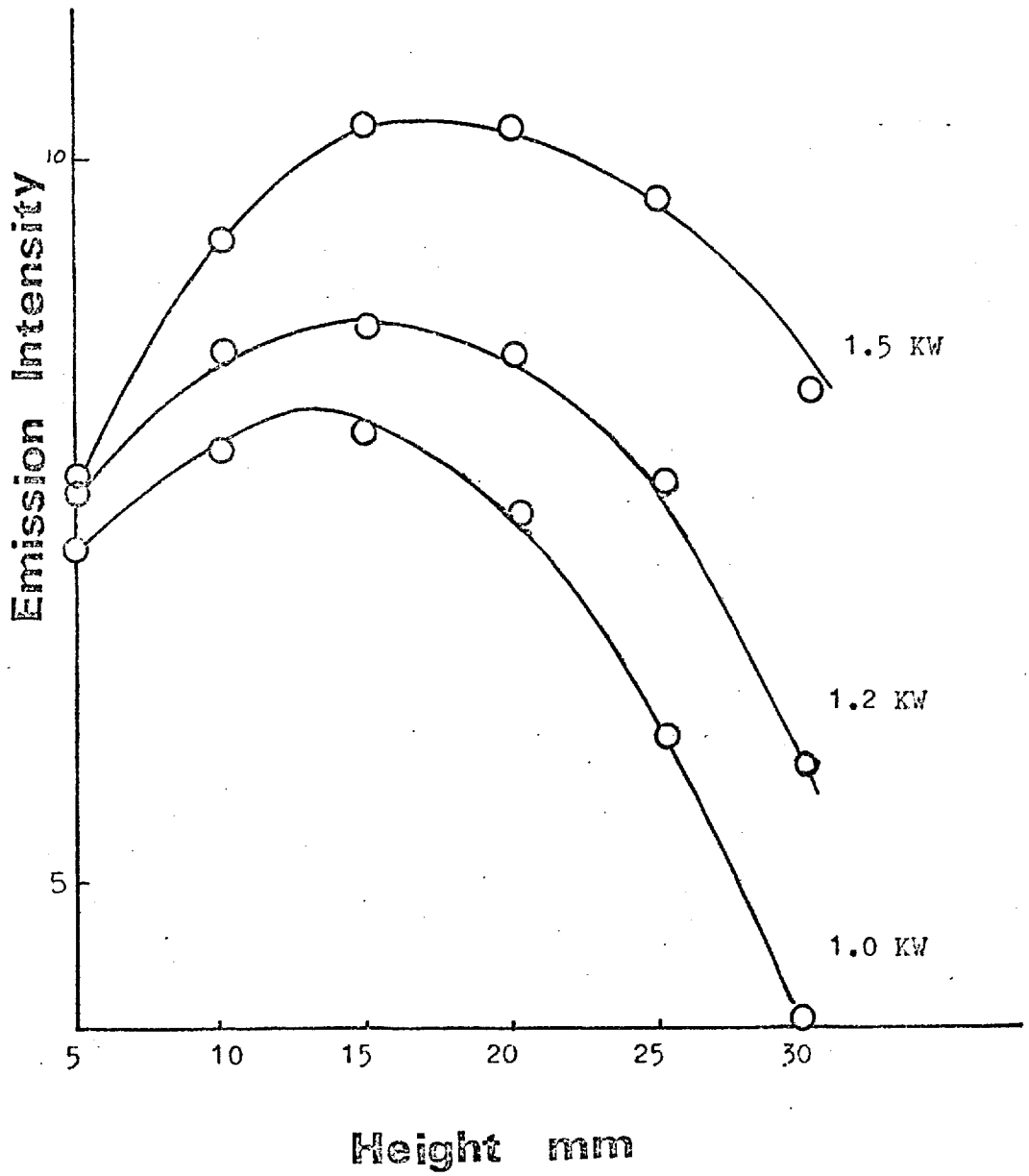


Fig. 4. 10 Effect of increasing power on BI 249.8 nm atom line intensity.

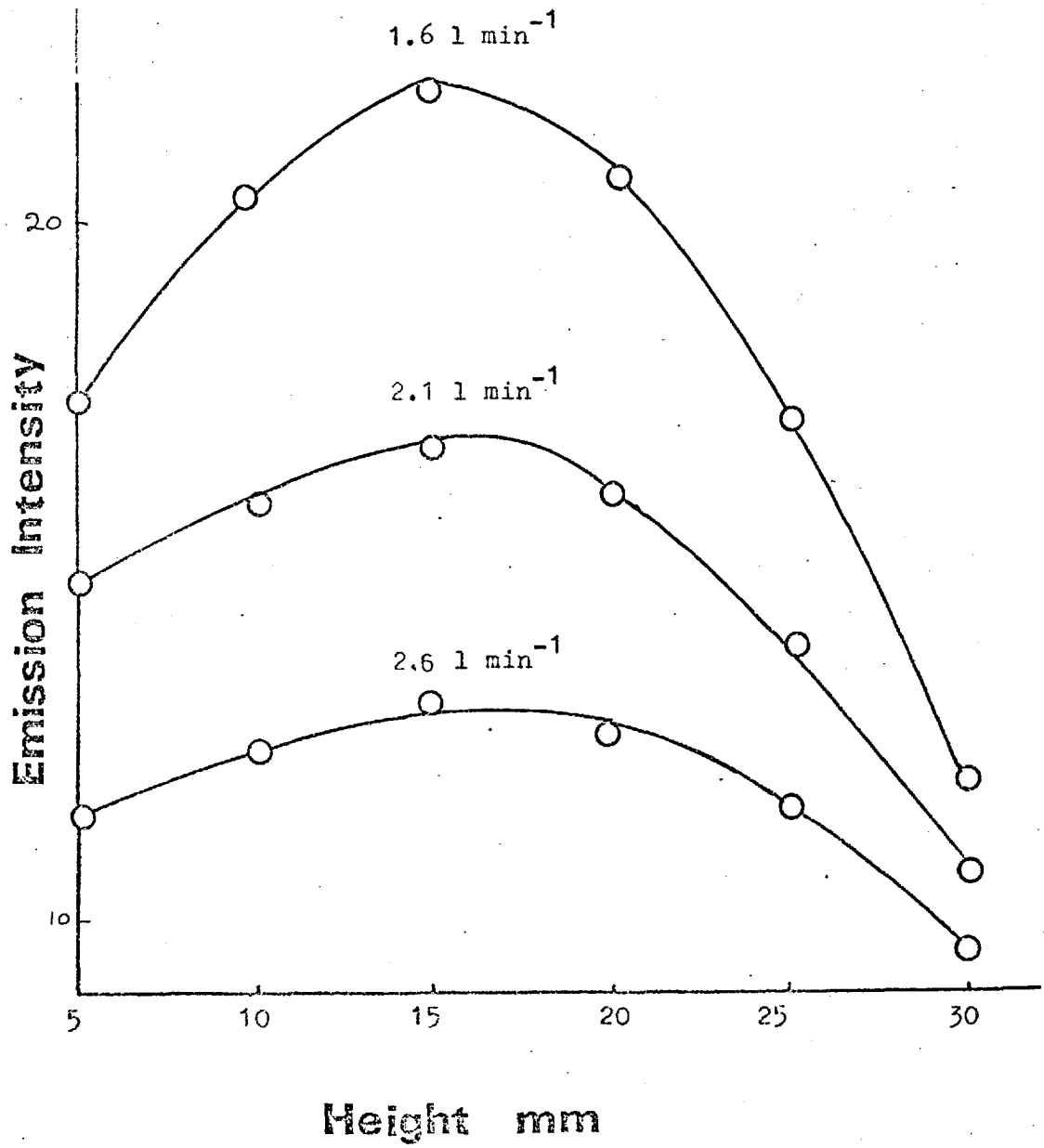


Fig. 4. 11. Effect of increasing injector gas flow rate on B I 249.8 nm atom line intensity.

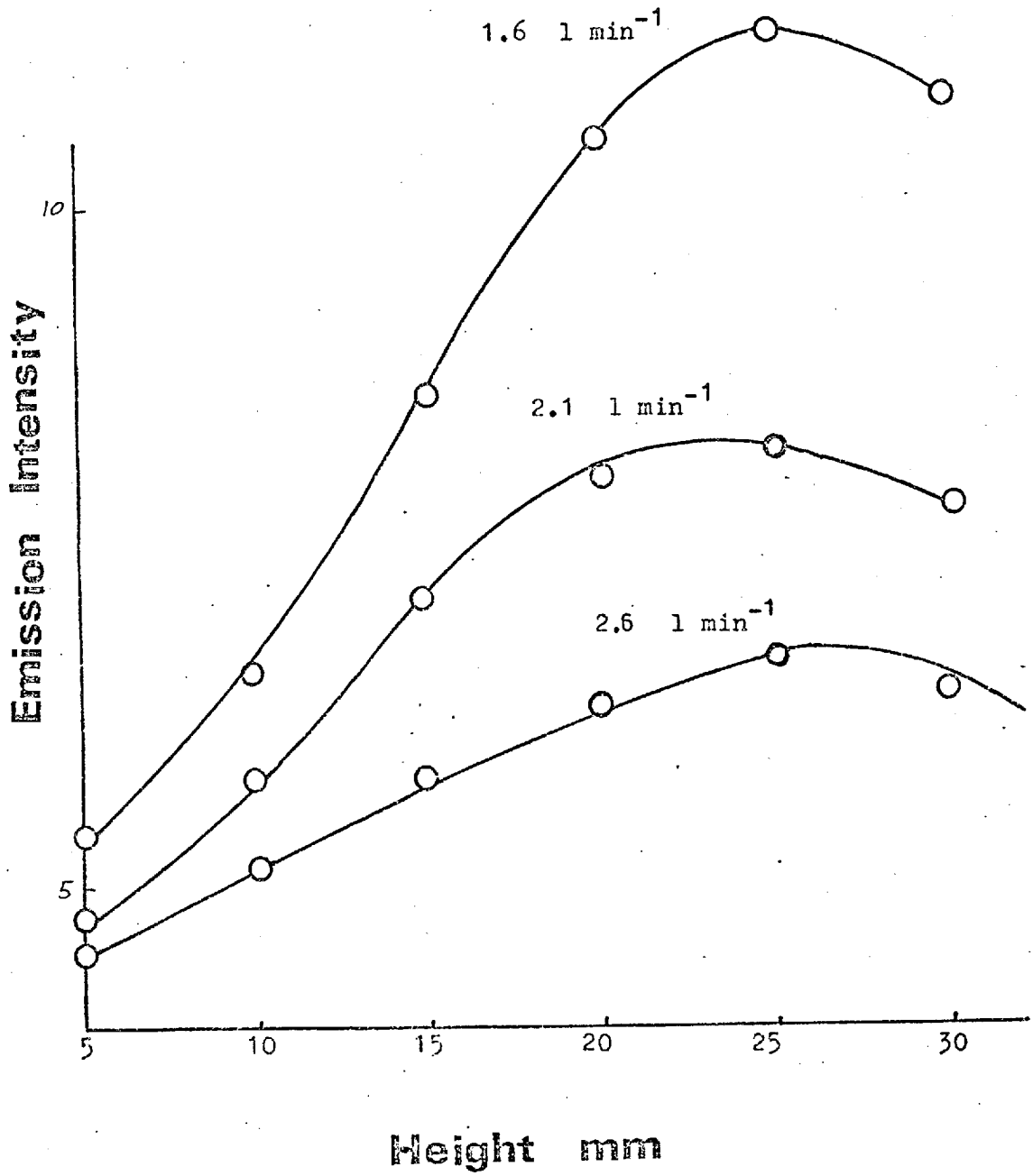


Fig. 4. 12. Effect of increasing injector gas flow rate on Co I 345.3 nm atom line intensity.

4.2 INTERFERENCE EFFECTS

The interference effects observed in ICPs are similar to those encountered in other high temperature sources. Because of the high temperature and inert atmosphere, the commonly found interferences related to the low temperature of flames and the complex composition of the flame gases, do not occur in the ICP. Before studying interference effects a rough classification of them is useful.

Spectral interferences are not included in this study because they are dependent on the spectral characteristics of the elements and the spectral band width of the spectrometer and do not characterise the source.

4.2.1 Classification of Interference Effects

Interference effects can be divided into three broad categories:

(I) Chemical Interferences;

These occur in the plasma as a result of chemical reactions affecting any of the processes, (solute vaporisation, volatilisation, dissociation), that govern the decomposition of the injected aerosol particles into free atoms (63).

Vaporisation interference occurs when the element of interest forms, or is released from, a refractory compound whose thermal stability reduces the efficiency of free atom formation. Examples of this are the Ca-PO4 and Ca-Al systems. A brief study of the literature showed that there is a disparity of results reported on Ca-PO4 and Ca-Al solute vaporisation interference. Al has been reported to enhance, suppress, and have no effect on the emission of Ca in the ICP. Edmonds and Horlick (76) have presented spatial profiles showing the effect of Al on Ca. They have concluded that by observing too low in the plasma a suppression

of/

of the Ca emission signal is observed, and an enhancement is seen by observing too high in the plasma. With, say a 5-10 mm observation window centered on the peak of the spatial pattern, no interference should be observed. Previous work has shown that Ca-Po4 and Ca-Al interference was negligible in our plasma system.

Volatilisation interference is attributed to the occlusion of the analyte in a less volatile matrix of the concomitant or its dispersion in a more volatile matrix. Gilbert (81) has listed elements such as B, Cr, Fe, Mo, Ti, etc., that may cause interference with various analyte elements by formation of mixed species of low volatility.

Dissociation interference occurs when the degree of dissociation of the species involving the analyte varies as the concentration of the concomitant varies.

(II) Ionisation Interference;

This occurs when ionisation of the analyte element is suppressed by the presence of an easily ionised concomitant species. Therefore, its magnitute depends on the ionization potential of the analyte and concomitant and on the type of the spectral line (atom or ion line).

(III) Non-Specific Interferences;

These include sample transport interferences (nebulisation interferences), solvent evaporation interferences and plasma shape interferences. Here one might include the interferences due to properties such as surface tension, density, viscosity and nebulizer type and geometry. For a concise classification of interference effects reference should be made to (4, 63,).

4.2.2 Ionization Interference Study

Interference/

Interference effects produced by easily ionizable element in electrically generated plasmas have been studied widely (82-86) and include papers concerned with ICP (80). Larson and coworkers (80) reported that 6900 μg/ml Na exerted little influence on the observed emission intensity of Ca, Cr and Cd in their ICP. The interferences caused by up to 5000 ppm K on the emission intensity produced by 10 ppm solutions of Ca, Mo and B at different heights of observations are presented in Figs 4.13-4.15. The ionization potentials of K, Ca, Mo and B are 4.34, 6.1, 7.06 and 8.28 ev. respectively. In these figures, the net emission intensity of the analyte in the absence of interferent element is normalized to 100 arbitrary units at each observational height.

The mechanism of ionization interferences of plasmas in local thermal equilibrium (LTE) has been well established (4, 6). Since the argon gas has a high ionization energy, the added analyte metal vapours furnish additional electrons at relatively low temperatures. However, the metal vapours make up only a small part of the plasma, so the bulk electron concentration remains low. Therefore, the electrons released by the ionization of easily ionizable elements increase the number density of electrons to a sufficient degree to suppress the ionization of the analyte species. It also increases the number of atom-electron and ion-electron collisions and thus increases the populations of the excited states. The curves plotted in Figs 4.13-4.15 tend to support this hypothesis. For the more easily ionized Ca, there is indeed an enhancement in atom line intensity with increasing concentration of K. For B, however, which is ionized to a much lesser degree, smaller enhancement in the neutral atomic line intensity is observed. It should be noted that

high/

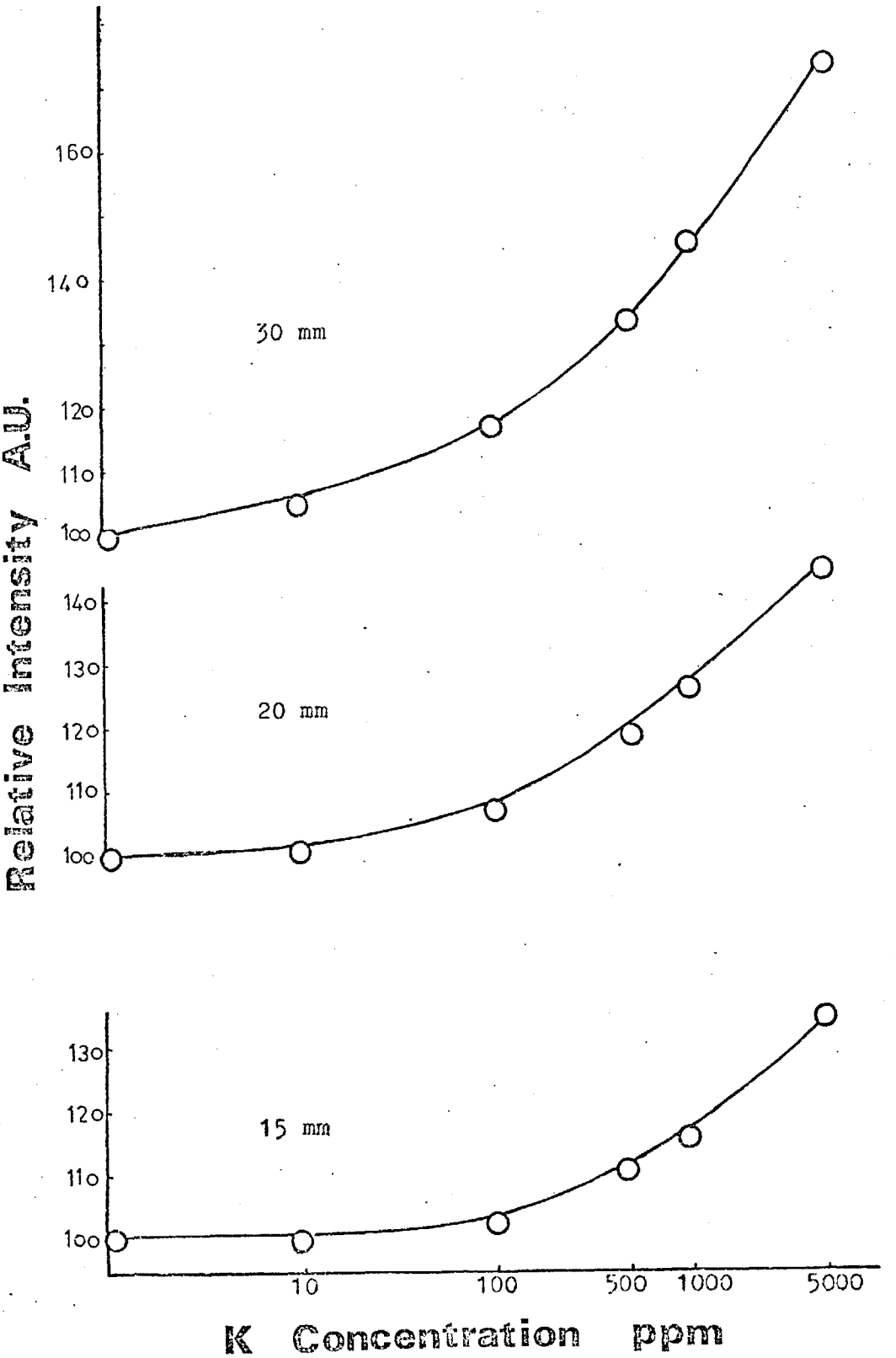


Fig. 4. 13. Effect of K on CaI 422.6 nm emission intensity at three heights of observation above load coil (10 ppm Ca)

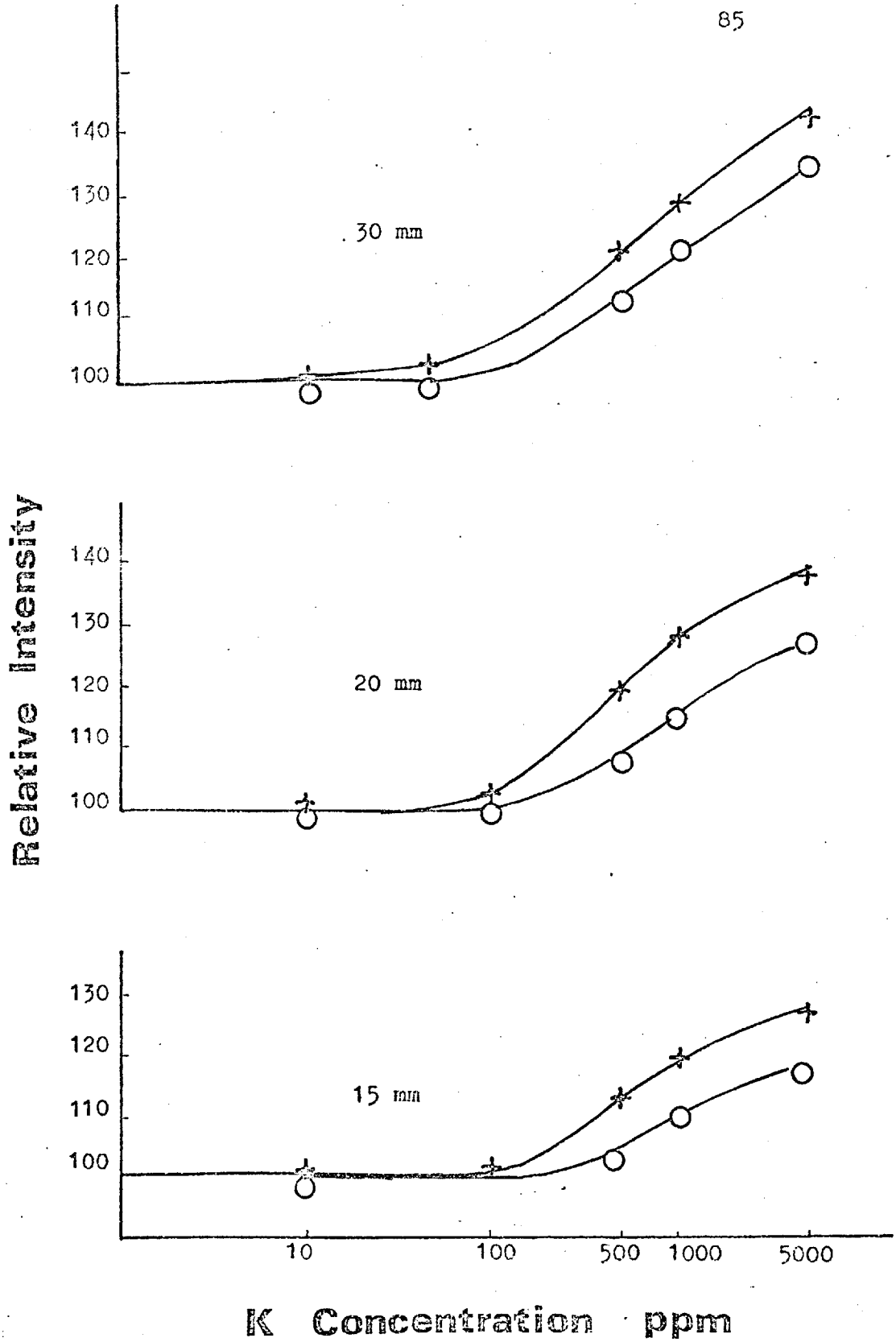


Fig. 4. 14. Effect of K on MoI 379.8 nm (+), and 390.3 nm (0) emission intensity at three heights of observation above load coil (10 ppm Mo)

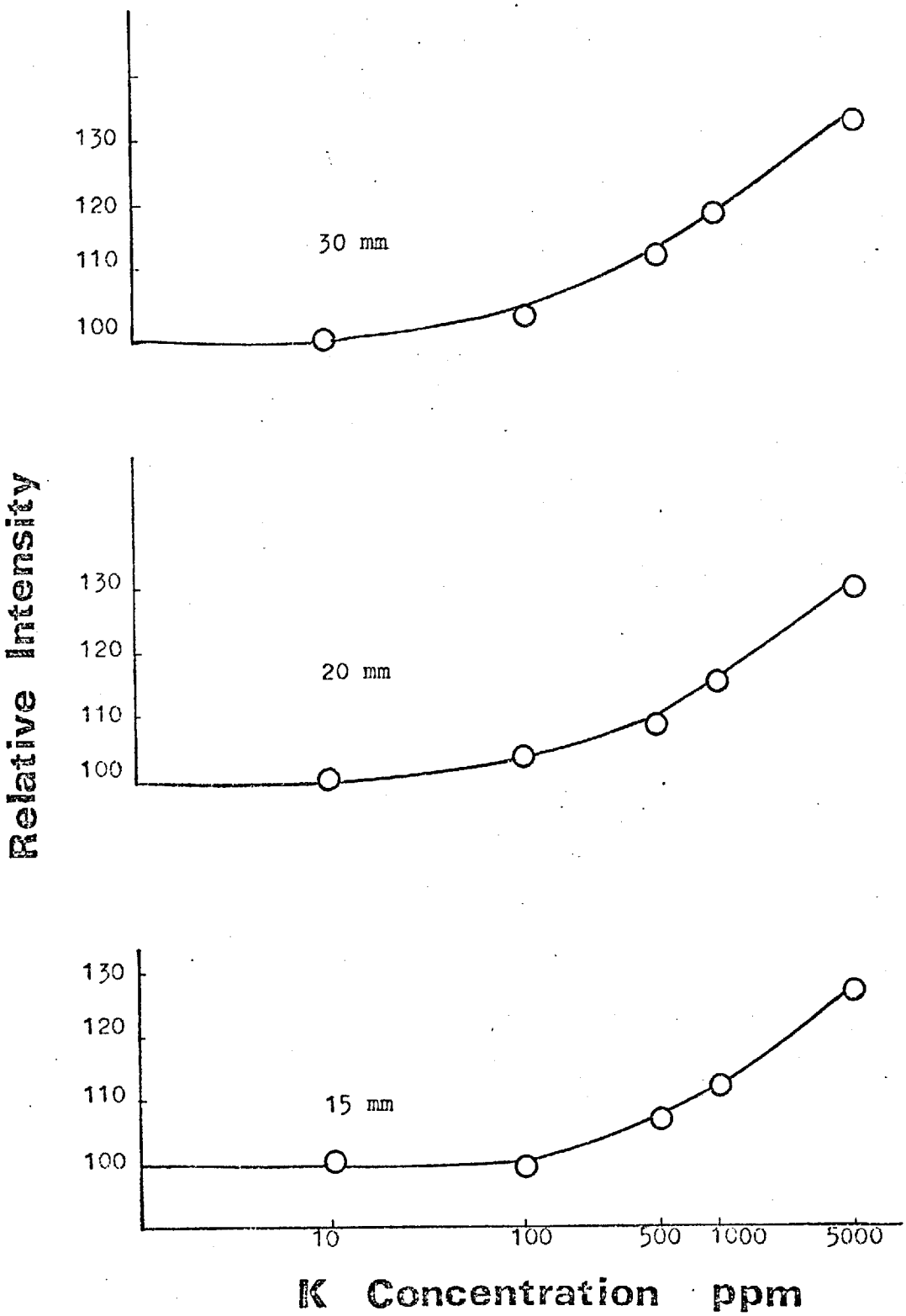


Fig. 4. 15. Effect of K on BI 249.8 nm emission intensity at three heights of observation above load coil (10 ppm B)

high concentrations of easily ionizable elements not only shift the ionization equilibrium but may also produce transport interference due to the higher viscosity.

Another interesting point to note in Figs 4.13-4.15 is that by increasing the height of observation the interference effect increases. This has been confirmed by the effect of Ca, Ba, Na, Mg, Mn, Al on Mo, Co and B atomic lines.

Fig. 4.14 also shows that less interference effect was observed at 390.3 nm than at 379.8 nm for Mo I. However, the 390.3 nm line is not as sensitive as the 379.8 nm line and it could only be used when low detection limits are not essential.

Fig. 4.16 shows the interference effects produced by K on Ca, Mo and B at two different injector flow rates. More enhancements were observed for all species at a flow rate of 2.6 l min^{-1}. This indicates that the operating parameters must be carefully controlled.

4.2.3 Dependence of Interference Effect on Interferent Concentration

In order to study the dependence of interference effects on the Interferent concentration, two sets of experiments were carried out:

(a) The concentration of the interfering element was kept constant and the interference was studied at different Interferent to analyte concentration ratios.

(b) The Interferent to analyte concentration ratios were kept constant and the interference was studied at different concentrations of Interferent.

Fig. 4.17 shows the interference effect of Na on Mo I for various concentration ratios of Na to Mo at constant Na concentration (5000

and/

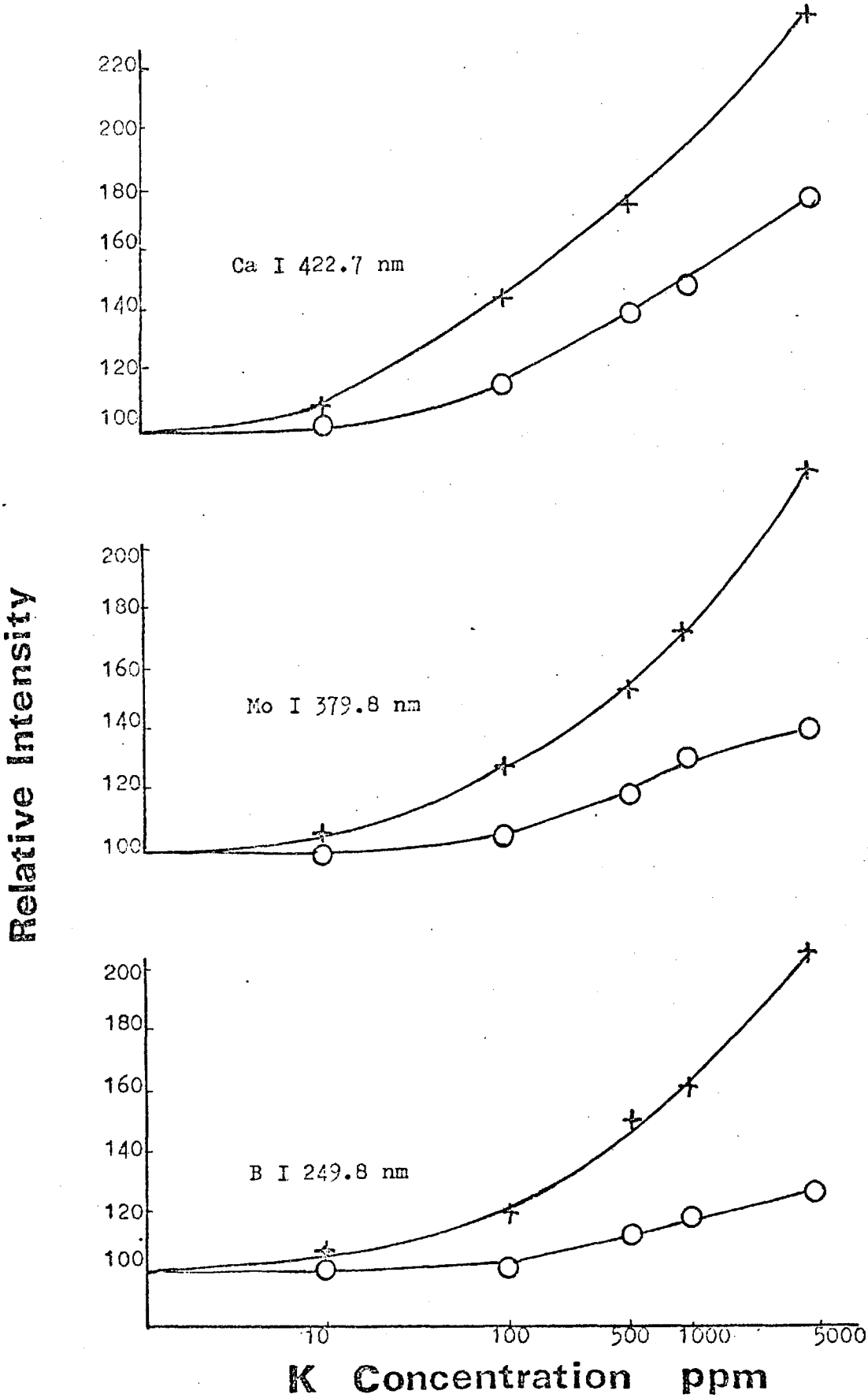


Fig. 4. 16. Comparison of the effect of K on 10 ppm B, Mo, and Ca emission intensity at two different injector flow rates (+)2.6 l/min and(0)1.6 l/min

and 1000 ppm). Fig. 4.18 shows similarly the effect of K on Ca I.

It was concluded from Figs 4.17-4.18 that if the concentration ratio of interferent to analyte is greater than 10^3, then the ionization interference effect tends to depend on the concentration of the interferent element only and not on the concentration ratio of interferent to analyte. This fact is important in real sample analysis because once the nature of the interference is identified buffering of the solution enables the analysis to be done without fear of matrix effect.

Fig. 4.19 shows the interference effect of Na on Mo I for various Na concentrations and constant Na to Mo concentration ratios (100 and 500 times). Fig. 4.20 shows similarly the effect of K on Ca. Figs 4.19, 4.20 support Figs 4.17, 4.18 and even though these two sets of experiments were carried out on different days and at different concentration ranges they are in a good agreement with each other.

Similar experiments were carried out with the effect of Ca on Mo, Al on Cd, Cu on Co and Ca on Co but the results differed from that of ionization interference. It seemed that other types of interferences were responsible and although some trends could be recognized, the main conclusion was that the picture was complex and further analysis of it in this stage of the investigation was not useful.

4.2.4 Mechanism of Al Interference on Mo

The enhancement of Mo I emission in the presence of Al has been observed in flame sources (44,87,97) and also in the ICP under operation in our laboratory. Enhancement effects of this kind in the ICP may be partly attributed to a lateral diffusion, as suggested by Boumans and de Boer (64). The lateral diffusion effect was first observed by

Koirtyohann/

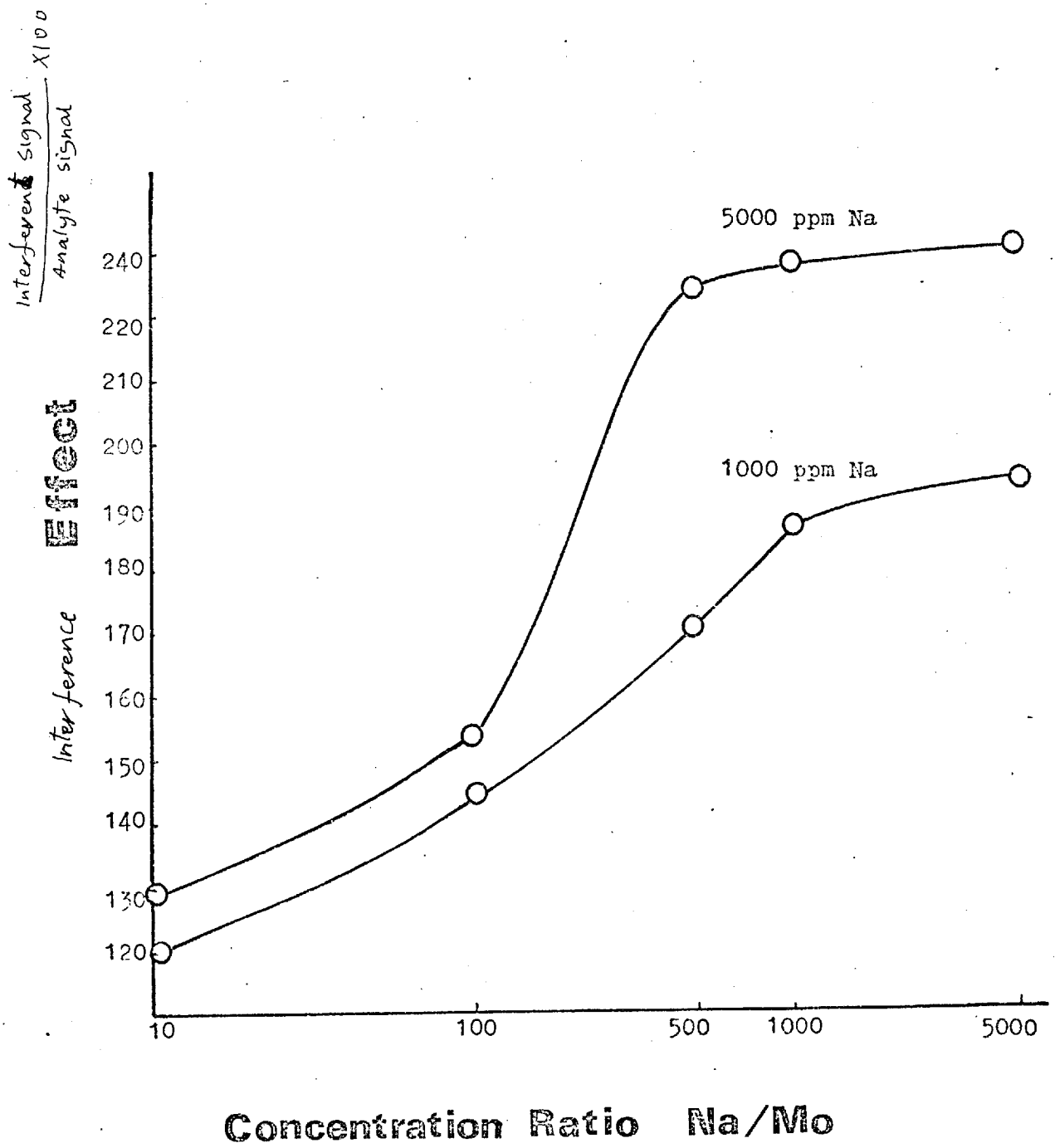


Fig. 4. 17. Interference effect of Na on MoI emission (379.8nm) for various concentration ratios of Na to Mo and constant Na concentration (1000 and 5000 ppm Na)

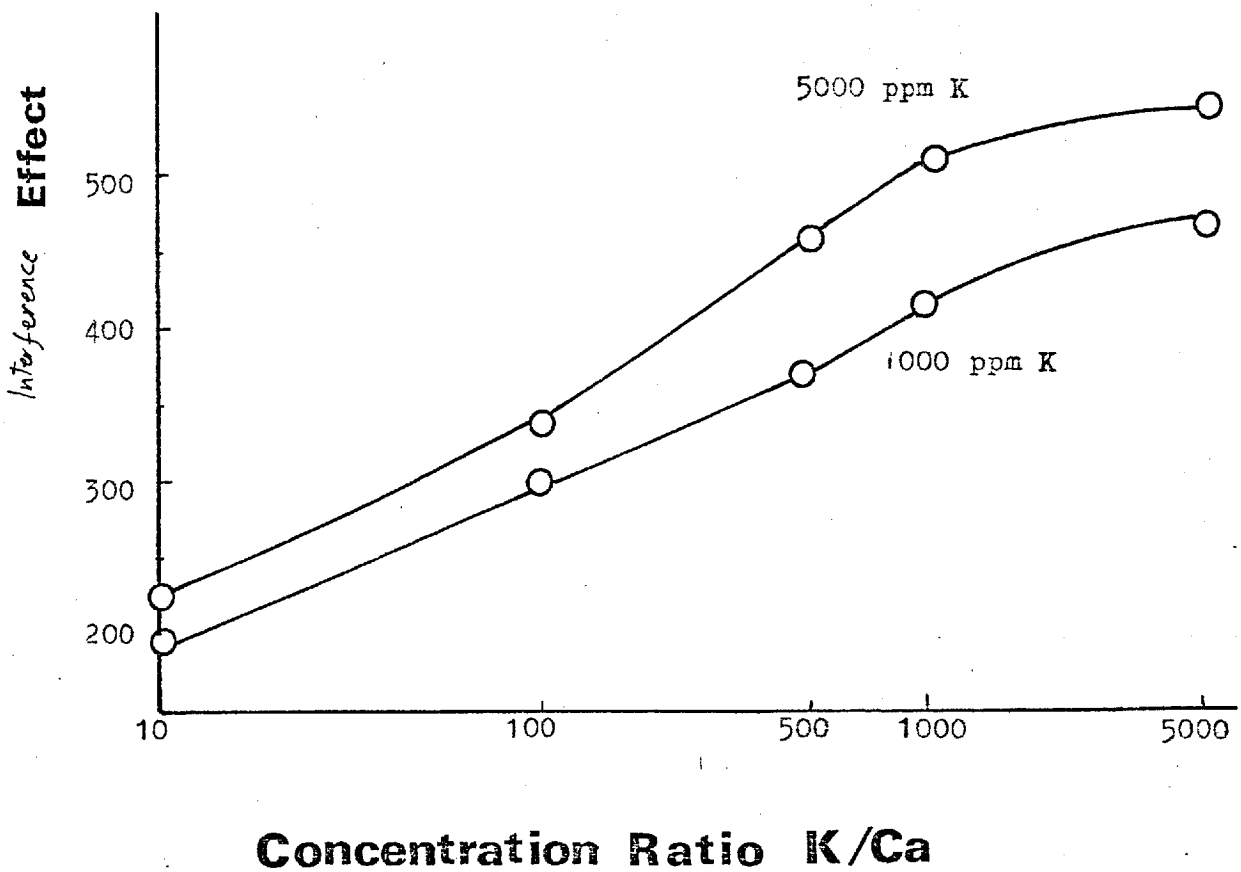


Fig. 4. 18. Interference effect of K on CaI emission (422.6nm) for various concentration ratios of K to Ca and constant K concentration (1000 and 5000 ppm K)

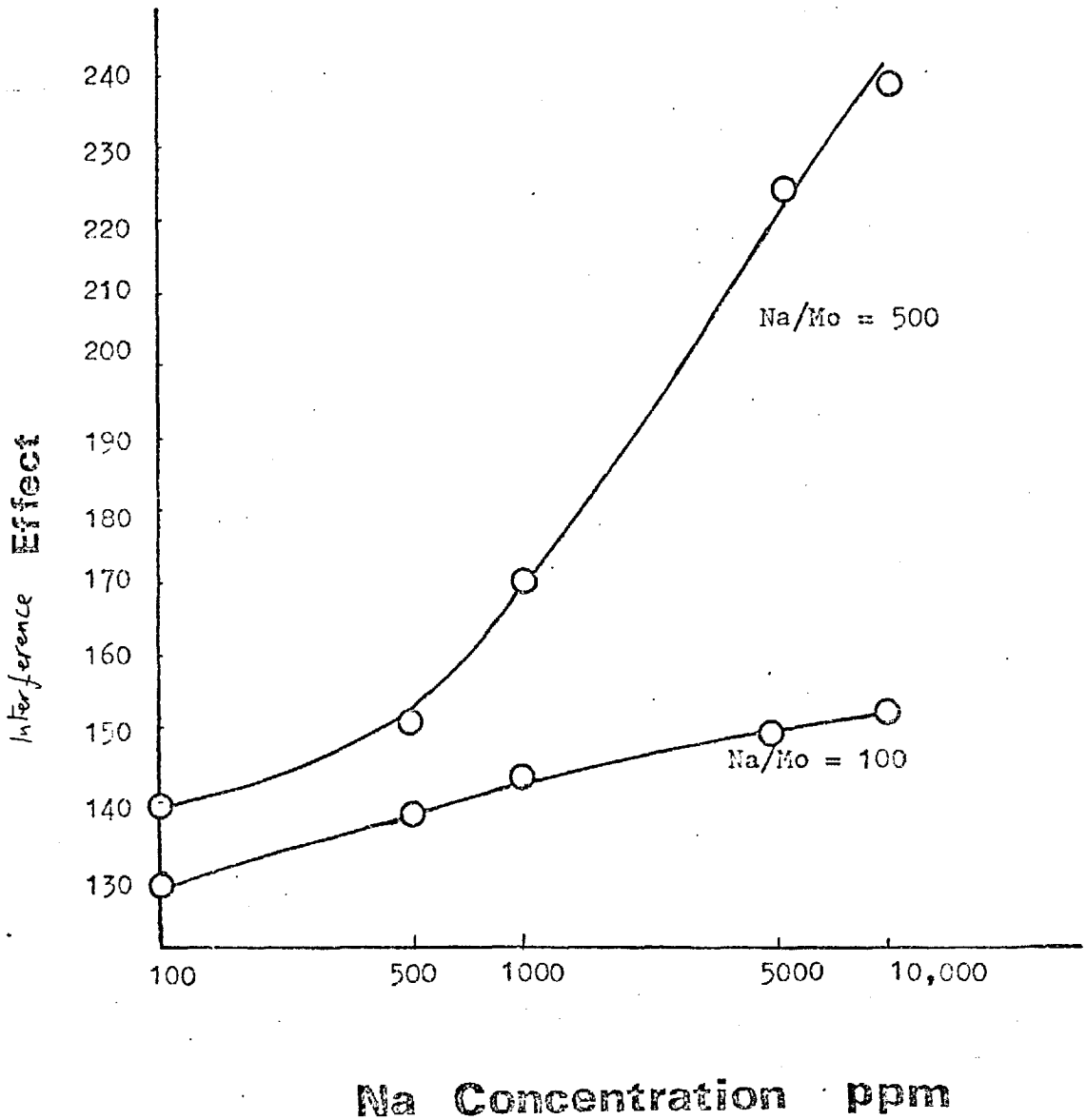


Fig. 4. 19. Interference effect of Na on MoI emission (379.8nm) for various concentrations of Na and constant concentration ratios of Na to Mo (100 and 500 times)

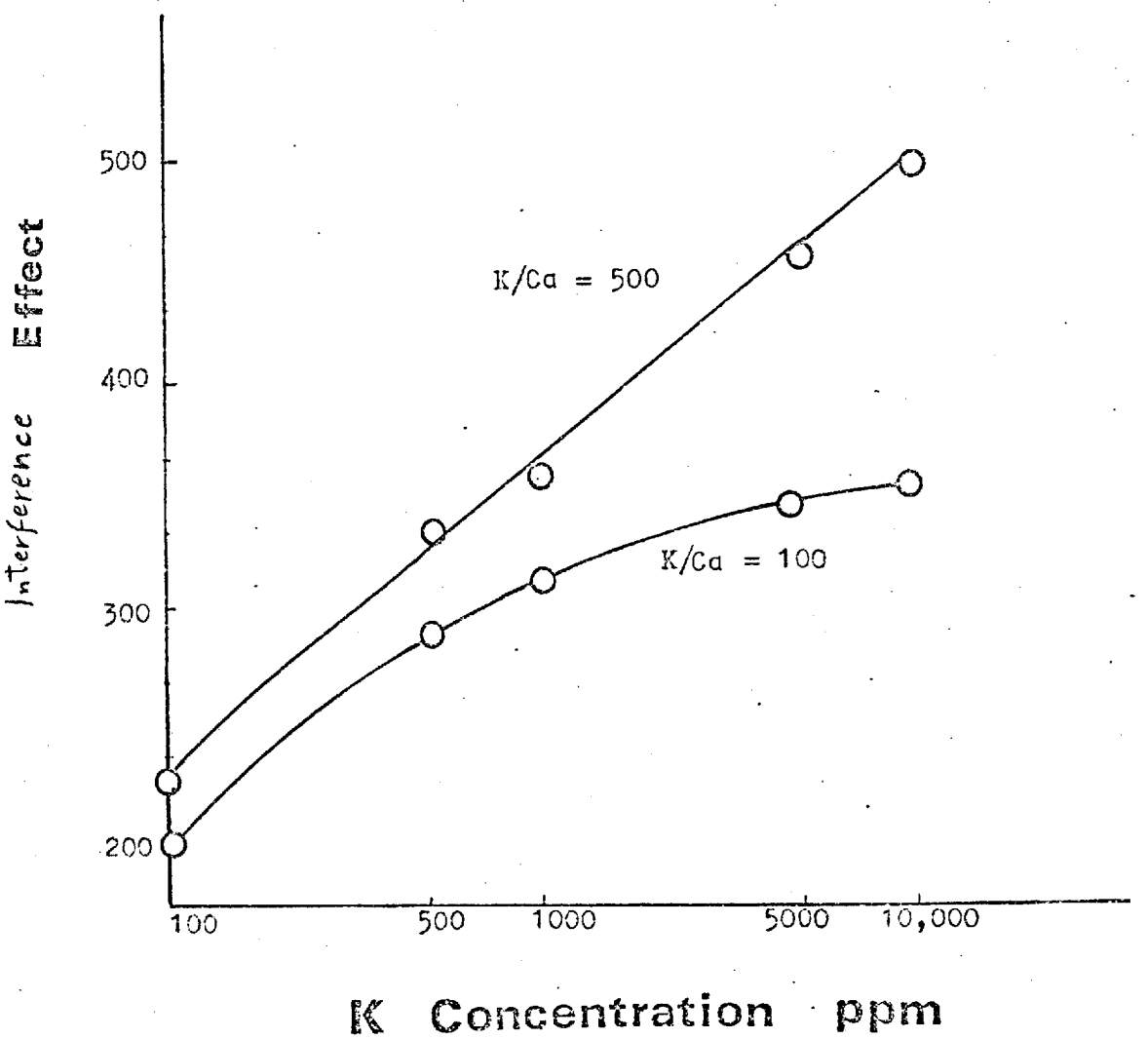


Fig. 4. 20. Interference effect of K on CaI emission (422.6nm) for various concentrations of K and constant concentration ratios of K to Ca (100 and 500 times)

Koirtyohann and Pickett (88) in a N_2O-C_2H_2 flame and later was more extensively studied by West et al (89). According to this hypothesis, the concomitant delays the production of free atoms, thus shortening the time available for lateral diffusion of the atoms before they enter the optical path. The atoms, therefore, diffuse a shorter distance and are concentrated at the flame center. The lateral diffusion hypothesis postulates a matrix effect that may be physical and non-specific as well as due to specific chemical reactions (89).

In the case of the ICP this would mean that the concomitant retards the atomization of the analyte during its passage through the central channel and this affects spatial distribution patterns. This conclusion is indeed supported in practice and as shown in Fig. 4.21 the optimum height of observation for Mo moved higher up in the plasma in the presence of Al.

Another and probably more satisfactory mechanism for the enhancement of Mo caused by Al may be explained on the basis of work by Rubeska (90-91). The suggested mechanism assumes that volatile Mo oxides are reduced to the less volatile metal and/or carbide, at high temperature, which prevents complete vaporisation. The presence of refractory oxides such as Al_2O_3 hinder reduction of Mo oxide before vaporisation either simply by shielding it from reducing gases or by reactions taking place in the condensed phase at high temperature. These reactions involve oxidation of the metal or carbide by oxygen from the refractory oxide (90-91). Thus the compound is vaporised in the volatile Mo form before dissociation to free atoms occurs.

4.3/

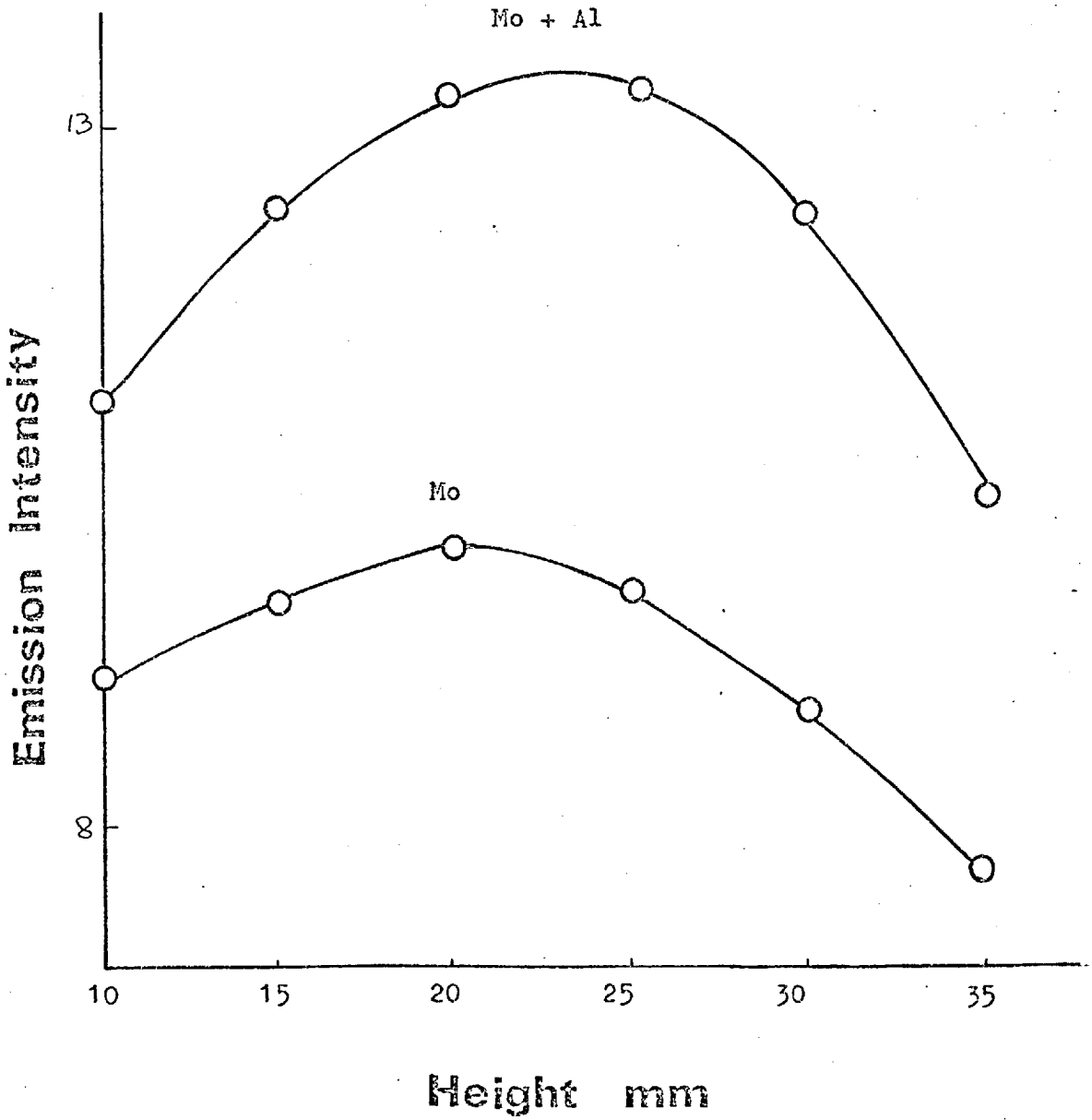


Fig. 4. 21. Variation of emission intensity at 379.8 nm with height of observation observed from solutions containing 10 ppm Mo and 10 ppm Mo + 5000 ppm Al.

4.3 DETECTION LIMITS

The term detection limit is used to define the lowest detectable concentration of the analyte in the sample solution. It is defined as the concentration of an element that will produce a signal that is twice the rms noise level. The detection limit depends on the instrumental stability and may vary considerably from instrument to instrument. Factors such as the sample matrix, gas pressures and flow rates, torch configuration, available power, type of nebulizer and generator used, and height of observation critically affect the detection limit.

Table 4.1 shows a compilation of the detection limits observed in this work [column 1], along with ICP-OES detection limits for compromise conditions published recently by Fassel and Kniseley (94) [column 2]. For comparison, the recent compilations of detection limits obtained by flame atomic absorption (AAS), emission (AE), and fluorescence (AFS) are also included (95, 96)

Table 4.1. Comparison of Experimental Detection Limits

	ICP ppm		Flame ppm		
Element	present work	Fassel-Kniseley (94)	AAS	AFS	AE (95, 96)
B	0.05	0.005	6	-	30
Cd	0.03	0.002	0.001	0.00001	0.8
Co	0.05	0.003	0.005	0.005	0.03
Ga	0.03	0.014	0.07	0.01	0.01
Ge	5	0.15	1	20	0.5
In	1	0.03	0.05	0.002	0.003
Mo	0.01	0.005	0.03	0.06	0.1

The detection limits for this work are in all cases worse than those reported by Fassel. This can be attributed to a number of factors, but particularly/

particularly the high R.F. noise level of our source. This noise is a characteristic of the generator type and cannot be removed without extensive modification of the R.F. oscillator. Another major factor is the difference in the rate of sample delivery to the plasma [2.8 ml/min sample uptake rate for aerosol argon flow of 1 l/min in the Fassel et al ICP (75) and 0.45 ml/min sample uptake rate for argon flow of 1.6 l/min in the our ICP]. The use of ultrasonic nebulisation in particular can often make a dramatic improvement. Another factor affecting the detection limit is the torch size and configuration. In small "Fassel type" torches, the power is dissipated in a smaller volume of gas, therefore the temperature is higher. Furthermore, in these torches the toroid is smaller, therefore the effective temperature experienced by the sample will also be higher for a given power input. Finally, the high resolution monochromator system used by Fassel plays an important role in the improvement of detection limits since it results in an improved signal/background ratio. There can also be differences in the detection limits due to different choice of analytical lines. It is, however, important to remember that with the possible exception of systems which are designed and optimized for one element, the blind acceptance of a low detection limit as an indicator of merit of the emission source is not recommended.

Butler et al (59) have shown that the detection limits observed under idealized conditions are transferable to "real-life" situations, i.e. in the presence of the sample matrix. They have demonstrated that the presence of a 0.5 wt % Fe matrix under standard operation condition showed no significant deterioration in the detection limit values of 12 elements. It should, however, be stated that the presence of matrix leads to some enhancement/

enhancement of the background intensity, and also to changes in the spatial profiles of the plasma. The net effect on the detection limits is a deterioration which is not greater than a factor of 2 under the conditions adopted in this work.

4.4 PRECISION

The reproducibility of intensity measurements is expressed as the relative standard deviation (RSD) at concentration levels 100 times the detection limit in aqueous solutions. The mean RSD of 4 spectral lines (B I 249.8, Co I 345.3, and Mo I 379.8 and 390.3 nm) was 0.85%.

CHAPTER V

THE APPLICATION OF THE INDUCTIVELY COUPLED PLASMA TO THE ANALYSIS OF SOIL SAMPLES

5.1 MOLYBDENUM

5.1.1 Introduction

The determination of Mo has been frequently reported in routine spectrochemical analysis of geological materials and soils (7, 97, 98). Because of the poor sensitivity of Mo by atomic absorption spectrometry its determination by this method has received less attention than most other elements. Several workers have employed with effect preliminary concentration by extraction with an organic solvent (99, 100). However, many chemists have preferred to use either the thiocyanate or toluene 3,4 dithiol colorimetric methods. The thiocyanate method is the most sensitive of colorimetric methods but it does have some major limitations, such as precipitation of Cu thiocyanate complex in the presence of relatively small amounts of Cu. This precipitate can adsorb some of the colour of the thiocyanate complex. Cr, W, Co and Pb can also interfere by either precipitating or by forming interfering coloured complexes with thiocyanate. Sutcliffe (97) has developed a simple and direct method for the determination of Mo in geological samples by atomic absorption spectrometry. The method is free from interference and as accurate as the thiocyanate method.

Robinson and Alexander (101) suggested that the normal level of Mo in soil is 2.5 ppm, based on nearly 1000 analyses of soils from all over the world. An average level of <0.05 and excess level of >0.1 ppm Mo in dry Scottish soil has been reported (102). (An excess level is a level at which an effect may arise with some type of plant material or with an animal consuming it.) The variation of this metal in plants is considerable, with levels up to several ppm being reported although less

than/

than 1 ppm is more usual.

5.1.2 Choice of Analytical Line

The two most sensitive Mo lines 379.8 and 390.3 nm can rarely be used in spectrochemical methods because of interferences. The CN band with emission peak at 388.3 nm interferes at 379.8 nm and the Fe 390.3 nm line which is very intense interferes at 390.3 nm. The Mo 317.0 nm line, however, being relatively sensitive and generally free from interference has been widely used. In the ICP source the effect of CN emission is minimal; therefore, the sensitive Mo 379.8 nm line can be used. Furthermore, with the present source, the emission spectrum for Mo in the region of 379.8 nm was found to be simple and the background was quite low. The emission spectrum in the region of 317.0 nm was very complex and of a high level (see Figs 5.1 and 5.2).

5.1.3 Standard Solutions

A stock solution containing 10'000 ppm Mo was prepared by dissolving ammonium molybdate in distilled water. Another stock solution was made in the same way but in 1M ammonium acetate solution. (Mo is extracted from soil samples in 1M ammonium acetate.) Stock solutions of interference ions were prepared from Analytical grade salts (generally chlorides) dissolved in deionised water. Necessary precautions were taken to avoid contamination.

5.1.4 Calibration Curves

Calibration curves established for Mo as ammonium molybdate in aqueous and in 1M ammonium acetate solutions at 379.8 nm are shown in Figs 5.3 and 5.4 respectively. In both cases significant deviation from linearity did not occur over the concentration range of 0.1-10'000 ppm. This long

linear/

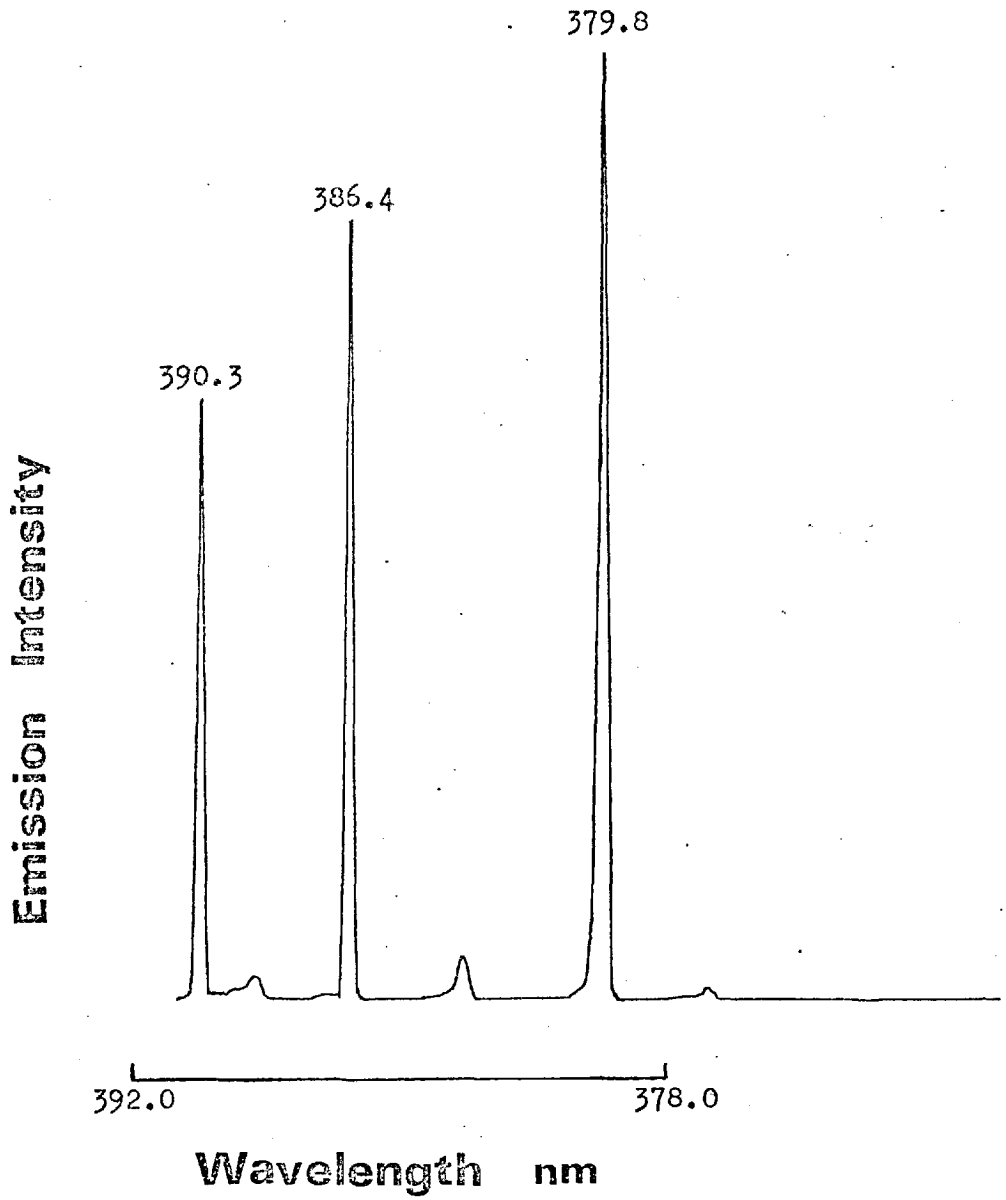


Fig. 5.1. Emission spectrum observed from 10ppm Mo over the wavelength range 378.0 - 392.0 nm.

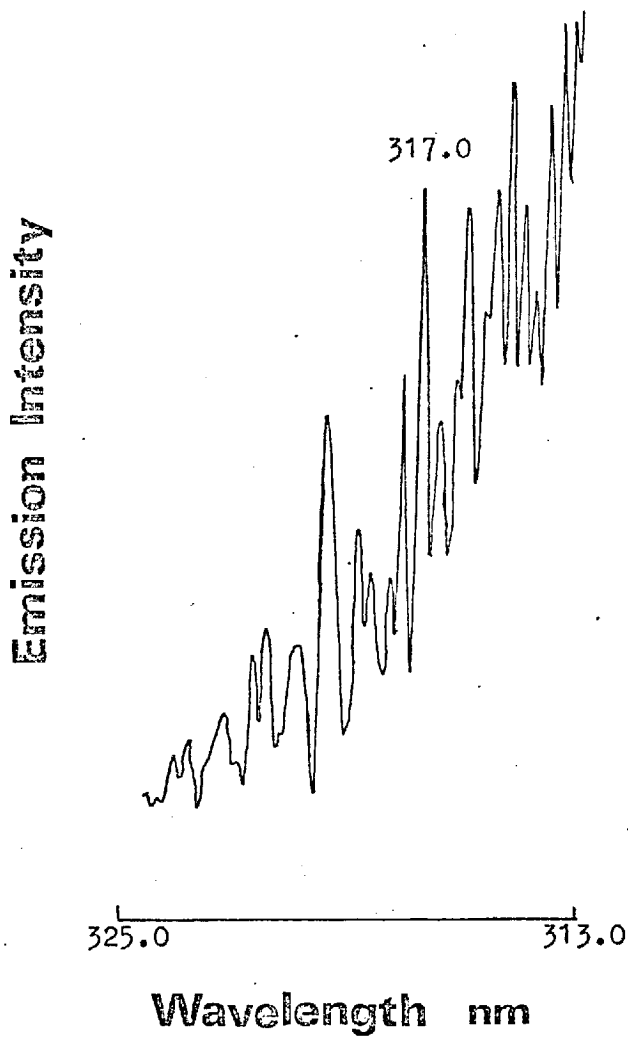


Fig. 5. 2. Emission spectrum observed from 10 ppm Mo over the wavelength range 313 - 325 nm.

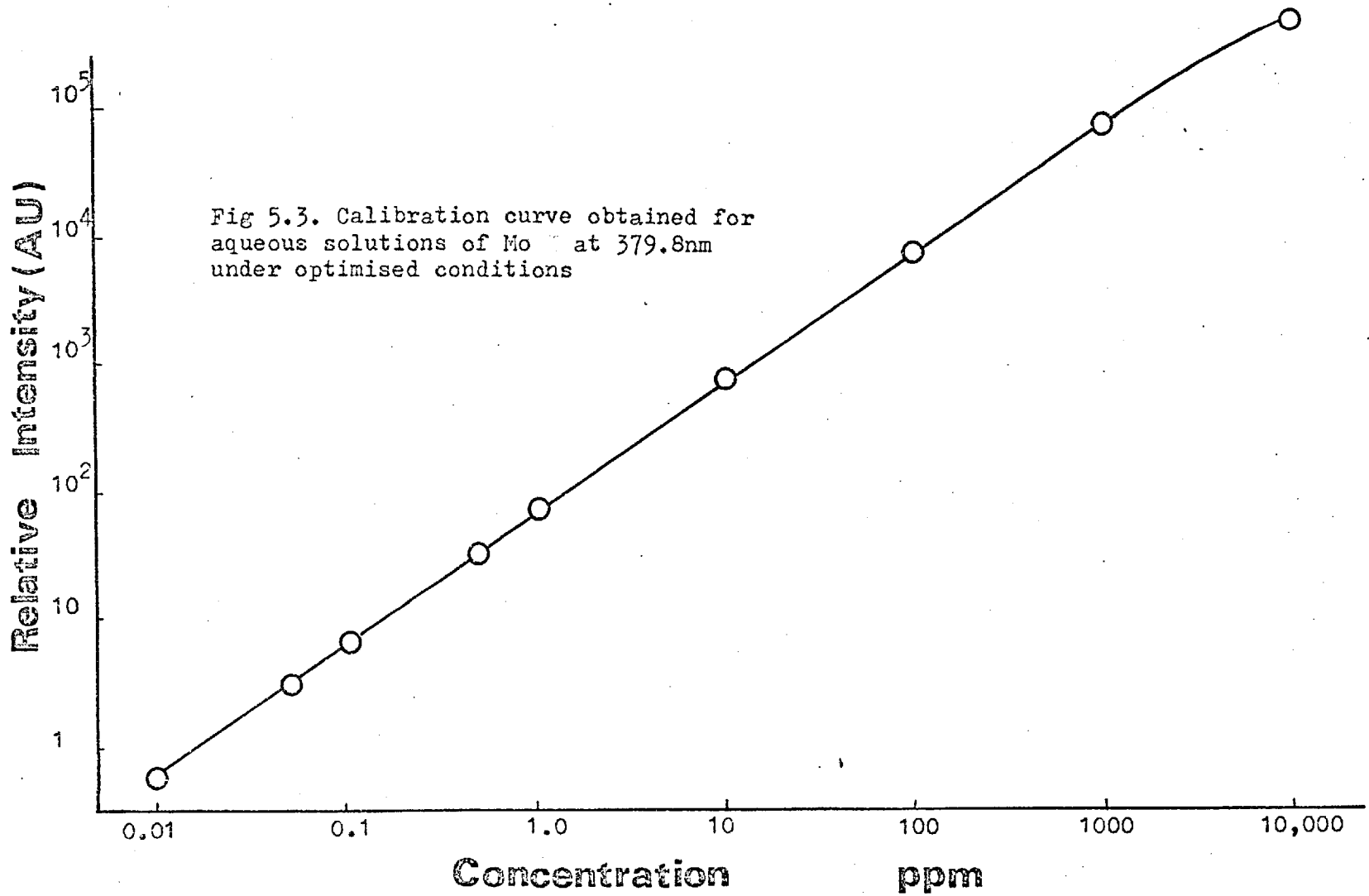


Fig 5.3. Calibration curve obtained for aqueous solutions of Mo at 379.8nm under optimised conditions

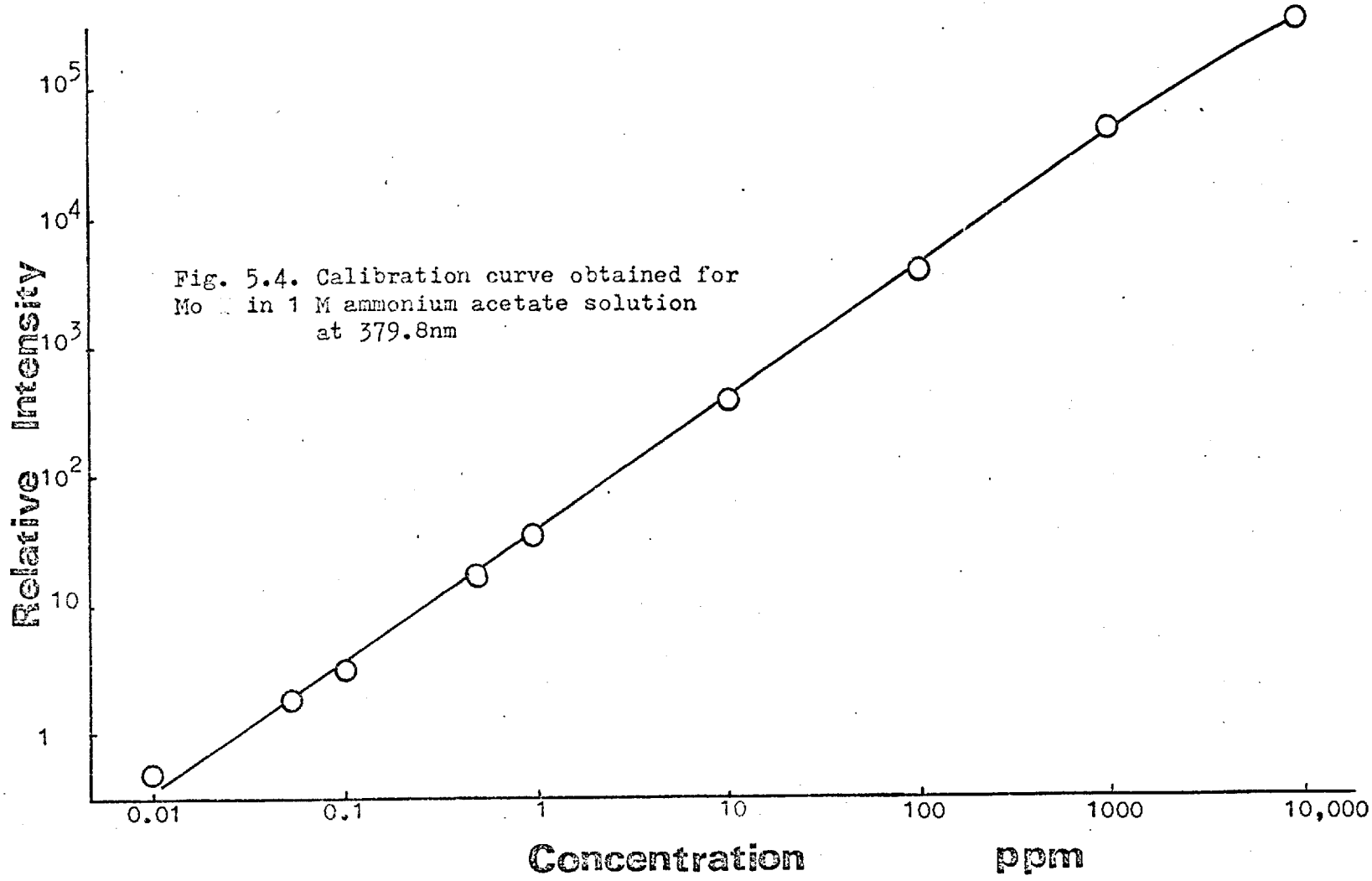


Fig. 5.4. Calibration curve obtained for Mo in 1 M ammonium acetate solution at 379.8nm

linear dynamic range of the calibration curves may be ascribed to the low background emission and the absence of self-absorption in the plasma. It is believed that there is little mixing between the central gas stream carrying the sample and the plasma gas where the discharge takes place. Therefore, all the analyte atoms are confined to the plasma central channel and the tailflame, in particular they do not occur in the cooler regions that surround the tailflame, so that the self-absorption is low.

The presence of ammonium acetate increased the background and reduced the Mo signal, which resulted in a raising of the detection limit from 0.005 ppm (for aqueous Mo solution) to 0.01 ppm. Fig. 5.5 shows the signals obtained for Mo in aqueous and in 1M ammonium acetate solutions. At this state a study of the emitted spectrum of the ICP was thought to be necessary to explain the reduction of detection power in the presence of ammonium acetate.

5.1.5 Emission Spectra

In order to demonstrate the increase in the background caused by ammonium acetate, the emission spectra of deionized water and ammonium acetate solution were obtained in the range of 350.0-400.0 nm (Figs 5.6 and 5.7). A high continuum background was observed above 375.0 nm for ammonium acetate, the background for water remaining low throughout the entire range.

Figs 5.6 and 5.7 also show the structural background observed in the plasma. In general it consists of Ar lines, OH band emission and weak band emission from NO , NH, CN and C2. Some of the emission lines have been identified on the spectrum. The continuum is largely attributed to the processes of ion recombination with electrons and the bremsstrahlung radiation/

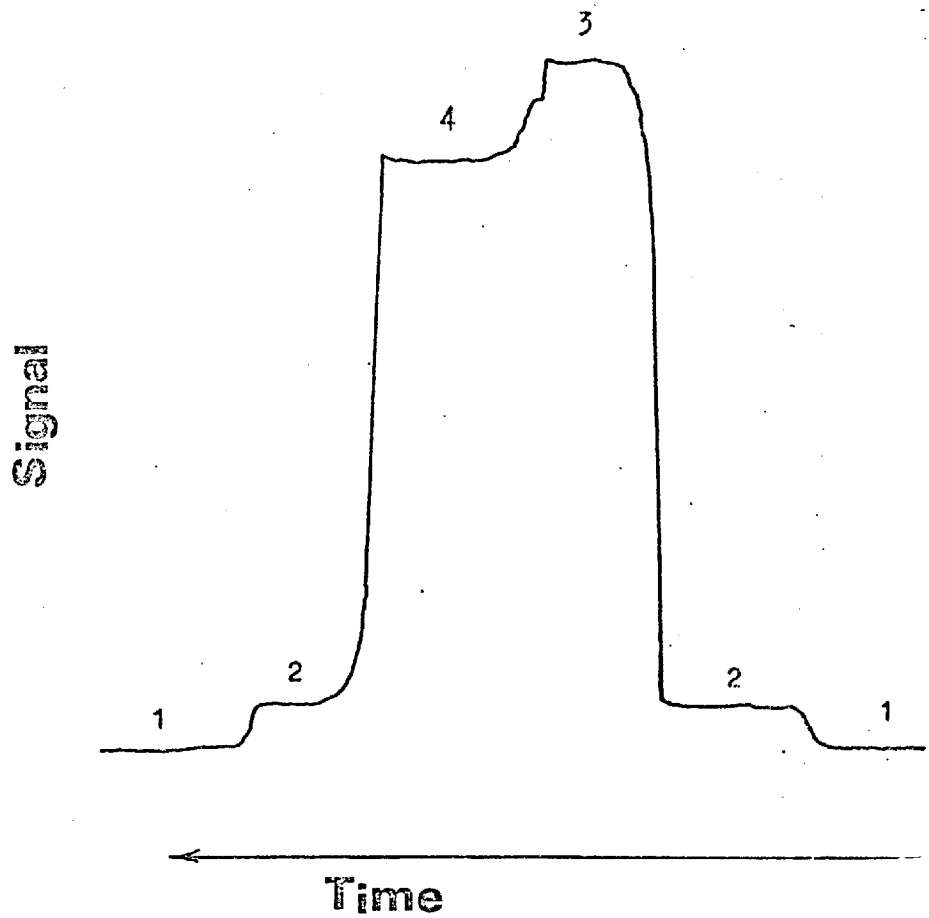


Fig. 5. 5. Effect of ammonium acetate solution on background and Mo signal at 379.8nm
1. water, 2. 1M ammonium acetate, 3. 10 ppm Mo and 4. 10 ppm Mo in 1M ammonium acetate

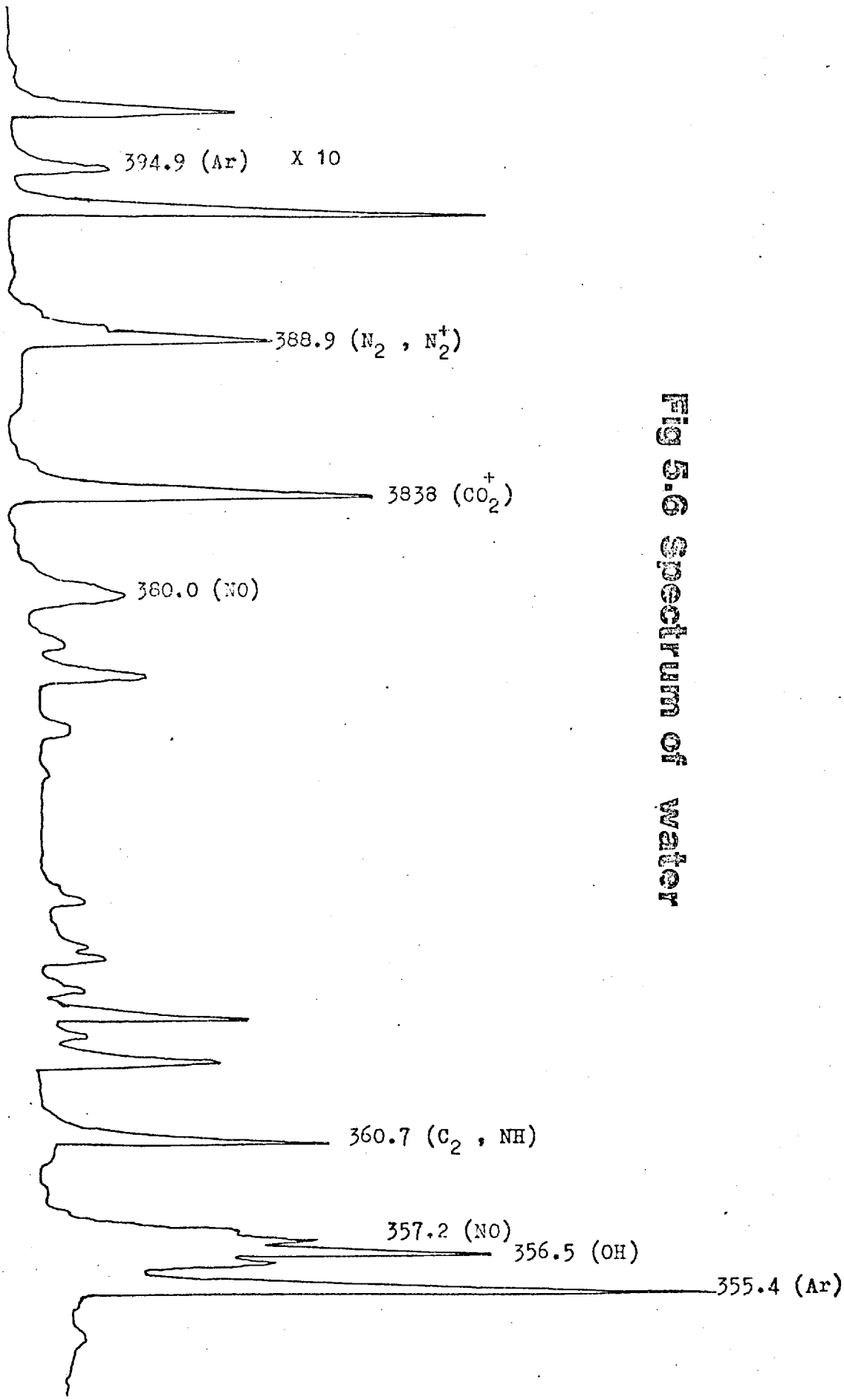


Fig 5.6 Spectrum of water

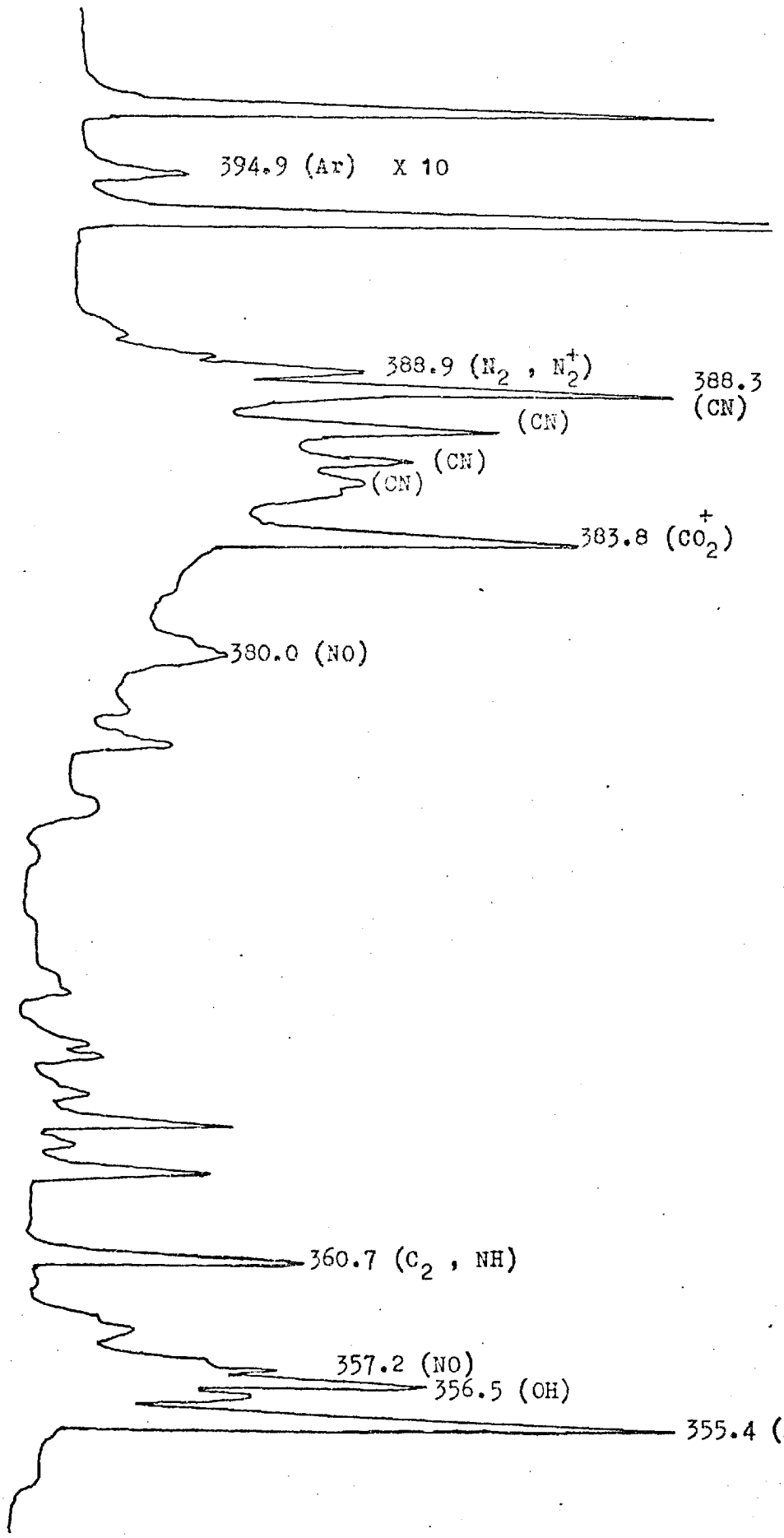


Fig 5.7 Spectrum of ammonium acetate

radiation caused by the deceleration of electrons in the neighbourhood of heavy ions. Therefore, the continuum depends strongly on the electron density.

5.1.6 Interference Effects

Interference effects of the following elements:- Na, K, Fe, Mg, Mn, Ca, and Al on Mo I 379.8 nm and 390.3 nm lines were observed when fifty-fold excesses of them were present in a solution containing 10 ppm Mo as aqueous ammonium molybdate. The magnitude of these interferences are shown in Table 5.1.

Table 5.1. Effect of Concomitants on Emission of 10 ppm Mo

Concomitant 500 ppm	Emission Intensity A.U. 379.8 nm	390.3 nm
None	100	100
Na	130	119
K	120	107
Fe	115	127
Mg	119	125
Mn	126	110
Ca	125	120
Al	120	115

Blank corrections were applied for all cases where it was necessary.

The experimental results suggest that the interference level increases with matrix concentration and may reach a value of 30% for atom lines. In contrast, in a high temperature N_2O-C_2H_2 flame, the matrix effects have been reported to range from -70 to +50% (89). The presence of acids such as HCl, HNO_3 slightly decreased the emission intensity of the Mo atom line.

Al has been widely used in flame spectroscopy as interferent suppressor and/

and therefore it was decided to investigate its usefulness in the ICP. The results presented in Chapter 4.2.4 showed that Al enhances Mo line emission (and therefore increases sensitivity) and also shifts the spatial emission peak. Table 5.2 shows the results of Al addition at the optimised viewing height for Mo (alone) in the range 0→6000 ppm Al.

Table 5.2. Effect of Al on Mo Emission

(Each solution containing 10 ppm Mo)

Al added ppm	0.0	10	100	500	1000	5000	6000
Relative Intensity	100	103	111	120	130	135	135

It can be seen that above 5000 ppm Al, there was no further effect on Mo line intensity and therefore experiments on interferent suppression were performed with 5000 ppm Al added to the solution. Table 5.3 indicates that Al at this level was highly effective in suppressing interference from most of the important concomitants found in soil extracts.

Table 5.3. Effect of Al as an Interference Suppressor

(Each solution containing 10 ppm Mo and 5000 ppm Al)

Metal tested	None	Na	K	Fe*	Mg	Mn	Ca
Amount added ppm	0.0	1000	2000	4000	4000	3000	2000
Relative Intensity	100	100	100	101	100	100	101

* Spectral interference is not included

5.1.7 Sample Preparation

A typical procedure for the extraction of Mo from soils is that employed at the Macaulay Institute, which is as follows:

A 50 g sample of soil is shaken overnight with 800 ml neutral normal ammonium/

ammonium acetate. The whole extract is filtered through an 18.5 cm Whatman No. 540 filter paper, as much of the soil as possible being transferred to the paper in order to minimize the passage of clay particles. The paper is washed several times with distilled water, and the filtrate evaporated to dryness, partially on a hot plate and then to completion on a steam bath. The residue is treated twice with 5 ml portions of redistilled HNO_3, then with 10 ml 6N redistilled HCl, the solution being taken to dryness after each addition. The residue is then taken up in 50 ml HCl and the extract filtered through a 9 cm Whatman No. 541 filter paper into a beaker. The solution is then diluted to the appropriate concentration. Some soils require more than two treatments with HNO_3 to oxidise the extracted organic matter completely.

Our experience has shown that with the ICP source there is no need for treatment with HNO_3, as organic matter at the concentration levels occurring in soil extracts do not cause any disturbance in the plasma. (See section 5.1.9.) However, some extracted solutions contained solid particles which made the nebulisation process unstable. In these cases samples were treated once with HNO_3 in order to obtain clear solutions free from particulates.

5.1.8 Analysis of Mo in Soil Extracts

In order to illustrate the capability of the ICP in the analysis of real samples, a few examples of applications are given in this chapter. Different soil samples each containing 25 g of soil in 50 ml of solution were analysed for Mo. Digestion with conc. HNO_3 was applied whenever it was necessary (to 10 ml of solution, 1 ml of conc. HNO_3 was added and the solution boiled to low volume and then diluted to 10 ml). The standard addition technique/

technique was used to determine Mo in soil samples and a typical analytical curve established by this method is shown in Fig. 5.8 for sample D41152. Background correction was applied in these determinations. The results of the analyses are shown in Table 5.2.

Table 5.4. Determination of Mo in Soil

	Extracts using ICP					
	concentration of Mo (ppm)		Matrix concentration (ppm)			
Sample	ICP	Macaulay	Ca	Mg	K	P
D41152	3.1	3.1	1140	-	85	22
D63405	0.30	0.31	2220	160	100	24
D63403	0.20	0.19	2290	250	140	25

The sensitivity was not sufficient to allow determination of Mo in three of the soil samples. Simple preconcentration was not possible because the solutions became so viscous that the nebulization was inhibited.

In the method of standard additions, it is assumed that the entire emission by the sample is due only to the element being determined. Any other emission, such as that due to nearby emitting lines, molecular bands, or light scattering, is added in equal amounts to the readings of the sample and the sample plus added standard. Therefore, the straight line plotted in Fig. 5.8 is shifted up by an amount equal to the background emission, and the unknown concentration will appear to be greater than it actually is. Thus, when this method is employed, the background should always be corrected. It should be noted that variation in the composition of the samples can produce varying degrees of spectral interferences, i.e. the contributions of interfering elements to the intensities of the lines of the analyte may be different from one sample

to/

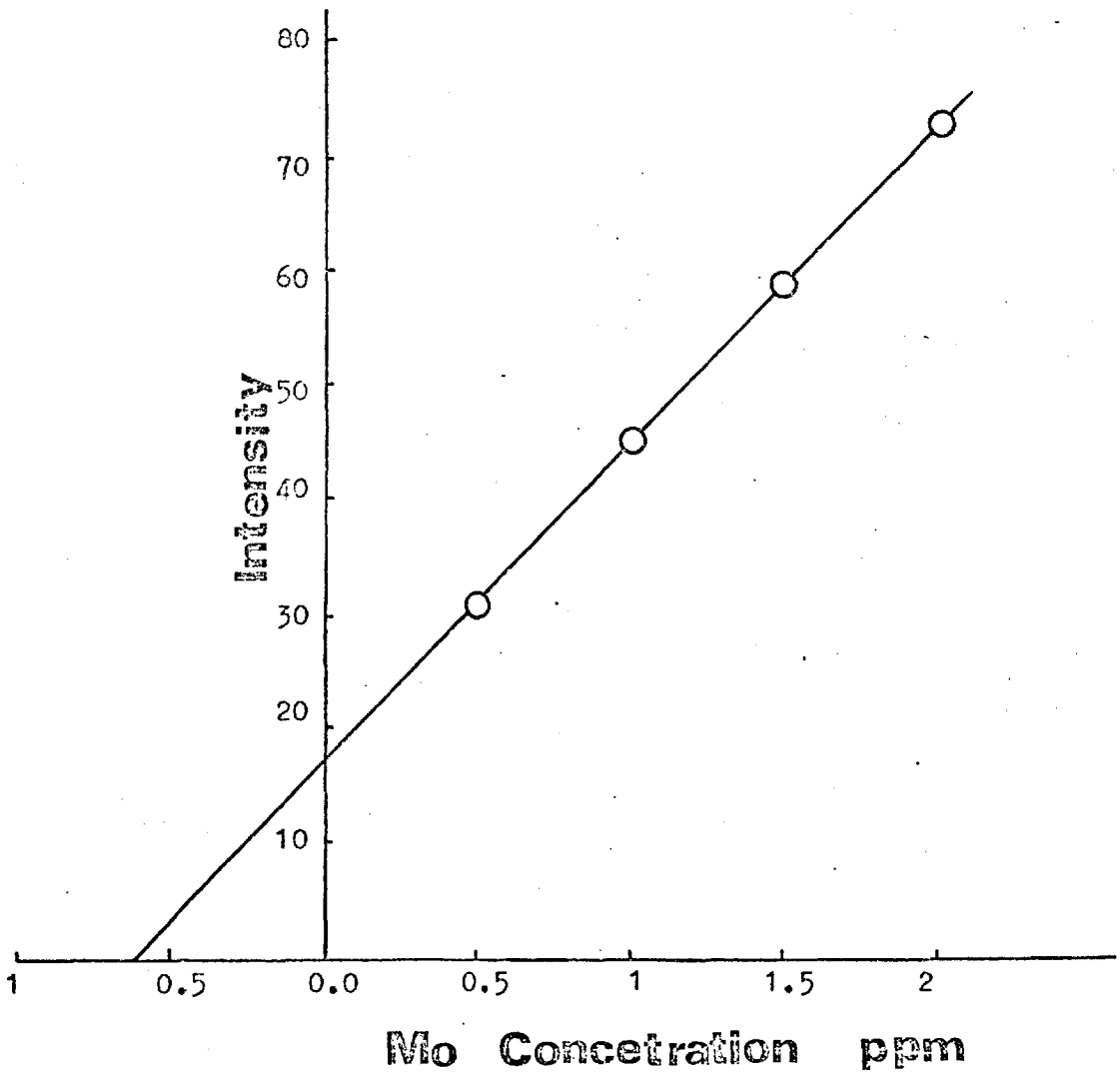


Fig. 5.8. Typical standard addition analytical curve for MoI at 379.8nm obtained from soil sample D41150 (five fold dilution)

to another. Therefore, the concentrations of possible interfering elements must also be determined in order to provide for checks and corrections. This procedure does not pose any difficulties in ICPs, because of the excellent multielement capability of the technique and the small matrix effects which permit calibrations with simple solutions.

5.1.9 Effect of Organic Matter on Mo Determination

In order to investigate the effect of organic matter on Mo emission intensity, ammonium acetate extractions of two soils with and without oxidation were studied. The following soil samples were selected:

D41150	50 g + 800 ml	NH_4OAC	0.24 ppm Mo
D41152	25 g + 400 ml	NH_4OAC	3.1 ppm Mo

Each soil was extracted four times, filtered, washed and evaporated to low bulk in the normal way. The four extracts from each soil were diluted to 200 mls in two graduated flasks. 50 ml was pipetted into each of the three beakers used for the filtration and remainder was retained in the 200 ml flasks as unoxidised extracts for each soil sample.

The first pair was oxidised with 5 ml conc. HNO_3, then treated with 5 ml 6N HCl and taken to dryness. The second pair was oxidised with two 5 ml conc. HNO_3, then treated with 10 ml 6N HCl and taken to dryness. The third pair was oxidised with three 5 ml conc. HNO_3, then treated with 15 ml 6N HCl and taken to dryness.

Finally, each extract was transferred to a 50 ml graduated flask and made up to mark. The solutions then were analysed for Mo by ICP. The Mo concentration obtained for each soil was the same in all four solutions (unoxidised, once, twice and three times oxidised with HNO_3). This indicates that the presence of organic matter in extracted solution does

not/

not affect the emission intensity of the Mo 379.8 nm atom line. Fig. 5.9 shows that the introduction of soil D41152 into the plasma as the oxidised and unoxidised solution gave the same signal and detection limit. As shown in the figure, the signal obtained for unoxidised Mo solution sample was rather pronounced and took more time to reach its maximum. This may be attributed to the fact that this solution was more viscous and affected the overall efficiency of the nebulizer and transport rate.

It has been shown that the presence of high concentrations of organic matrices such as oils, petroleum products, pharmaceutical products can cause instability in the ICP (74). The solvent tends to burn and cause instability of the discharge. This effect was observed in the plasma in the determination of Sn in organic materials dissolved in 10% acetone, 75% ethanol and 10% acid.

5.1.10 Molybdenum Determination in the Presence of Zirconium

The determination of Mo in the presence of Zr by arc spectrography has been found to give low results for Mo content. It was at first thought that Mo was being lost from the electrode in the presence of Zr. Experiments with radiactive Mo, however, showed that this was not the case (112). It is now believed that a stable Zr-Mo carbide is formed on the electrode, which does not volatilise even at the arc temperature of 6000 K and that this is responsible for the low results.

The ICP was successfully applied to the determination of Mo in the range 0.1-2.0 ppm in 0.1 M HCl solution containing Fe up to 15 ppm, Zr up to 50 ppm and 8 Hydroxy-quinoline (8HQ) up to about 2000 ppm. Standards prepared in 0.06 M HCl gave a linear calibration over the range 0.1-2.0 ppm Mo with pen-recorder deflections of about 30% full scale for 1 ppm/

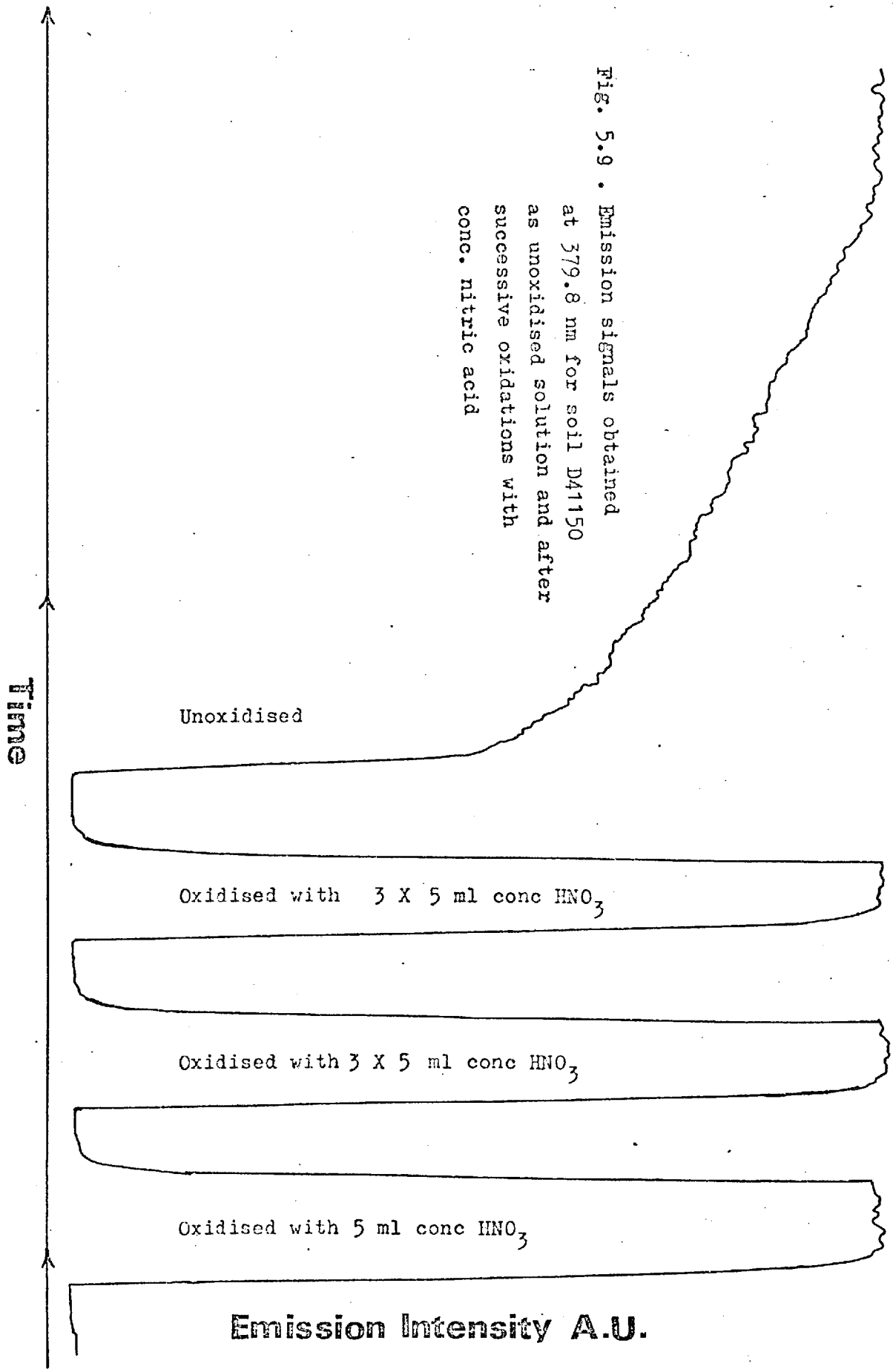


Fig. 5.9 . Emission signals obtained at 379.8 nm for soil D41150 as unoxidised solution and after successive oxidations with conc. nitric acid

1 ppm Mo. The presence of Fe, Al, Zr or 8 HQ did not have any measurable effect on this sensitivity; Fe, Al and Zr each increased the background signal while 8 HQ had no noticeable effect.

The background caused by the presence of Fe arose almost certainly from a simple line interference on Mo 379.8 nm and was linearly related to the Fe concentration in solution, 120 ppm Fe giving a signal equal to that of 1 ppm Mo. Thus, it was possible to make a good correction for Fe-background when the Fe content was known or determined independently. An investigation of the Al and Zr backgrounds indicated that the Mo determinations required the Zr and Al to be held constant. Good agreement was reached with colorimetric Mo determinations carried out at Macaulay Institute.

5.2 COBALT

5.2.1 Introduction

Co is essential for the nutrition of ruminants. It is present in nearly all soils, but it is not uniformly distributed. Gregers-Hansen (103) studied seven Danish soil types by neutron activation analysis and found a total Co concentration of 1.5-8.4 ppm. The contents normally found in Scottish soil range from 0.05-2.5 ppm Co extractable by acetic acid or EDTA, and about one-tenth of this by ammonium acetate (104). A deficiency level of <0.3 ppm, common level of 0.3-5 ppm and excess level of >50 ppm has been reported (102). Soils containing less than 2 ppm of this metal commonly present "sick" areas, whereas those with more than this are generally healthy (105).

The common incidence of Co-deficiency in sheep on Scottish soils led Ure and Mitchell (104) to develop a more rapid analytical method for the determination of extractable Co, than that provided by the Cathode-Layer-arc spectrographic technique following chemical concentration (106). They applied an atomic absorption method which was capable of assessing extractable Co in the range of 0.05-2.5 ppm. The application of the ICP for analysis of Co in soil will be studied here.

5.2.2 Choice of Analytical Line

The Co I 345.3 nm line is the most sensitive and most commonly used line. However, like all transition elements, Co has many sensitive lines, and the analyst has a wide selection. The Co 340.5 nm line sometimes suffers interference from Ti 340.5 nm in certain rocks, soils and minerals, while the Co 345.3 nm line is free from interference.

Other/

Other sensitive Co lines are: 352.9, 346.5 and 228.6 nm. The Co 345.3 nm line is used throughout this work and the spectrum obtained in the range of 342.0-350.0 nm is shown in Fig. 5.10.

5.2.3 Standard Solutions

A stock solution containing 10'000 ppm of Co was prepared by dissolving $CoCl_2, 6H_2O$ (20.1840 g) in distilled water and diluting to volume (500 ml). Another stock solution was made in the same way but in 0.5 N acetic acid.

5.2.4 Calibration Curves

The analytical curves were established by measuring the relative intensity of the Co I 345.3 nm line emitted when standard solutions were run. Figs 5.11 and 5.12 show the calibration curves obtained for Co in aqueous and in 0.5 N acetic acid solutions. The analytical curves are linear over a wide concentration which enables the determination of both the major and trace constituents in a sample at a single dilution level. In contrast, analytical curves obtained by flame atomic emission and absorption are generally linear only over 1.5 to 2 orders of magnitude (107), thus several sample dilutions are often necessary for the determination of both major and minor constituents.

5.2.5 Interference Effects

In the acetic acid extraction of Co from soils appreciable amounts of constituents which might interfere with the determination are also extracted. The normal ranges of these are: 200-4000 ppm Ca, 20-1000 ppm Mg, 250-2500 ppm Al, 5-200 ppm Fe, 20-1000 ppm K and 10-500 ppm Na. Therefore, the interference effects of the major constituents on the Co 345.3 nm line were studied, and the results are shown/

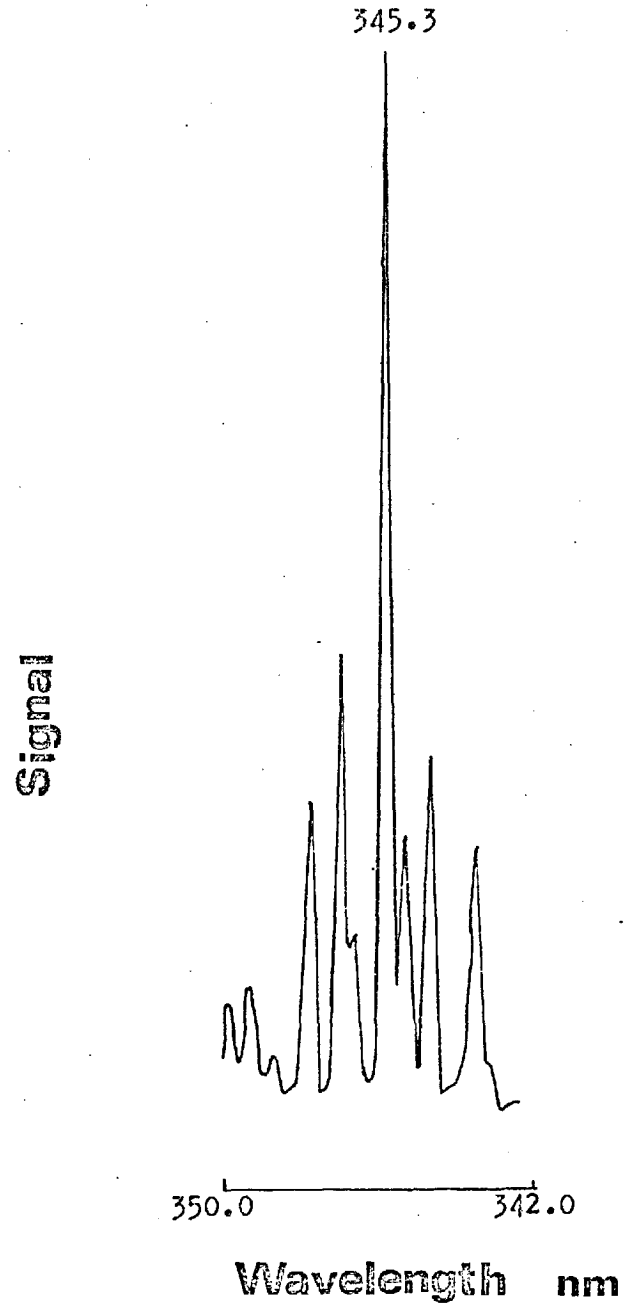


Fig. 5.10. Emission spectrum observed for 10ppm Co over the wavelengh range 342 - 350 nm

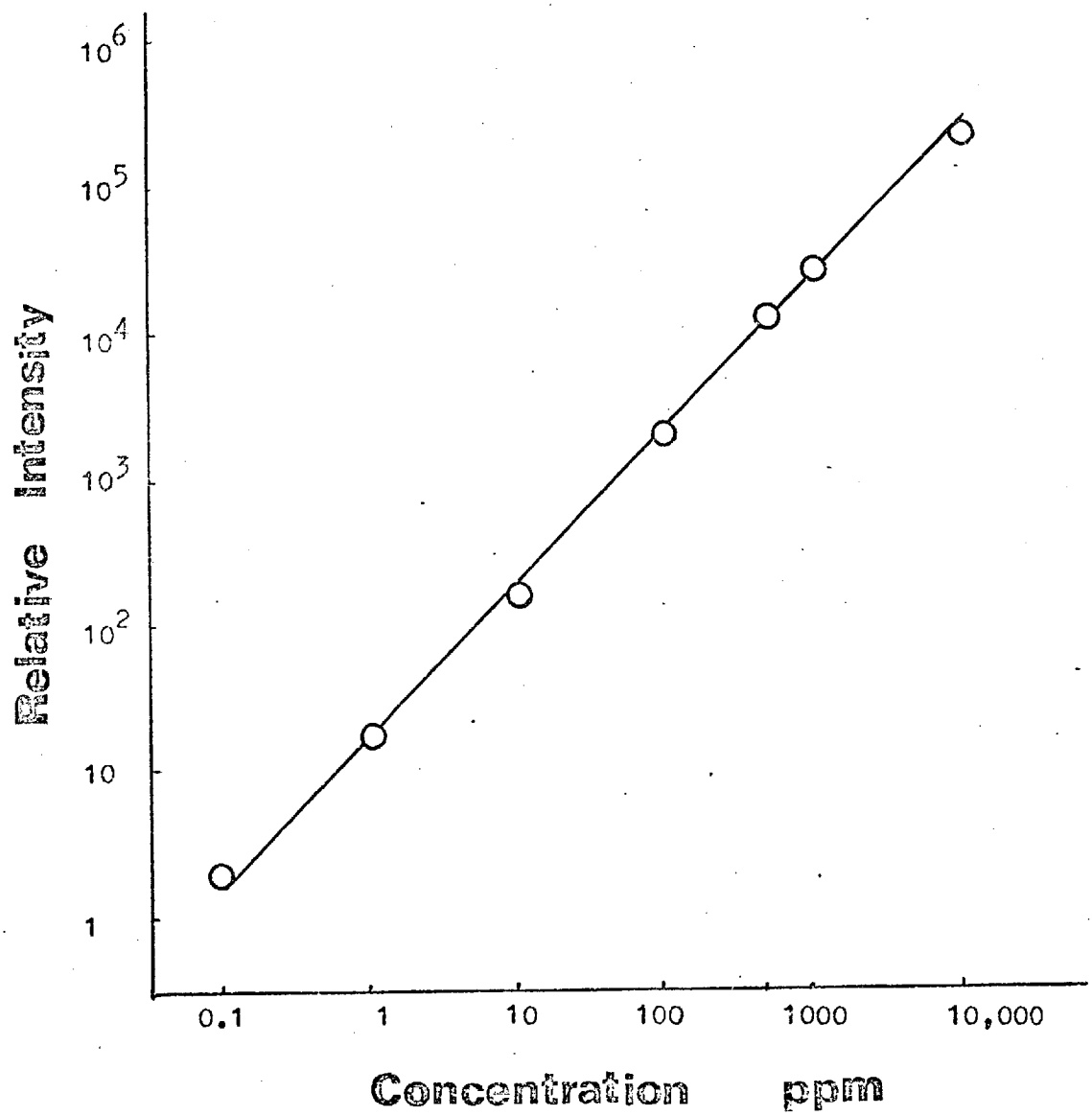


Fig. 5.11. Calibration curve obtained for aqueous solutions of CoI at 345.3nm under optimum conditions

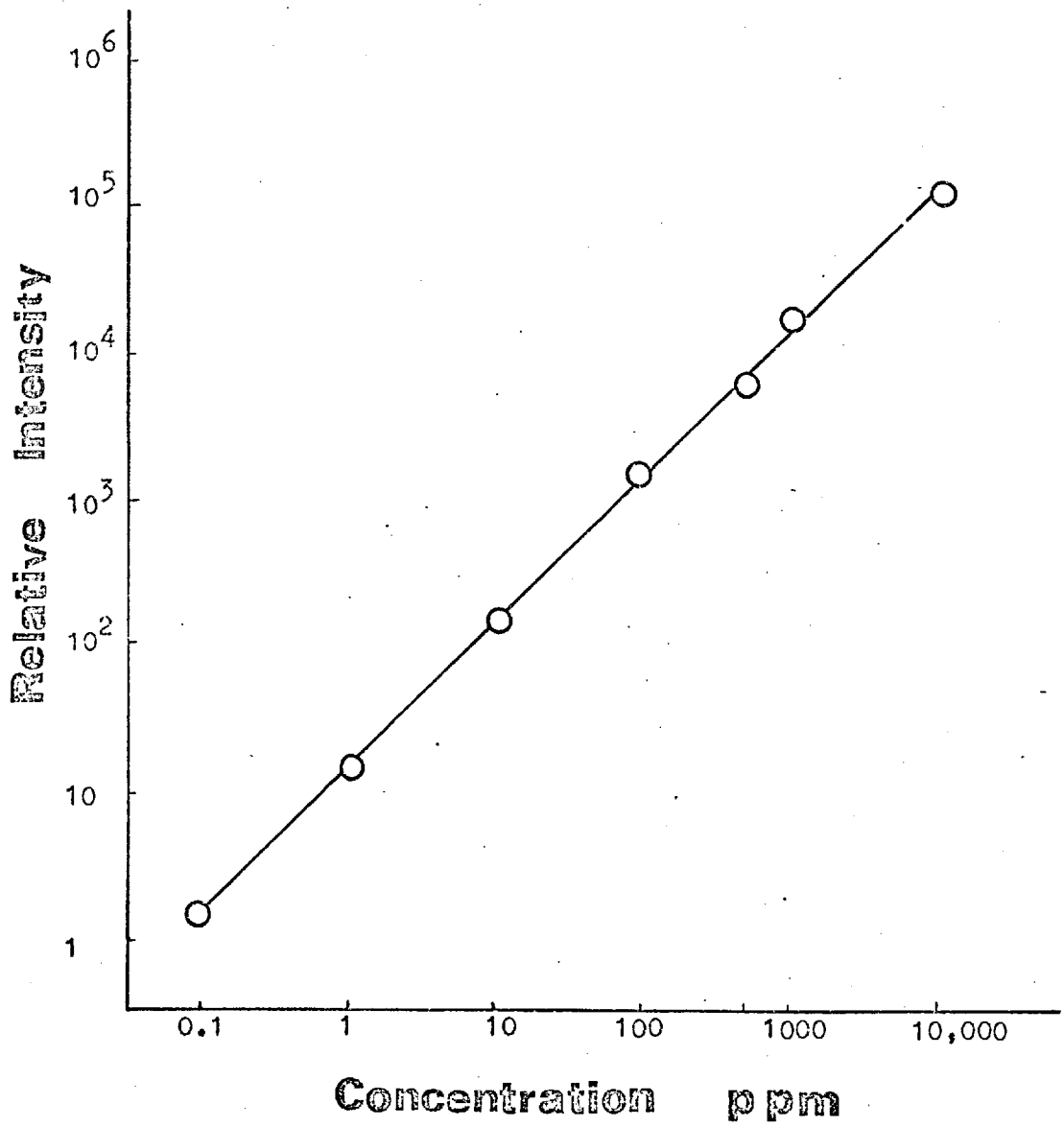


Fig. 5.12. Calibration curve obtained for CoI in 1M ammonium acetate solution at 345.3 nm

shown in Table 5.5.

Table 5.5. Effect of Concomitants on Emission of 10 ppm Co

Concomitant 500 ppm	Emission Intensity A.U.
None	100
Ca	101
Mg	110
Al	125
Fe	130
K	104
Na	115
Cu	103
Ba	130

The magnitudes of the interferences are fairly small and should not present any analytical problems. However, the presence of Fe and Mg, in the concentration ranges occurring in Scottish soils, can be troublesome; therefore, close matching of sample and standard composition is required. The presence of 2.2 and 1.8 Molar hydrochloric acid and sulphuric acid respectively reduced the emission intensity of 10 ppm Co about 10%, while the presence of 2.45 and 3.2 Molar acetic acid and nitric acid enhanced the signal by approximately 10-15%.

5.2.6 Sample Preparation

A 20g sample of air-dried soil is shaken overnight on an end-over-end shaker with 800 ml 0.5 N acetic acid solution. The whole extract is filtered in the same manner as ammonium acetate extracts (section 5.1.7) and is evaporated to dryness. The residue is then taken up in 100 ml, 0.1 N HCl (102).

5.2.7 Analysis of Co in Soil Extracts

The/

The method of standard addition, being found to be a convenient way to compensate for matrix effects, was used to determine Co in acetic acid extracts of soils. In this procedure the effects of decreased flow rate due to increased viscosity of the sample, interelement effects, and other physical and chemical interferences occur to the same extent with the standard as with the sample. Table 5.6 summarises the results of Co determinations in soil extracts obtained by the ICP. Each value shown is the mean of three results. For comparison the results obtained at the Macaulay Institute by the atomic absorption method have also been given in Table 5.6.

Table 5.6. Determination of Co in Soil Extracts using ICP

	Concentration of Co (ppm)	
Sample	ICP	Macaulay
D46753	0.18	0.18
D41148	0.28	0.28
D44193	0.37	0.36
D40458	0.50	0.50
D88787	1.00	0.95
D44187	1.10	1.10

5.3 BORON

5.3.1 Introduction

B is the only element which is essential to plants but not to animals or humans. Although it is necessary for the growth of higher plants, excess amounts in the soil can induce toxicity in plants. A deficiency level of <0.5 ppm, common level of 0.5-3 ppm and excess level of >4 ppm in Scottish soils has been reported (102). However, the total

B/

B content of a soil is not a reliable indicator of the need for B fertilizers because not all of it is readily available.

B has a very simple spectrum. Most spectrochemists have used the sensitive doublet components B 249.7 and 249.8 nm lines. The emission spectrum obtained from the ICP in the range of 205.0-255.0 nm is shown in Fig. 5.13.

Very little work has been described on B atomic absorption or emission. Goldschmidt and Peters (108), who were the first to investigate the geochemistry of B, used Cathode Layer arc excitation and Cu electrodes. A more accurate method has been described by Landergren who employed Sb as an internal standard (109). The porous-cup solution spark method has also been used to determine B in soil extracts (102). In the porous-cup method the solution is introduced into a carbon or graphite tubular upper electrode which has thin porous base. A spark is induced between the moist base of the cup and a pointed counter electrode. This method has certain advantages over the conventional d.c. arc method. Firstly, standard solutions with matrix composition, both chemical and physical, similar to that of the sample solutions are very easily prepared; and secondly, the solutions are homogeneous.

5.3.2 Calibration Curves

A stock solution containing 10'000 ppm B was prepared by dissolving [5.715 g] boric acid in 100 ml deionized water. All other B standard solutions were prepared by diluting the stock solution and they were kept in plastic containers to avoid contamination.

A calibration curve was established under optimized conditions for/

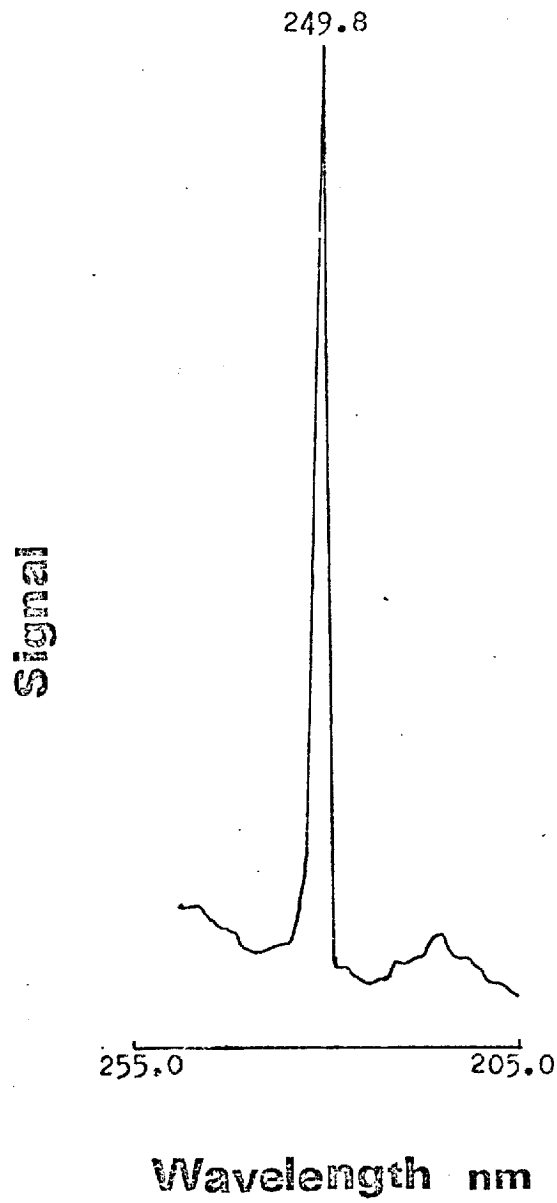


Fig. 5. 13. Emission spectrum observed for 10 ppm Co over the wavelength range 205 - 255 nm

for the B 249.8 nm emission line, and this is shown in Fig. 5.14. As can be seen from the graph the calibration curve is linear over a wide range of concentration.

5.3.3 Interference Effects

The interferences of the following elements:- Na, K, Fe, Mg, Mn, Cu, Ca and Al on the B 249.8 nm emission line were observed when fifty-fold excesses of them were present in a solution containing 10 ppm B. The results of these observations are shown in Table 5.7.

Table 5.7. Effect of Concomitant on Emission of 10 ppm B

Concomitant 500 ppm	Emission Intensity
None	100
Na	118
K	107
Fe	108
Mg	108
Mn	100
Cu	105
Ca	106
Al	100

The presence of 2 N sulphuric acid had no significant effect on the B emission line but the presence of 2 N hydrochloric acid and 2 N nitric acid suppressed the signal by approximately 10%. The magnitude of these interferences however was quite small and did not present any difficulties in the analysis of B in soil extracts.

5.3.4 Sample Preparation

Fifty grams of air-dried soil are boiled under reflux with 100 ml water for 10 minutes. After standing to cool partially, the extract is/

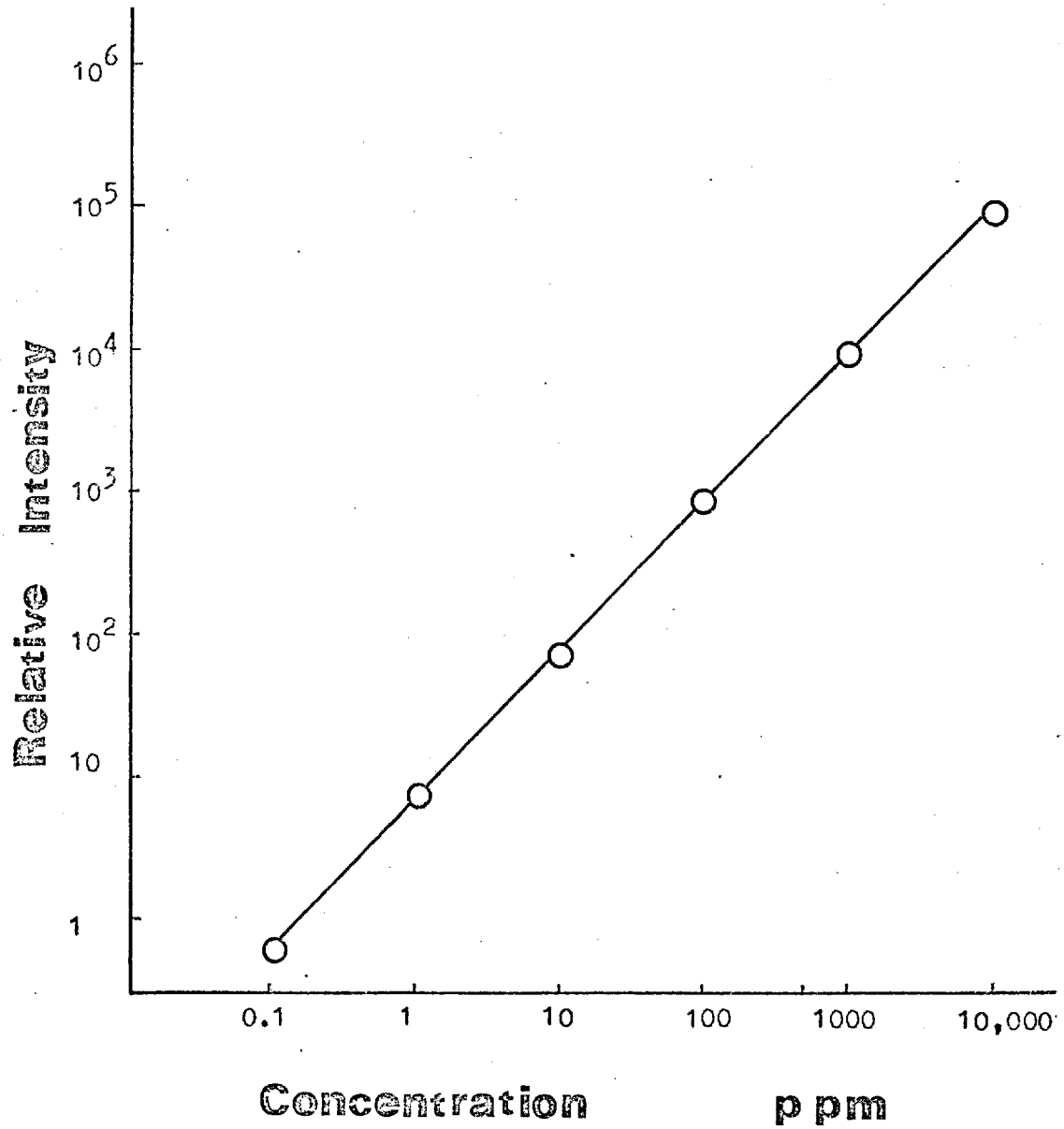


Fig. 5. 14. Calibration curve obtained for aqueous solutions of BI at 249.8 nm under optimised conditions.

is filtered through an 18.5 cm Whatman No. 3 filter paper into a conical beaker and a 40 ml aliquot of the filtrate transferred to a silica beaker. The solution is taken to dryness and the residue oxidised with 10 ml 6% H_2O_2. The residue is then taken up in 5 ml 1.5 N HCl and diluted to volume (102).

5.3.5 Analysis of B in Soil Extracts

As stated above the interferences on B in the ICP are negligible. Therefore, the simple method of directly using the analytical calibration curve was applied. In order to confirm the results obtained by the direct method, the standard addition method was also used. The results of B determination in six different soils are shown in Table 5.8. Each result is the mean of three determinations.

Table 5.8. Determination of B in Soil Extracts Using ICP

	Concentration of B ppm		
Sample	Macaulay	Direct Method	Standard Addition
D18668	0.46	0.37	0.36
69	0.51	0.49	0.49
70	0.71	0.62	0.62
71	0.69	0.57	0.56
72	0.45	0.44	0.44
73	0.47	0.46	0.43

The results obtained by the direct and standard addition methods are in good agreement but lower than the results obtained by a colorimetric determination carried out at Macaulay Institute. This difference in results is possibly because of contamination in the colorimetric procedure which requires tedious preconcentration steps and the use of concentrated H_2SO_4 which is supplied by the manufacturers in soda glass Winchesters.

CHAPTER VI

CONCLUSION

CONCLUSION

An ideal excitation source for use in emission spectrometry for elemental analysis must have the following desirable characteristics: the ability to excite any element, satisfactory freedom from interference effects, outstanding detection limits, capability for simultaneous multielement determinations, wide linear range, simplicity, stability, ease of operation, capability for accepting samples as solids, powders, solutions or gases and finally portability.

The ICP torch having a high excitation temperature and long residence time for the sample species is capable of exciting all elements. The temperature, residence time characteristics together with the inert nature of the support gas minimise chemical interferences. Matrix effects such as ionization suppression in the plasma apparently do occur although there are some unresolved difficulties in assigning this mechanism. Fassel et al (80) maintain that interference effects are eliminated, while Boumans and de Boer (64) have reported interference effects up to 35% for atom lines. The detection limits obtained with our ICP are comparable to other excitation sources although some improvements are needed. Very high detection powers for many elements (0.02-10 ng/ml) have been reported with improved instrumentation (particularly the nebulizer and generator) (36).

The experimental results have shown that the operating parameters (i.e. the sample uptake rate, gas flow rates, power input and observation height) critically affect both detection limits and interference effects. It was found in general that the detection power deteriorated when the parameters/

parameters were altered to achieve minimal interference. Furthermore, the operating parameters have inter-relative effects (see chapter 4) and it would therefore seem that by their manipulation a great deal of control is possible over the emission characteristics of analyte elements. Thus it is, in theory, possible to find compromise conditions under which both the extent of the interferences and the detection power are so balanced for individual elements that the requirements for simultaneous multielement analysis are fulfilled. Indeed, such conditions have been found in practice (60, 63).

Linear calibration curves covering concentration ranges of over 4-5 orders of magnitude were observed for Mo, Co, and B (see chapter 5). The system is simple, stable and no severe difficulties have been encountered in its operation. Solution samples have been successfully employed during this work, and previous work concerning powder nebulization has yielded promising results (92). The system is not portable and the cost of the plasma torch equipment and the large argon consumption make the technique rather expensive. However, it appears to be economical if it is used for SME determinations.

The great disadvantage of the emission technique is that the selectivity is dependent upon the ability of the monochromator to separate the spectral line of the analyte from all other lines in the spectrum. Owing to its high excitation temperature, the plasma torch produces spectra that are fairly rich in lines so that monochromators giving medium or high resolution are required.

SUGGESTIONS FOR SYSTEM IMPROVEMENT

This work was carried out with a generator which was some 12 years old/

old and a monochromator which was originally designed for atomic absorption work. In order to realize the full potential of the R.F. plasma system some improvements in the instrumentation should be made and the author thinks that the system should consist of the following components:

(I) A modern generator with stable frequency and power which is properly shielded to prevent R.F. leakage. The power of the generator can be chosen according to the requirements of the experiments.

(II) An adjustable torch assembly similar to that described by Ohls and Krefta (119) which allows optimum positioning of the three silica tubes with respect to each other. The torch should be movable on both horizontal and vertical axes in order to study the spatial characteristics of the plasma.

(III) A torch housing which is sufficiently well shielded to prevent R.F. leakage. This should have three viewing apertures to allow the simultaneous measurement of signal, background emission and an internal standard line.

(IV) An ultrasonic nebulizer combined with a desolvation system.

(V) A high resolution monochromator which will allow better separation of spectral lines. This must also have a sufficiently large aperture to allow the detection of weak signals.

The results shown in this work, taken together with those found in the literature, indicate that the plasma torch is an excellent excitation source and the future of plasma emission spectrometry is very promising.

REFERENCES

REFERENCES

1. E. H. Holt and R. E. Haskell, Foundation of Plasma Dynamics, Macmillan Company, New York, 1965.
2. P. W. J. M. Boumans and F. J. de Boer, Spectrochim. Acta, 1975, 30B, 449.
3. B. L. Sharp, Annual Review of the Analytical Sciences, Vol. 4, The Chemical Society, 1976.
4. E. L. Grove, Editor, Analytical Emission Spectroscopy, Part II, Dekker, New York, 1972.
5. G. Svehla, Editor, Comprehensive Analytical Chemistry, Vol. V, Elsevier Scientific Publishing Company, Oxford, 1975.
6. P. W. J. M. Boumans, Theory of Spectrochemical Excitation, Hilger and Watts, Ltd., London, 1966.
7. L. H. Ahrens and S. R. Taylor, Spectrochemical Analysis, Pergamon Press, London, 1961.
8. H. Gerdien and A. Lotz, Z. Tech. Phys., 1923, 4, 157.
9. R. Peters, Naturwissenschaften, 1954, 41, 571.
10. R. Weiss, Z. Phys., 1954, 138, 170.
11. G. M. Giannini, Sci. Am., 1957, 197 No. 280.
12. M. Margoshes and B. F. Scribner, Spectrochim. Acta, 1959, 15, 138.
13. V. V. Korolev and E. E. Vains htein, Zh. Anal. Khim, 1959, 14, 658. 1960, 15, 686.
14. National Academy of Science, National Research Council, "The Development and Possible Applications of Plasmas and Related High Temperature Generating Devices", The Division of Engineering and/

and Industrial Research, Washington, 1960.

15. J. A. Browing, Technique for Producing Plasma Jets, Thermal Dynamic Corp., ARS, Aug. 1959.

16. S. Greenfield, H. McD. McGeachin and P. B. Smith, Talanta, 1975, 22, 1.

17. S. Greenfield, H. McD. McGeachin and P. B. Smith, Talanta, 1975, 22, 553.

18. V. A. Fassel in, "Colloquium Spectrocopicum Internationale XVI, Heidelberg, Oktober 1971; Planary Lectures and Reports", Adam Hilger Ltd., London, 1972, P.63.

19. R. F. Browner and J. D. Winefordner, Spectrochim. Acta, 1973, 28B, 263.

20. L. G. Bachurina, I. I. Devyatkin, V. M. Perminova and N. I. Tsemko, Zh. Prikl. Spektrosk., 1971, 15, 401.

21. L. G. Bachurina, I. I. Devyatkin, V. M. Perminova, N. I. Tsemko, S. A. Savostin and L. K. Chuprina, Zavodsk. Lab., 1973, 39, 225.

22. A. D. Stokes, J. Phys. D: Appl. Phys., 1971, 4, 916.

23. T. B. Reed, J. Appl. Phys, 1961, 32, 821, 2534.

24. T. B. Reed, Int. Sci. Technol., 1962 (June), No. 6, 42.

25. V. A. Fassel and R. N. Kniseley, Anal. Chem., 1974, 46, 1155A.

26. R. H. Wendt and V. A. Fassel, Anal. Chem., 1965, 37, 920.

27. R. H. Wendt and V. A. Fassel, Anal. Chem., 1966, 38, 337.

28. C. Veillon and M. Margoshes, Spectrochim. Acta, 1968, 23B, 553.

29. C. Bordonali and M. A. Biancifiori in 'Proc. XIV Colloquium Spectrocopium International' 1968.

30. S. Greenfield, I. L. L. Jones and C. T. Berry, Analyst, 1964, 89, 713.

31/

31. V. A. Fassel and G. W. Dickinson, Anal. Chem., 1968, 40, 247.

32. V. A. Fassel and G. W. Dickinson, Anal. Chem., 1969, 41, 1021.

33. H. C. Hoare and R. A. Moslyn, Anal. Chem., 1967, 39, 1153.

34. R. Mavrodineanu and R. C. Hughes, Spectrochim. Acta, 1963, 19, 1309.

35. R. M. Dagnall, D. J. Smith, T. S. West and S. Greenfield, Anal. Chim. Acta, 1971, 54, 397.

36. P. W. J. M. Boumans and F. J. de Boer, Spectrochim. Acta, 1972, 27B, 391.

37. R. H. Scot, V. A. Fassel, R. N. Kniseley and D. E. Nixon, Anal. Chem., 1974, 46, 75.

38. K. W. Busch and G. H. Morrison, Anal. Chem., 1973, 45, 712A.

39. D. G. Mitchell, K. W. Jackson and K. M. Aldous, Anal. Chem., 1973, 45, 1215A.

40. D. Truitt and J. W. Robinson, Anal. Chim. Acta, 1970, 49, 401.

41. D. Truitt and J. W. Robinson, Anal. Chim. Acta, 1970, 51, 61.

42. J. F. Alder and J. M. Mermet, Spectrochim. Acta, 1973, 28B, 421.

43. S. Greenfield, H. McD. McGeachin and P. B. Smith, Talanta, 1976, 23, 1.

44. T. V. Ramakrishna, P. W. West and J. W. Robinson, Anal. Chim. Acta, 1969, 44, 437.

45. S. Greenfield, Proc. Soc. Anal. Chem., 1965, 2, 111.

46. S. Greenfield, P. B. Smith, A. E. Breeze and N. M. D. Chilton, Anal. Chim. Acta, 1968, 41, 385.

47. W. Barnett and V. A. Fassel, Spectrochim Acta, 1968, 23B, 643.

48. J. M. Mermet and J. P. Robin, Anal. Chem., 1968, 40, 1918.

49. I. Kleinmann and V. Svoboda, Anal. Chem., 1969, 41, 1029.

50/

50. G. H. Morrison and Y. Talmi, Anal. Chem., 1970, 42, 809.

51. R. M. Barnes and S. Nickdel, J. Appl. Phys, 1976, 47, 3929.

52. G. F. Kirkbright, A. F. Ward and T. S. West, Anal. Chim. Acta, 1972, 62, 241.

53. G. F. Kirkbright, A. F. Ward and T. S. West, Anal. Chim. Acta, 1973, 64, 353.

54. J. C. Souilliart and J. P. Robin, Analysis, 1972, 1, 427.

55. P. W. J. M. Boumans, F. J. de Boer and J. W. de Ruiter, Philips Tech. Rev., 1973, 33, 50.

56. S. Greenfield, I. L. L. Jones, H. McD. McGeachin and P. B. Smith, Anal. Chim. Acta, 1975, 74, 225.

57. M. L. Thorpe, N. A. S. A. Contractors Report CR-1143, 1968.

58. S. Greenfield, Proc. Analyt. Div. Chem. Soc., Sept. 1976, 279.

59. C. C. Butler, R. N. Kniseley and V. A. Fassel, Anal. Chem., 1975, 47, 825.

60. V. A. Fassel, C. A. Peterson, F. N. Abercrombie and R. N. Kniseley, Anal. Chem., 1976, 48, 516.

61. A. Montaser and V. A. Fassel, Anal. Chem., 1976, 48, 1490.

62. G. F. Larson and V. A. Fassel, Anal. Chem., 1976, 48, 1161.

63. P. W. J. M. Boumans and F. J. de Boer, Spectrochim. Acta, 1975, 30B, 309.

64. P. W. J. M. Boumans and F. J. de Boer, Spectrochim. Acta, 1976, 31B, 355.

65. P. W. J. M. Boumans and F. J. de Boer, Proc. Anal. Div. Chem. Soc., May 1975, 140.

66. S. Greenfield, P. B. Smith, Anal. Chim. Acta, 1972, 59, 341.

67/

67. S. Greenfield, C. T. Berry and L. G. Bunch, Spectroscopy with a High Frequency Plasma Torch, Radyne Publication, 1965.

68. S. Greenfield and P. B. Smith, Anal. Chim. Acta, 1971, 57, 209.

69. A. E. Crawford, 'Ultrasonic Engineering', Butterworths, London, 1955.

70. J. M. Mermet and J. Robin, Proc. Colloq. Spectrosc. Int. 14th, 1967, 2, 715.

71. S. Greenfield, Metron, 1971, 3, 224.

72. A. E. Watson, G. M. Russell and G. Balaes, National Inst. for Metallurgy, Report No. 1815, 1976.

73. D. J. Smith, Ph.D. Thesis, London University, 1971.

74. A. F. Ward, Ph.D. Thesis, London University, 1973.

75. K. W. Olsen, W. J. Hass Jr. and V. A. Fassel, Anal. Chem., 1977, 49, 632.

76. T. E. Edmonds and G. Horlick, 1976, in press.

77. G. R. Kornblum and L. de Galan, Spectrochim. Acta, 1974, 29B, 249.

78. R. M. Barnes and R. G. Schleicher, Spectrochim. Acta, 1975, 30B, 109.

79. D. J. Kalnicky, R. N. Kniseley and V. A. Fassel, Spectrochim. Acta, 1975, 30B, 511.

80. G. F. Larson, V. A. Fassel, R. H. Scott and R. N. Kniseley, Anal. Chem., 1975, 47, 238.

81. P. T. Gilbert Jr, "Analysis Instrumentation", Proc. Xth Nat. Anal. Inst. Symp., San Francisco, Plenum Press, New York, 1964.

82. K. Kitagawa and T. Takeuchi, Anal. Chim. Acta, 1972, 60, 309.

83. S. Murayama, H. Matsuno and M. Yamamoto, Spectrochim. Acta, 1968, 23B, 513.

84. S. Murayama, Spectrochim. Acta, 1970, 25B, 191.

85/

85. H. Kawaguchi, M. Hasegawa and A. Mizuike, Spectrochim. Acta, 1972, 27B, 205.

86. H. Schirrmeister, Spectrochim. Acta, 1968, 23B, 709.

87. J. C. Van Loon, Atom. Absorption Newsl., 1972, 11, No. 3.

88. S. R. Koirtyohann and E. E. Pickett, Anal. Chem., 1968, 40, 2068.

89. A. C. West, V. A. Fassel and R. N. Kniseley, Anal. Chem., 1973, 45, 1586.

90. I. Rubeska, Anal. Chem., 1976, 48, 1640.

91. I. Rubeska, Can. J. Spectrosc., 1975, 20, 156.

92. J. Goulter, Ph.D. Thesis, London University, 1976.

93. D. E. Nixon, V. A. Fassel and R. N. Kniseley, Anal. Chem., 1974, 46, 210.

94. V. A. Fassel and R. N. Kniseley, Anal. Chem., 1974, 46, 1110A.

95. J. D. Winefordner, V. Svoboda and L. J. Cline, "CRC, Critical Reviews in Analytical Chemistry", August 1970.

96. N. Omentto, L. M. Fraser and J. D. Winefordner, Appl. Spectrosc. Rev., 1973, 7(2), 147.

97. P. Sutcliffe, Analyst, 1976, 101, 949.

98. G. D. Christian and F. J. Feldman, Atomic Absorption Spectroscopy, Wiley Interscience, 1970.

99. L. R. P. Butler and P. M. Mathews, Anal. Chim. Acta, 1966, 36, 319.

100. D. Hutchinson, Analyst, 1972, 97, 118.

101. W. O. Robinson and T. Alexander, Soil Science, 1953, 75, 287.

102. The Macaulay Institute for Soil Research, 1971, Bulletin 2.

103. B. Gregers-Hansen, Trans. Int. Congr. Soil Sci., 8th, Bucharest, 1964, 3, 63.

104. A. M. Ure and R. L. Mitchell, Spectrochim. Acta, 1967, 23B, 79.

105/

105. F. A. Gilbert, Mineral Nutrition and the Balance of Life, Univ. of Oklahoma Press, Norman, 1957.

106. R. L. Mitchell, Tech. Commun. No. 444, Commonwealth Bureau of Solids, Harpenden, 1964.

107. P. J. T. Zeegers, R. Smith and J. D. Winefordner, Anal. Chem., 1968, 40(13), 27A.

108. V. M. Goldschmidt and C. L. Petters, The geochemistry of Boron, Nachr. Ges. Wiss. Göttingen, Math-Phys.Kl.,1932, 402 and 528.

109. S. Landergren, Contribution to Geochemistry of Boron, I. Spectrochemical det. of Boron in Silicate Rocks and Sediments, Ark. Kemi. Min. Geol., 1945, 19A, No.25.

110. A. C. G. Mitchell and M. W. Zemansky, Resonance Radiation and Excited Atoms, Cambridge University Press, 1971.

111. G. R. Kornblum and L. De Galan, Spectrochim Acta, 1977, 32B, 71.

112. J. C. Burridge, Macaulay Institute for Soil Research, Private Communication.

113. H. G. C. Human, R. H. Scott, A. R. Oaks and C. D. West, Analyst, 1976, 101, 265.

114. J. B. Jones Jr, Commun. in Soil Science and Plant Analysis, 1977, 8(4), 349.

115. J. F. Alder, A. M. Gunn and G. F. Kirkbright, Anal. Chim. Acta, 1977, 92, 43.

116. C. W. Fuller, Editor, Annual Reports on Analytical Atomic Spectroscopy, Vol. 6, The Chemical Society, 1977.

117. G. F. Kirkbright, Proc. Anal. Div. Chem. Soc., January, 1975, P.15.

118. F. E. Lichte and S. R. Koirtyohann, ICP Inf. Newsl., 1976, 1, 200.

119/

119. K. Ohls and K. Krefta, ICP Inf. Newsl., 1976, 1, 168.

120. C. Allemand and R. M. Barnes, Initiation of an Induction Heated Air Plasma, 27th Pittsburg Conference on Anal. Chem. and Appl. Spectroscopy, March 1-5, 1976, Cleveland, Ohio, U.S.A.

121. C. Allemand and R. M. Barnes, Initiation and Operational Characteristics of Various Torch Configuration, 27th Pittsburg Conference on Anal. Chem. and Appl. Spectroscopy, March 1-5, 1976, Cleveland, Ohio, U.S.A.